MODELLING BONE MARROW EXTRACELLULAR MATRIX INTERACTIONS REVEAL CD36-DEPENDENT VULNERABILITIES IN ACUTE MYELOID LEUKEMIA

Zhaklina Cifligu

A THESIS SUBMITTED TO THE FACULTY OF GRADUATE STUDIES IN PARTIAL FULFILMENT OF THE REQUIREMENTS FOR THE DEGREE OF MASTER OF SCIENCE

GRADUATE PROGRAM IN BIOLOGY
YORK UNIVERSITY
TORONTO, ONTARIO
DECEMBER 2025

Abstract

Understanding how the bone marrow microenvironment influences metabolic dependencies is crucial for improving therapeutic strategies in acute myeloid leukemia (AML). CD36, a fatty acid transporter associated with lipid uptake and chemoresistance in AML, may be functionally influenced by interactions with the extracellular matrix (ECM). This thesis investigated whether ECM engagement alters CD36-dependent responses in AML. OCI-AML2 cells were cultured on either standard polystyrene (PS) or an ECM-based scaffold and assessed following CD36 inhibition. Scaffold-cultured cells exhibited reduced viability, fatty acid uptake, and clonogenic capacity under CD36 inhibition compared to PS culture. Primary AML samples were then evaluated to assess patient-specific responses. ECM scaffold culture revealed phenotypic adaptations following CD36 inhibition, including reduced fatty acid uptake and increased CD11b expression for two patient samples, suggestive of enhanced ECM interaction and myeloid differentiation. Overall, these findings demonstrate that ECM interactions modulate CD36-dependent vulnerabilities in AML not evident under standard PS culture conditions.

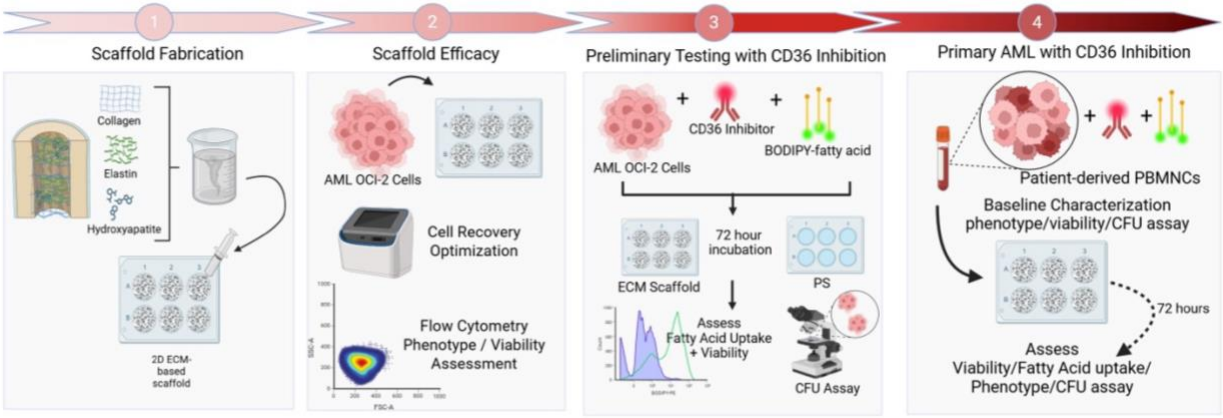

Graphical Abstract. An extracellular matrix (ECM) scaffold was first fabricated to model the bone marrow microenvironment. The scaffold was then validated using AML2-OCI cells to confirm its ability to support proliferation, viability, and phenotypic maintenance relative to standard polystyrene (PS) culture. Following successful validation, CD36 inhibition was tested to assess effects on viability, fatty acid uptake, proliferation, and clonogenic capacity (CFU assay) under PS versus scaffold conditions. Having established ECM-dependent responses in the cell line model, the same approach was subsequently applied to primary AML patient samples to determine whether the ECM scaffold similarly modulates CD36-dependent functional and phenotypic outcomes in a patient-specific context.

Acknowledgments

I would like to express my immense gratitude to Dr. Eleftherios Sachlos for entrusting me with this project, along with his unwavering support and encouragement throughout my journey. Your mentorship has shaped not only this thesis but also my personal growth as a scientist. Exposing me to this world of research is an influence I will carry throughout my life.

I am also deeply appreciative of Dr. Mark Bayfield on my supervisory committee for his invaluable time, thoughtful insights, and support. My gratitude is also extended to the rest of the defence committee for their time, consideration, and feedback. Additionally, the generous funding from CIHR and NSERC helped make this research possible. I extend my gratitude to Dr. Minden, Princess Margaret Cancer Centre, and the patients who generously donated their samples. Working with their precious samples has been a humbling honour and a constant reminder of why this work matters.

I would especially like to thank Milad Falahat Chian for dedicating countless hours to training me, teaching me new techniques, and continuously mentoring me throughout every stage of this research. His patience, generosity and guidance have been instrumental in my development as a researcher. I also want to thank Samira Kabira for being the best lab friend anyone can ask for; your friendship and support mean so much to me. Additionally, I extend my appreciation to the other lab members: Farrah Sawh for always being available to answer my questions, Adriana Pagnani for her kindness and many coffee breaks, and Joab Ogato for his moral support and encouragement. Thank you to Sara Hajari and Vladislava Sadetckaia for their preliminary efforts in laying out the foundation of this work, which I am honoured to have continued.

Lastly, I am greatly indebted to my family and friends for their unwavering support in pursuing my passion. Your unconditional love and motivation have helped me overcome every challenge I've faced. Thank you for being a constant source of strength and light throughout my journey.

Table of Contents

Abstract ..... *ii*

Acknowledgments ..... *iii*

List of Abbreviations ..... *vii*

List of Figures ..... *viii*

Chapter 1: Introduction *1*

1.1 Bone Marrow Niche Components **1**

1.1.1 Hematopoietic stem cells (HSCs) 1

1.1.2 Bone Marrow Niche 2

1.1.3 The Extracellular Matrix of the Bone Marrow 3

1.1.3.1 Collagen 3

1.1.3.2 Elastin 4

1.1.3.3 Hydroxyapatite 4

1.2 Acute Myeloid Leukemia **4**

1.2.1 Overview of AML 4

Figure 2. Schematic of the Pathology of Acute Myeloid Leukemia. 5

1.2.2 AML classification 6

1.2.3 Flow cytometry for studying AML 6

1.2.3.1 Stem/Progenitor Markers 7

1.2.3.2 Myeloid Blast Markers 8

1.2.3.3 Maturation/Differentiation Markers 9

1.2.3.3 Lymphoid Lineage Markers 11

1.2.4 AML treatment 11

1.2.5 Leukemic Stem Cells (LSCs) 12

1.3: Cancer Metabolism **12**

1.3.1: HSC Metabolism 13

1.3.2 AML metabolism 13

1.3.2.1 Fatty Acid Metabolism in AML 14

1.3.2.2 CD36 14

1.3.2.3 Role of CD36 in AML 15

1.3.2.4 Therapeutic implications of CD36 in AML 15

1.4 Altered Metabolism with ECM Interactions in AML **17**

1.4.1 Integrins and AML 17

1.5 Hypothesis, Aim and Objectives **17**

Chapter 2: Methods *19*

2.1 Scaffold Fabrication **19**

Figure 3. Schematic of 2D scaffold fabrication process 19

2.2 CFU Assay **20**

2.3 Flow Cytometry Panel Design **20**

2.4 Preliminary testing with AML OCI2 cells **20**

2.4.1 AML OCI-2 Cell Culture 20

2.4.2 Optimization of Cell Recovery from Scaffolds 20

2.4.3 Characterizing Phenotype of AML OCI-2 Cells 21

2.3.4 Titration of Blocking Antibody FA6-152 Concentrations 21
2.3.5 CD36 Inhibition on Lipid Uptake Assay 22

2.4 Primary AML PBMNC Cell Culture 22
2.4.1 Assessment of CD36 Inhibition in Scaffold-based Cultures of Primary AML Cells 22
Figure 4. Experimental workflow to assess CD36 inhibition in scaffold-based cultures of Primary AML cells. 23

Chapter 3: Results 23

3.1 Optimizing Cell Recovery Assay 23
Figure 5. Optimizing Recovery of OCI-AML2 cells on ECM Scaffold. 24

3.2 Flow Cytometry-Based Characterization of Surface Markers and Viability Analysis in OCI-AML2 Cells 24
Figure 6. Representative flow cytometry of AML OCI-2 cell phenotype and survival. 26
3.2.1 Scaffold-cultured cells Exhibit Elevated CD36 Expression 26
Figure 6. Effect of Culture Condition on Surface Marker MFIs 27

3.3 Titration of FA6-152 Blocking Antibody Concentrations 27
Figure 7. Testing Different Concentrations of Blocking Antibody FA6-152 on AML OCI-2 Cells. .. 28

3.4 CD36 Inhibition Reduces Proliferation and Fatty Acid Uptake for Scaffold-Cultured AML OCI2 Cells 28
Figure 8. Effect of CD36 inhibition on AML-OCI2 Cells. 30

3.5 Baseline Characterization of Primary AML Samples 30
3.5.1 AML Patient-Specific Variation in CD36 Expression and Fatty Acid Uptake 31
Figure 9. Baseline CD36 frequency and Fatty Acid Uptake of Primary AML blasts with Acute CD36 inhibition. 32
3.5.2 Baseline Phenotypic Profiles of Patient-Derived AML Samples 32
Figure 10. Baseline Phenotype of AML Primary PBMNCs with Flow Cytometric Analysis. 34
3.5.3 Baseline Viability of AML Patient Samples 34
Figure 11. Baseline Viability and Absolute Cell Count of Primary AML cells. 35
3.5.4 Baseline Frequencies of Stem Cell-Like Subpopulations 35
3.5.5 Baseline Colony-Forming Unit Potential 35

3.6 Effect of CD36 Inhibition on AML Cell Viability and Proliferation 36
Figure 12. Baseline Stem-like Populations and Clonogenic Capacity of Primary AML Patient Samples. 37
Figure 13. Effect of CD36 Inhibition on Primary AML Cell Viability and Proliferation following 72-hour culture on PS or scaffold. 38

3.7 Effect of CD36 Inhibition on Fatty Acid Uptake 38
Figure 14. Fatty Acid Uptake in Primary AML Patients with CD36 Inhibition. 40

3.8 Effect of CD36 Inhibition on AML Phenotype 40
3.8.1 Variation in Phenotypic Responses Under Inhibition Across Primary AML Blasts 41
3.8.2 CD36 Inhibition Elicits Limited but Distinct Phenotypic Changes Within the ECM Scaffold 42
Figure 16. Effect of CD36 Inhibition on AML Phenotype under different culture conditions. 42
3.8.3 Upregulation of CD11b on Scaffold-Cultured Cells under Inhibition 43
Figure 17. Effect of CD36 Inhibition on Primary AML Myeloid Differentiation. 43
3.8.4 CD36 Inhibition Promotes Broad Myeloid Marker Increases Under PS, but Limited CD11b Upregulation within ECM Scaffold 44
Figure 18. Effect of CD36 Inhibition on Compiled AML Phenotype under Different Culture Conditions. 44

3.9 Effect of CD36 Inhibition on Clonogenic Potential 45
Figure 19. Effect of CD36 Inhibition on Primary AML Clonogenic Potential. 45
Chapter 4: Discussion 46
4.1 Scaffold Efficacy 46
4.2.1 Scaffold Efficacy with Primary AML Cells 48
4.3 Patient Heterogeneity and CD36 Expression 49
4.4 Effect of CD36 Inhibition on AML Clonogenic Capacity 50
4.5 Effect of CD36 Inhibition and ECM Scaffold on Fatty Acid Uptake 52
4.6 Effect of CD36 Inhibition on Primary AML Proliferation and Viability 54
4.7 Phenotype Analysis 55
Chapter 5. Concluding Remarks 59
5.1 Conclusion 59
References 62
Appendix 78

List of Abbreviations

AML	Acute Myeloid Leukemia
Akt	Protein Kinase B
BCL-2	B-Cell Lymphoma 2
BM	Bone Marrow
BSA	Bovine Serum Albumin
CD	Cluster of Differentiation
CFU	Colony-Forming Unit
DRD2 / DRDs	Dopamine Receptor D2 / Dopamine Receptors
ECM	Extracellular Matrix
ETC	Electron Transport Chain
FA	Fatty Acid
FAO	Fatty Acid Oxidation
FBS	Fetal Bovine Serum
FSC-A	Forward Scatter Area
GPCR	G Protein-Coupled Receptor
GVHD	Graft-Versus-Host Disease
HIF-1 / HIF-1α	Hypoxia-Inducible Factor-1 Alpha
HLA-DR	Human Leukocyte Antigen – DR Isotype
HSC	Hematopoietic Stem Cell
IL-3 / IL3-R	Interleukin-3 / Interleukin-3 Receptor
ILK	Integrin-Linked Kinase
LSC	Leukemic Stem Cell
LOX	Lysis Oxidase
LT-HSC	Long-Term Hematopoietic Stem Cell
MAPK	Mitogen-Activated Protein Kinase
MPAL	Mixed phenotype acute leukemia
MFI	Mean Fluorescence Intensity
MSC	Mesenchymal Stromal Cell
NOS	Not otherwise specified
NF-κB	Nuclear Factor Kappa B
NK	Natural Killer Cell
OXPHOS / OxPhos	Oxidative Phosphorylation
PBS	Phosphate-Buffered Saline
PEF	PBS, EDTA, FBS
PI3K	Phosphoinositide 3-Kinase
PS	Polystyrene
ROS	Reactive Oxygen Species
SCF	Stem Cell Factor
shRNA	Short-Hairpin RNA
SSC-A	Side Scatter Area
SSO	Sulfo-N-succinimidyl Oleate
TCA	Tricarboxylic Acid Cycle
2D / 3D	Two Dimensional / Three Dimensional
7-AAD	7-aminoactinomycin D

List of Figures

Graphical Abstract. ……..……..ii
Figure 1. Visualization of the Pathology of Acute Myeloid Leukemia. 5
Figure 2. Schematic of 2D scaffold fabrication process 19
Figure 3. Experimental workflow to assess CD36 inhibition in scaffold-based cultures of Primary AML cells. 23
Figure 4. Optimizing Recovery of OCI-AML2 cells on ECM Scaffold. 24
Figure 5. Representative flow cytometry of AML OCI-2 cell phenotype and survival. 26
Figure 6. Effect of Culture Condition on Surface Marker MFIs 27
Figure 7. Testing Different Concentrations of Blocking Antibody FA6-152 on AML OCI-2 Cells. 28
Figure 8. Effect of CD36 Inhibition on AML-OCI2 Cells. 30
Figure 9. Baseline CD36 Frequency and Fatty Acid Uptake of Primary AML blasts with Acute CD36 inhibition. 32
Figure 10. Baseline Phenotype of AML Primary PBMNCs with Flow Cytometric Analysis. 34
Figure 11. Baseline Viability and Absolute Cell Count of Primary AML cells. 35
Figure 12. Baseline Stem-like Populations and Clonogenic Capacity of Primary AML Patient Samples. 37
Figure 13. Effect of CD36 Inhibition on Primary AML Cell Viability and Proliferation following 72-hour culture on PS or scaffold. 38
Figure 14. Fatty Acid Uptake in Primary AML Patients with CD36 Inhibition. 40
Figure 15. Representative Bodipy Fluorescence Histograms of Fatty Acid Uptake in Primary AML Patients with CD36 Inhibition. 81
Figure 16. Effect of CD36 Inhibition on AML Phenotype under different culture conditions. 42
Figure 17. Effect of CD36 Inhibition on Primary AML Myeloid Differentiation. 43
Figure 18. Effect of CD36 Inhibition on Compiled AML Phenotype under different culture conditions. 44
Figure 19. Effect of CD36 Inhibition on Primary AML Clonogenic Potential. 45

Chapter 1: Introduction

1.1 Bone Marrow Niche Components

1.1.1 Hematopoietic stem cells (HSCs)

The hematopoietic system is a collective organization of the body's blood-forming organs and tissues that are responsible for generating and replenishing every blood cell in the body. Hematopoiesis, the process of blood production, is organized hierarchically, with hematopoietic stem cells (HSCs) at its apex.

HSCs were discovered by two Canadian scientists, Till and McCulloch, in the 1960s. They provided the first direct evidence that HSCs can both self-renew and reconstitute multilineage hematopoiesis in irradiated mice through bone marrow transplants[1].

HSC self-renewal refers to their ability to divide and produce identical copies of themselves, thereby sustaining a consistent, lifelong reservoir of stem cells in the bone marrow[2]. HSC multipotency refers to their ability to give rise to or differentiate into either myeloid- or lymphoid-lineage cells. They do this by dividing asymmetrically, in which one daughter cell retains self-renewal characteristics while the other differentiates into a specialized cell type[3]. HSCs can give rise to multipotent progenitors that lack self-renewal capacity, but differentiate into specialized common progenitors that are either myeloid or lymphoid[4]. Myeloid progenitors can then differentiate into more specialized myeloid-lineage-specific cells, such as erythrocytes, megakaryocytes, monocytes (which give rise to dendritic cells and macrophages), and granulocytes (which give rise to basophils, eosinophils, and neutrophils). Lymphoid progenitors give rise to T cells, B cells, and natural killer (NK) cells.

Besides their biological importance, HSCs are also significant from a therapeutic standpoint. For example, a single HSC can produce lifelong complete hematopoietic reconstitution in a lethally irradiated recipient mouse[7]. Generating or maintaining HSCs from autologous tissues (obtained from the same individual) has been a topic of interest for cellular transplantation therapy, *in vitro* hematological disease modelling, drug discovery, and toxicology studies. Bone marrow transplantation (BMT) is the most established cellular replacement and remains the only curative

treatment for patients suffering from a variety of hematologic disorders such as sickle cell anemia, leukemias, and lymphomas[8]. However, even the most robust current protocols achieve a modest expansion of long-term (LT) repopulating HSCs, and they often have reduced multilineage and migratory potential compared with fresh HSCs[9]. This is attributed to cells being removed from their native environment, where they no longer receive the full spectrum of extrinsic cues from surrounding cells and the extracellular matrix (ECM), which support their proliferation and maintenance[10].

1.1.2 Bone Marrow Niche

Hematopoiesis occurs in the bone marrow, where the rare population of HSCs are tightly regulated in a specialized microenvironment known as the bone marrow (BM) niche. It is a complex area in which the niche represents an intricate interplay among different cell types (hematopoietic and non-hematopoietic) and extracellular components, including the ECM, chemical, and physical factors. These factors coordinately regulate the balance between HSC quiescence, activation, and subsequent processes of cell fate determination, proliferation, self-renewal and differentiation[11].

The several non-hematopoietic cells that comprise the BM niche include mesenchymal stromal cells (MSCs), osteoblasts, adipocytes, endothelial cells, and neural cells. MSCs are crucial multipotent cells in the BM niche that interact with and maintain HSC quiescence, homing, apoptosis, and differentiation by producing key cells, cytokines, chemokines, and ECM components[12,13]. MSCs can differentiate into osteoblasts, which support bone tissue regeneration, or adipocytes (fat cells), which serve as energy reservoirs for surrounding cells under stressful conditions[14].

There are two anatomically distinct compartments within the BM niche: the endosteal and vascular niche. The endosteal niche is located along the inner bone surface lined by osteoblasts[15]. HSCs residing in this niche are maintained in a quiescent state to preserve their self-renewal capacity[16].

The vascular niche surrounds the bone marrow blood vessels, specifically the sinusoidal and arteriolar vessels within the bone marrow cavity. Endothelial cells form the lining of blood vessels that not only supply essential nutrients and oxygen throughout the body but are also significant sources of cytokines such as CXCL12 and stem cell factor (SCF), which regulate HSC function.

HSCs residing in this niche are metabolically active and rapidly give rise to differentiated progenies[17]. Additionally, the extracellular matrix surrounding this niche acts as a dynamic scaffold that enhances cellular interactions and regulates the release and localization of signalling molecules[18].

1.1.3 The Extracellular Matrix of the Bone Marrow

In addition to the cellular components that make up the BM niche, the ECM also plays a pivotal role in hematopoiesis. The ECM is a complex, dynamic three-dimensional meshwork composed of various proteins that not only provide structural support but also bind, sequester, and distribute growth factors that directly affect stem cell fate and hematopoietic regulation. Additionally, mechanical characteristics such as stiffness and elasticity have been shown to play roles in cell polarity, differentiation, proliferation, and survival[20].

The ECM is continuously remodelled by ECM-modifying enzymes such as lysis oxidase (LOX), matrix metalloproteinases, and plasmin[21]. The balance between matrix assembly, crosslinking, and degradation modulates tissue stiffness, which, in turn, plays roles in HSC maintenance, differentiation, and disease progression[22]. Adhesion of HSCs/HPCs to ECM proteins regulates their maintenance, self-renewal, and differentiation within the BM niche[23]. ECM-cell interactions are commonly mediated by integrins, which are α/β heterodimer receptors, critical for cell survival, cancer growth, and metastasis[24].

1.1.3.1 Collagen

The most abundant and major structural ECM protein in bone marrow is collagen type I. However, collagen types II, III, V, and XI are also present, which collectively play essential roles in bone structure, tensile strength, and stiffness of the ECM and tissues[25]. The structure of collagen is comprised of three individual alpha chains that form a triple-helical structure of elongated fibres. Each alpha chain is formed from repeating Gly-X-Y triplets, where X and Y can be any amino acid. The rod-like domain of collagen fibrils provides the central biochemical scaffold for cell attachment and anchorage[26]. The biosynthesis of collagen is a complex, multi-step process that is

predominantly produced by fibroblasts and occurs via the chain association and folding of procollagens (soluble precursors) and subsequent post-translational modifications[27]. The posttranslational modifications of collagens have often been found to undergo tremendous alterations during the development of cancer, driving the ECM to a stiffer state, which is critical to the progression of tumors[28]. Collagen is one of the most widely used biopolymers in tissue engineering, as it replicates the native matrix chemistry and stiffness that engage HSC/HSPC integrins, thereby promoting stem cell anchorage, quiescence, and retention.

1.1.3.2 Elastin

Elastin is a fibrous protein known for providing structural resilience, contributing to the biomechanical properties of the BM ECM[30]. It is found in connective tissue that confers elasticity and resilience. Elastin is secreted by elastogenic cells, such as fibroblasts, smooth muscle cells, and endothelial cells, as a monomer (tropoelastin). It is cross-linked by LOX into insoluble fibres that are highly resilient and resistant to deformation. It is most often intertwined with collagen fibrils to regulate stretching and prevent tissue damage, as the elastic fibres can endure billions of expansions and recoils without breaking down[32]. Elastin has been widely used to recapitulate the biomechanical component of the BM niche in hematological studies, as it supports HSC retention and function.

1.1.3.3 Hydroxyapatite

Hydroxyapatite is the main inorganic component of the ECM or hard tissues such as bone. It is a calcium-phosphate mineral, and can be a synthetic ceramic considered to have good biocompatibility[35]. It provides tissue stiffness and topography, which HSCs sense, leading to increased cell adhesion and motility[36]. As a result, it is classically implemented in hematological studies that recapitulate bone marrow niches as a scaffold[37].

1.2 Acute Myeloid Leukemia

1.2.1 Overview of AML

Acute Myeloid Leukemia (AML) is an aggressive hematological malignancy characterized by the clonal expansion of undifferentiated myeloid progenitors within the bone marrow and peripheral blood[38]. These leukemic blasts proliferate uncontrollably through the acquisition of self-renewal

while failing to differentiate into functional blood cells of the myeloid lineage (Fig. 1). The dysfunctional blasts ultimately outcompete and displace the generation of terminally differentiated blood cells, and also deplete the healthy HSC pool[39]. As a result, hematopoiesis is impaired due to the lack of normal blood cells from the myeloid lineage, including red blood cells, platelets, and granulocytes, which significantly contributes to the severe morbidity in this disease[40].

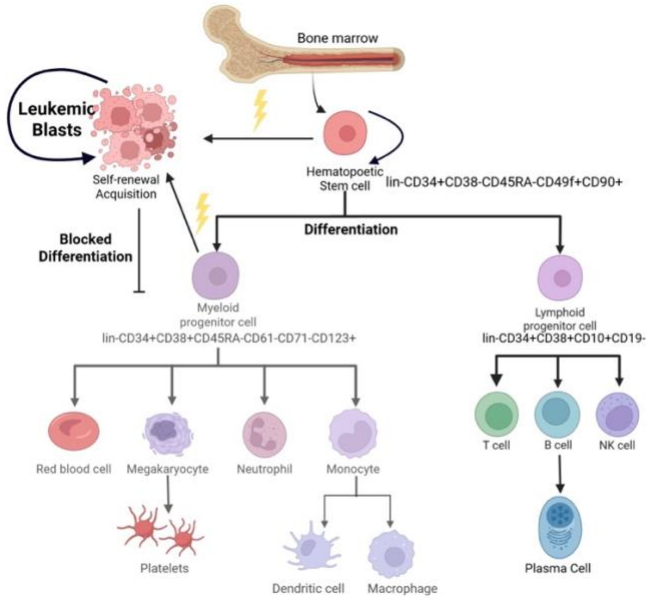

Figure 1. *Schematic of the Pathology of Acute Myeloid Leukemia.* In the normal hematopoietic system, hematopoietic stem cells (HSCs) differentiate into myeloid or lymphoid progenitor cells and eventually produce mature hematopoietic cells. In AML, HSCs or myeloid progenitors acquire genetic mutations which acquire self-renewal ability, allowing them to proliferate uncontrollably in the bone marrow. They are unable to properly differentiate into cells from the myeloid lineage, ultimately outcompeting hematopoiesis and leading to bone marrow failure without intervention. Image created with BioRender.com.

Clinically, AML typically presents with signs of bone marrow failure, such as fatigue, anemia, recurrent infections, and bleeding, due to pancytopenia (decreased red blood cells, white blood cells, and platelets). Diagnosis is confirmed by the presence of ≥20% blasts in the bone marrow or peripheral blood, or by the detection of specific chromosomal abnormalities, regardless of blast percentage[42].

1.2.2 AML classification

AML is a highly heterogeneous disease at both the cytogenetic and molecular levels, reflecting a diversity of cytogenetic aberrations, molecular mutations, and epigenetic modifications[43]. They collectively influence clinical manifestations, disease progression, and response to therapy. This poses significant challenges to disease classification and treatment stratification.

AML subtypes are classified by the WHO system, which divides AML into several broad groups based on genetic, morphological, and clinical criteria. One primary group includes AML with genetic abnormalities such as translocations between chromosomes 8 and 21 (t(8;21)), inversions or translocations involving chromosome 16 (inv(16)), and rearrangements affecting chromosome 11. Therapy-related AML is classified separately and includes cases that arise following exposure to chemotherapy or radiation. Cases that do not meet the criteria for these categories fall under AML not otherwise specified (NOS), which includes morphologic subtypes from the older FAB (French-American-British) classification system, such as undifferentiated AML (M0), AML with minimal maturation (M1), AML with maturation (M2), acute promyelocytic AML (M3), acute myelomonocytic leukemia (M4), acute monocytic leukemia (M5), acute erythroid leukemia (M6), acute megakaryoblast leukemia (M7), acute basophilic leukemia, and acute panmyelosis with myelofibrosis[44]. Rare cases exhibiting both myeloid and lymphoid markers are referred to as mixed phenotype acute leukemias (MPAL), reflecting features of both AML and acute lymphoblastic leukemia (ALL). This comprehensive classification framework aids in accurate diagnosis, risk stratification, and selection of appropriate therapy.

1.2.3 Flow cytometry for studying AML

Diagnosing and classifying AML involves an integrated approach that combines clinical, morphologic, immunophenotypic, and genetic data[45,46]. Immunophenotyping using flow cytometry serves as a standard, powerful tool in identifying and enumerating leukemic blasts, assigning lineage, and detecting aberrant immunophenotypic features. Flow cytometry is a technique that rapidly analyzes single cells as they flow past multiple lasers while suspended in a buffered salt-based solution[47]. Each cell is analyzed for visible light scatter, which is measured in two different directions: 1) the forward direction, or forward scatter (FSC), which indicates the relative size of the cell, and 2) at a side direction at 90° known as the side scatter (SSC), which indicates the internal complexity or granularity of the cell. Cells can also be analyzed using

multiple fluorescence parameters, in which samples are stained with fluorescent dyes or fluorescently conjugated antibodies to detect extracellular surface markers for identification. Antibody panels are optimized to employ a broad array of markers to distinguish leukemic blasts from normal cells and to characterize aberrant phenotypes. AML panels typically include markers spanning stem/progenitor antigens, myeloid differentiation antigens, and lineage-specific (T-cell, B-cell, NK) to identify normal subsets and any abnormal expression on blasts[48].

1.2.3.1 Stem/Progenitor Markers

CD34 is a family member of single-pass transmembrane sialomucin (O-glycosylated) glycoproteins, and is expressed on HSCs, HSPCs, AML blasts and LSCs. It is highly expressed in AML blasts and is associated with several genetic aberrations characteristic of AML development[49]. The role of CD34 is to enhance lymphocyte adhesion through binding to L-selectin, which mediates the homing of HSCs and HPCs to the bone marrow niche or stromal cells[50]. It can also prevent cell lineage differentiation, maintaining progenitor cells in an immature state. In AML diagnostics, CD34 is included to identify blast populations with stem/progenitor features. CD34+ blasts (often co-expressing CD117) are a hallmark of many AML cases, and the presence of CD34 on leukemic blasts has poor prognostic implications, as studies have shown that CD34+ blasts are associated with higher relapse rates than CD34-negative cases[51,49]. This correlation likely reflects the enrichment of chemoresistant leukemic stem cells (LSCs) in CD34+ populations, in which they have been shown to reside in protective microenvironments and maintain quiescence[52].

CD117 (also known as c-Kit) is a type III receptor tyrosine kinase and an early myeloid antigen expressed on HSCs and some myeloid precursors, and is essential for their survival, proliferation, and differentiation[53]. These functions are mediated by receptor binding to SCF. In normal cases, it is expressed in 4% of mononuclear cells in the bone marrow, whereas in AML it is expressed in roughly 60-80% of blasts[54]. CD117 is a standard marker used to delineate immature AML blasts with minimal residual disease (MRD) analysis[55]. Metabolically, CD117 signalling can upregulate nutrient uptake and biosynthetic pathways (via PI3K/mTOR) to meet the demands of proliferation[56].

CD123 is the alpha chain of the interleukin-3 receptor (IL3-R), typically expressed on HSCs[57]. IL-3R is part of a family of membrane receptors that regulates hematopoietic cell growth, proliferation, survival, and differentiation[58]. It is present on a range of early and mature hematopoietic progenitors, as well as on both myeloid and lymphoid lineages and more committed cell populations[59]. The binding of IL-3 to CD123 results in activation of a series of signalling pathways, including the JAK/STAT, Ras-MAPK, and phosphatidylinositol 3-kinase (PI3K) pathways[60]. Elevated CD123 expression is common in leukemic stem cells and is associated with increased blast proliferation, resistance to apoptosis, and a poor prognosis, making it a useful diagnostic and therapeutic biomarker in myeloid leukemias. A high frequency of $CD34^{+}CD38^{low}CD123^{+}$ blasts at diagnosis is predictive of adverse outcomes[62], highlighting its association with the most therapy-resistant LSC fraction.

Dopamine receptors (DRDs) are a class of G protein-coupled receptors (GPCRs) that were first characterized in the nervous system as mediators of learning, memory and regulation of sympathetic tone[63]. However, over the past decade, it has been shown that D2-type receptors, such as DRD2, are linked to AML self-renewal properties, and the high expression of DRs on leukemic stem cells can be selectively targeted with DR antagonists such as thioridazine[63].

1.2.3.2 Myeloid Blast Markers

CD33 is a classic myeloid differentiation antigen, as it is expressed on all normal myeloid cells downstream of the common myeloid progenitor. It plays a role in modulating inflammatory and immune responses by dampening tyrosine kinase-driven signalling pathways[58,59,65]. It is detected in about 88% of AML patients in leukemic blasts and LSCs[66]; however, it does not appear on the surface of normal primitive or multipotent progenitor cells, which makes it a favourable target for immunotherapy of AML[67].

HLA-DR is the most abundant MHC class II antigen, which is normally expressed on antigen-presenting cells (e.g. monocytes, dendritic cells, B cells) and on early myeloid progenitors. HLA class II antigens are involved in the adaptive immune response by presenting peptides derived from extracellular pathogens to CD4+ T-cell helper cells[68]. HLA-DR is reportedly absent or downregulated in various cancerous hematological malignancies, such as in 15-17% cases of

AML[69,70]. Loss of HLA-DR antigen expression is recognized as a mechanism of immune surveillance escape and is associated with post-transplant relapses after allogeneic HSC transplantation[71]. Studies have reported that up to 50% of AML patients with post-transplant relapse are associated with complete or partial loss of HLA-DR and other HLA class II molecules[72].

1.2.3.3 Maturation/Differentiation Markers

CD64 is a high-affinity IgG Fc receptor expressed primarily on monocytes, macrophages, and dendritic cells[73]. IgG antibodies bind to foreign antigens (such as pathogens, viruses) to form an antigen-antibody immune complex. The CD64 antigen functions in both innate and adaptive immune responses through facilitating cellular processes such as endocytosis, phagocytosis, antigen presentation, antibody-dependent cellular cytotoxicity, and cytokine release[74]. The presence of CD64 indicates an acquisition of monocytic lineage and effector machinery. In AML, strong CD64 expression (coupled with CD25 expression) is a hallmark of monocytic differentiation (for FAB subtypes M4 and M5)[75]. Thus, CD64 is included to catch those cases and monitor if blasts begin showing monocytic maturation. While leukemic blasts are not effective phagocytes, the upregulation of CD64 indicates that their metabolism rewires depending on the type of action. Classical M1 activation drives glycolysis, whereas M2 activation leads to reliance on FAO via CD36 and mitochondrial biogenesis[76] to promote tissue repair and metabolic homeostasis[76].

CD11b is an adhesion molecule that pairs with CD18 to form the integrin Mac-1, which is responsible for mediating leukocyte attachment to the endothelium or ECM proteins[77], and in cell movement[77]. Classical findings have shown that Mac-1 preferentially binds to denatured ECM proteins, such as fibronectin, laminin, vitronectin, and thrombospondin[78]. It also contributes to the binding of granulocytes to collagen. CD11b is lowly expressed on CD34+ progenitors, and its expression is increased upon activation of monocytes and granulocytes[79]. Hence, it commonly serves as a robust marker of myeloid differentiation.

CD15 is a classic myeloid antigen expressed on most terminally differentiated myeloid and monocytic lineages[80]. CD15 interacts with E-, L-, and P-selectins, facilitating adhesion to

endothelial cells. It also facilitates phagocytosis and chemotaxis[81]. CD15 expression in the absence of HLA-DR is used to define granulocytic-like AML or to detect asynchronous maturation or aberrant co-expression patterns[82]. CD15 is a favourable prognostic marker in AML[83, 84].

CD16 is a low-affinity IgG receptor expressed on mature neutrophils, NK cells, and macrophages. Functionally, CD16 enables neutrophils and NK cells to perform antibody-dependent cellular cytotoxicity. The absence of this maturation marker, alongside CD11b and CD15, is used to distinguish myeloblasts from mature or maturing myeloid cells[85]. The co-expression of CD16 and CD56 is associated with an adverse prognosis of aberrant NK marker expression[86].

CD71, also known as transferrin receptor 1, is an integral membrane glycoprotein that plays a vital role in the cellular uptake of iron[87]. CD71 is commonly used as an erythroid-associated antigen, although all proliferating cells in the hematopoietic system express CD71[88]. Hence, it is also well known as a marker for cell proliferation and activation. Higher CD71 expression is present in poorly differentiated AMLs with severe anemia than in well-differentiated ones[89]. Therefore, higher CD71 expression enables blasts to meet their high proliferative demands by importing iron for DNA synthesis and metabolism. However, the clinical significance of CD71 in AML remains unclear[90].

CD38 is a transmembrane glycoprotein found on the surface of many immune cells, and acts as a receptor and catalytic enzyme[91]. As a receptor, it is primarily involved in cell adhesion and migration through binding with CD31, and also related to cell activation, proliferation and differentiation[92]. It also acts as an NADase ectoenzyme, ultimately mediating Ca2+ influx, activating various signalling pathways, and participating in effector cell-mediated immunosuppression[93]. It is commonly used as a negative selection marker for HSCs and LSCs, and studies have shown that CD34+CD38- LSCs are associated with unfavourable prognosis, have chemotherapy-resistant properties, and are thereby possibly responsible for the outgrowth of MRD causing relapse[98].

CD45 (the leukocyte common antigen) is a receptor protein tyrosine phosphatase present on all malignant and non-malignant nucleated hematopoietic cells and their precursors, except mature

erythrocytes and platelets[95]. Blasts typically show dim to moderate CD45 expression or are completely negative due to their block in differentiation. In contrast, normal cells exhibit a wider range of CD45 expression[85]. Hence, the marker serves as a backbone for initial flow cytometry gating steps for blast identification in AML

1.2.3.3 Lymphoid Lineage Markers

Expression markers CD4, CD5, CD10, and CD56 are commonly used to identify cells of the lymphoid lineage and to recognize aberrant lymphoid antigen expression in AML. In these aberrant antigen cases, blasts of one lineage do not exhibit the markers of normal differentiation but express unusual markers in which lymphoid-associated antigens are expressed in myeloblasts[96]. This is thought to adversely influence remission rates and overall survival, although the mechanisms underlying this pathology are unknown.

1.2.4 AML treatment

The most standard treatment for AML is induction chemotherapy, which is typically a combination of daunorubicin for three days and cytarabine for seven days (commonly known as '3+7')[97]. Recently, venetoclax has been administered in combination with other drugs and is currently under investigation through phase 1b clinical trials in the US and Canada[98]. Many other various chemotherapeutic agents are used depending on the AML subtype; however, these treatment regimens are accompanied by significant adverse effects, including increased risk of infection, cognitive decline, heart problems, thyroid dysfunction, and numerous other systemic complications[99]. Although this method reduces the presence of leukemic blasts, most adult patients die despite achieving initial complete remission, including those treated with aggressive multi-agent chemotherapy and allogeneic stem cell transplantation[100]. Allogeneic stem cell transplantation is typically administered following chemotherapy. It uses healthy blood-forming stem cells from an HLA-matched donor, ideally restoring the bone marrow's ability to form new blood cells and generating a new immune system for the patient. However, graft-versus-host disease (GVHD) is a common complication that can arise from this, where the donor stem cells (the graft) attack the patient's healthy cells (the host). Long-term outcomes have not improved significantly for over 3 decades, due to a likelihood of relapse nearing 40-60%[101]. This has resulted in an average 5-year survival rate of 5-10% for those aged over 60, and only about 40% for younger

patients[100]. Additionally, long-term survival for patients younger than 60 years old is 35-45%, and 10-15% in patients 60 years and older[102]. These poor outcomes have been considered attributable to chemotherapeutic resistance and post-treatment persistence of leukemia regenerating cells (LRCs), where it has been hypothesized that they are derived from leukemic stem cells (LSCs)[103].

1.2.5 Leukemic Stem Cells (LSCs)

There is increasing evidence that the development of solid and hematological tumours depends on the presence of tumour-initiating cells or tumour stem cells[104]. The first proof of this stem cell concept came from studies by John Dick and colleagues, in which they demonstrated that a small subset of malignant cells in the BM or peripheral blood of most AML patients can regenerate the same AML phenotype when transplanted into recipient animals[105,106]. In AML, these cells are referred to as leukemia-initiating cells (LICs) or LSCs[107]. This supports the notion that AML is a hierarchical disease driven by LSCs, which possess self-renewal and leukemia-initiating capacity[106]. These, along with other studies, have defined LSCs to share a similar immunophenotype with normal HSCs, as CD34+CD38-, rendering selective targeting extremely difficult[108]. Ongoing efforts have been made to identify novel markers and immunological targets in LSC[109]; however, the expression of these markers is heterogeneous among patients[110], and some phenotypic markers may be expressed by both malignant and normal cells[111]. This further reinforces the notion that immunophenotype identification may not be sufficient to target LSCs selectively. Emerging evidence indicates that LSCs have distinct metabolic programs compared to normal HSCs and bulk leukemic blasts that can be therapeutically targeted[112].

1.3: Cancer Metabolism

Metabolic reprogramming in cancer cells has long been recognized as a hallmark of cancer since the discovery of “the Warburg effect” in the 1920s. Normal cells primarily rely on mitochondrial oxidative phosphorylation to generate ATP, yet cancer cells rely on aerobic glycolysis, even in the presence of oxygen[113]. This phenomenon has famously been termed “the Warburg effect”. Emerging literature has highlighted that leukemia progression is tightly linked to metabolic alterations involving key metabolites and their pathways[114]. These metabolic shifts cooperate with underlying genetic and epigenetic changes to sustain leukemic growth and confer drug

resistance[115,116]. Accordingly, uncovering and exploiting these metabolic dependencies have emerged as therapeutically actionable vulnerabilities in AML and other types of malignancies[117].

1.3.1: HSC Metabolism

Normal HSCs, LSCs, and AML blasts have distinct and unique metabolic profiles[118]. In the endosteal niche, HSCs remain largely quiescent and constitute the long-term, self-renewing population as LT-HSCs[119]. LT-HSCs preserve their capacity for self-renewal by existing in a state of quiescence to be protected from proliferative and genomic stress[120, 121].They exhibit low metabolic activity by relying on low rates of anaerobic glycolysis while limiting the TCA cycle and mitochondrial oxidative phosphorylation (OxPhos)[123,124]. Limiting OxPhos protects HSCs from accumulating high levels of reactive oxygen species (ROS), which are generated by mitochondria during normal bioenergetic metabolism[124]. ROS generation can lead to mitochondrial DNA mutations, which in turn induce premature aging and thus lower HSC self-renewal capacity[125]. It can also trigger programmed cell death pathways[126]. The metabolic status of anaerobic glycolysis in HSCs is largely mediated by hypoxia-inducible factor (HIF-1). HIF-1 is highly elevated in LT-HSCs and is involved in the response and metabolic adaptation to environmental conditions, in which it upregulates crucial glycolytic enzymes (such as Pfk-1) to promote this process. Additionally, HIF-1 limits mitochondrial OxPhos by actively suppressing the TCA cycle and ROS production[127]. When HSCs are activated to proliferate or differentiate, they undergo a metabolic shift of mitochondrial biogenesis, OxPhos, and elevated ROS to meet higher energy and biosynthetic demands, driving HSC differentiation to short-term repopulating cells and further on to myeloid differentiation[128 129].

1.3.2 AML metabolism

AML blasts exhibit increased glycolytic activity to supply the required energy for proliferation, which contributes to the aggressive phenotype of the disease[130]. Studies have shown that inhibiting glycolysis in AML cells increases their sensitivity to classical chemotherapeutics such as cytarabine[131].

LSCs are less metabolically active than AML blasts and retain similar metabolic profiles as healthy HSCs; however, they exploit OxPhos to a greater extent. For instance, several components of the ETC complexes (which fuel the proton gradient for ATP synthesis) are more abundant in LSCs than in HSCs[132]. Additionally, LSCs overexpress B cell lymphoma 2 (BCL-2), which helps regulate OxPhos and prevents apoptosis[130]. LSCs are also able to lower ROS levels by upregulating the expression of HIF-1α[1]. OxPhos in *de novo* LSCs is predominantly fueled by amino acids,[133] but in relapse it switches to fatty acid oxidation (FAO), leading to decreased sensitivity to venetoclax-based regimens[134]. The heavy reliance on FAO via lipid metabolism is crucial for their survival and function[135,136], hence ongoing efforts are directed towards perturbing this pathway.

1.3.2.1 Fatty Acid Metabolism in AML

Increased lipid accumulation is a common metabolic alteration in the tumour microenvironment, providing energy for cancer cell growth and migration[137]. Fatty acids (FAs) serve as the backbone for most lipid groups and are essential sources of energy for beta oxidation or fatty acid oxidation. Several transporter proteins facilitate fatty acid transport, such as fatty acid binding proteins (FABP), fatty acid transport proteins (FATP), caveolin-1, and fatty acid translocase (FAT/CD36)[138]. AML patients have a distinct lipid signature compared with healthy controls[139,140], and several reports have observed differences in lipid species correlating with specific cytogenetic and prognostic groups. Leukemic blasts can program BM adipocytes to generate a pro-tumour microenvironment that supports their survival[144]. They do this by inducing adipocyte lipolysis (the breakdown of stored triglycerides into glycerol and free fatty acids, which are released) and by importing the released FAs through CD36[133].

1.3.2.2 CD36

CD36 is a membrane glycoprotein that belongs to the scavenger receptor class B scavenger receptor superfamily[145]. It is expressed in a wide variety of cell types, such as monocytes, macrophages, platelets, erythrocytes, dendritic cells, adipocytes, endothelial cells, muscle cells, and cardiomyocytes[146]. The primary role of CD36 is as a transporter of long-chain fatty acids[147]. The noncanonical functions of CD36 include its role in immune evasion, in which it activates the

NFKB pathway by sensing oxidized low-density lipoproteins (oxLDLs), and its enhancement of myeloid differentiation primary response 88 palmitoylation[148]. Together, this hijacks T cell activity, thereby suppressing antitumor immunity and fostering a permissive environment that allows leukemic blasts to persist and expand. In fact, monocytic AML samples showed higher CD36 expression and greater T cell suppression than nonmonocytic AML samples[148]. Interestingly, CD36 was initially used as a marker for common myeloid progenitors[149] before its role in FA transport was associated with cancer cell metabolism in various tumours, such as ovarian cancer[150], breast cancer[151], and, importantly, AML[139].

1.3.2.3 Role of CD36 in AML

CD36 has recently been identified as an independent prognostic marker in AML[152]. For AML patients uniformly treated with standard "3+7" intensive chemotherapy, those with CD36-high blasts exhibited significantly lower event-free survival, reduced overall survival, and a higher cumulative incidence of relapse compared to cases with CD36-low expression (<20% positive blasts). Moreover, CD36-high AML was enriched for intermediate- and adverse-risk karyotypes and showed a higher frequency of genetic abnormalities, including KMT2A (11q23) rearrangements and t(9;22)/BCR-ABL1 translocations. Collectively, these findings suggest that CD36 expression correlates with more aggressive disease phenotypes driven by adverse genetic features.

1.3.2.4 Therapeutic implications of CD36 in AML

CD36 has been implicated in AML disease progression by facilitating leukemic cell migration and promoting the occurrence of extramedullary disease in AML patients[153]. Farge *et al*. demonstrated that these effects were reduced upon antibody or siRNA-mediated inhibition of CD36 in AML cell lines and xenograft models. In another study, they found that CD36 expression was increased in residual AML blasts after chemotherapy. To determine whether CD36 drives relapse, they knocked down CD36 with shRNA in AML cells and transplanted the cells into immunodeficient mice. In the absence of chemotherapy, CD36 depletion did not alter survival, indicating CD36 is not essential for baseline leukemic growth. However, following chemotherapy, CD36-deficient cells were associated with significantly prolonged survival, whereas CD36-expressing cells demonstrated overall survival. These findings suggest that CD36 facilitates the recovery and

proliferation of residual leukemic cells post-treatment, thereby promoting relapse. Additional studies have also shown that particularly LSCs expressing CD36 have improved survival and chemoresistance[139,154].

Thus, CD36 has emerged as a potential pharmacological target for inhibiting fatty acid uptake in AML. CD36-specific antibodies, fatty acid analogs, and a drug-like small molecule (SMS121) have been reported to block the activity of CD36 (Table 1). Although there are currently no clinical trials targeting CD36 in AML, recent progress has been made in the first CD36-targeting clinical trial for solid tumors[155]. VT1021, a cyclic peptide, induces the expression of TSP-1 in myeloid-derived suppressor cells so that TSP-1 binding to CD36 induces tumour and endothelial cell apoptosis.

Table 1: Strategies for blocking CD36 and their reported effects in AML.

Inhibitor	Reported Effects	Study Context	References
SMS121 (Small-molecule antagonist)	Binds CD36 and blocks lipid uptake (reversible by excess FA) and decreased cell viability	AML cell lines, co-culture with adipocytes	Abacka et al, 2024[142]
SSO (Sulfo-N-succinimidyl oleate)	-Inhibits FA uptake -Induced apoptosis in cells -Reversed FA-driven chemoresistance (Ara-C)	Mouse xenograft models	Zhang et al, 2022[156] Akhtari et al, 2020[2026-01-30 6:31:00 AM]
CD36 shRNA (Genetic suppression of CD36 expression)	-Reduces AML cell proliferation, induced apoptosis in vitro -Delays leukemia progression -Enhanced chemotherapy response -Lowered MRD	AML cell lines, mouse models	Guo et al, 2024[148]
Neutralizing antibody (FA6-152)	Reduces migration, blocks binding of CD36 to TSP1	AML cell lines (U937, OCI-AML3), primary AML patient samples	Farge et al, 2022[153] Zheng et al, 2022[157]

1.4 Altered Metabolism with ECM Interactions in AML

1.4.1 Integrins and AML

AML cells can exploit components of the ECM in the bone marrow niche that have been shown to promote their resistance to chemotherapy and pro-survival signalling[158]. HSCs and LSCs express a repertoire of membrane receptors that interact with the ECM niche[159]. Importantly, they express integrins that participate in cell-cell or cell-ECM adhesion, which critically modulate cellular function and response[160]. For example, binding of collagen to α2β1 integrin protects against doxorubicin-induced DNA damage by inhibiting Rac-1 activation, thereby contributing to pro-survival and chemoresistance[161]. Similarly, LSCs and AML blasts overexpress CD44, which binds various ECM proteins (collagens, laminins, hyaluronic acid, osteopontin, and fibronectin), and this is associated with increased chemotherapy resistance and cancer aggressiveness[162,163]. Importantly, chemotherapy-resistant AML cells heavily rely on OxPhos and lipid metabolism for energy production and survival[164]. This suggests that ECM-mediated adhesion reinforces this metabolic state.

A key mediator linking integrin signalling to various cell signalling pathways is integrin-linked kinase (ILK). It is a central scaffolding protein that binds to the cytoplasmic domains of β-integrins and forms multiprotein complexes which connect them to the actin cytoskeleton[165]. This facilitates cellular adhesion and activates intracellular signalling pathways such as NF-κB, PI3K/Akt-mTOR, Wnt/β-Catenin, and MAPK[166,167]. These pathways promote aberrant cancer functions, including survival, self-renewal, proliferation, metastasis, invasion, and resistance to chemotherapy[165,167]. ILK is a focal adhesion component required for LSC self-renewal and maintenance of quiescence[169]. Notably, inhibition of ILK in quiescent LSCs was shown to reduce the expression of CD36[169]. Hence, ECM-integrin engagement is somehow connected to CD36-dependent lipid metabolism; however, the mechanistic basis of this regulation remains poorly understood.

1.5 Hypothesis, Aim and Objectives

Despite increasing recognition of the role of lipid metabolism and how AML can directly utilize the ECM to aid its survival, little is known about how extracellular matrix interactions shape CD36

function. Given that AML cells heavily depend on metabolic adaptation and engagement with the ECM of the bone marrow niche to support their survival, microenvironmental cues likely shape the functional role of key metabolic receptors. CD36, which is involved in lipid uptake and AML survival, may interact with ECM components that reinforce these metabolic demands. Therefore, it is hypothesized that CD36 interacts with extracellular matrix components within the bone marrow niche to regulate lipid metabolism and survival in AML. The following section outlines the aims of this thesis, which are designed to address this neglected area and establish a framework for evaluating CD36 as a therapeutic vulnerability within the ECM environment.

Aim 1: Validate an ECM scaffold as a preliminary model for assessing whether CD36 inhibition in AML OCI-2 cells elicits enhanced functional responses compared to conventional 2D culture, prior to testing on patient-derived samples.

Former lab members previously developed the fabrication and composition of the ECM scaffold used in this study to support primary AML viability and stemness. To assess if the ECM interacts with CD36, AML OCI-2 cells were initially used to: (i) optimize cell recovery from the scaffold, (ii) characterize viability and phenotype, (iii) evaluate the impact of CD36 inhibition on viability, phenotype, colony-forming unit potential, and fatty acid uptake compared to PS. This approach serves as a foundational step towards identifying if inhibiting CD36 elicits differential cellular responses when they are cultured on PS vs the ECM scaffold.

Aim 2: Characterize primary AML responses to CD36 inhibition on the ECM scaffold versus PS. Following initial validation using AML cell lines, the next aim was to assess if CD36 inhibition induces measurable changes for ECM-cultured cells compared to PS in thawed AML patient peripheral blood mononuclear cells (ID: 120313s). Patient samples were cultured on either PS or ECM scaffolds with and without CD36 inhibition, and the effects were assessed through (i) colony-forming unit (CFU) output to evaluate clonogenic potential, flow cytometry to assess (ii) viability, (iii) fatty acid uptake, and (iv) phenotypic changes. This approach helps determine whether targeting CD36 in a niche-mimicking environment reveals functional vulnerabilities that are less apparent in traditional 2D culture systems.

Chapter 2: Methods

2.1 Scaffold Fabrication

The production of 2D scaffolds to mimic the native bone marrow ECM involves incorporating various ECM proteins, such as collagen type 1, elastin, and hydroxyapatite (Figure 1). Type 1 collagen (derived from Bovine Achilles Tendon) is mixed with 0.05M acetic acid (prepared from diluted Glacial acetic acid, Cat.# 695092, Sigma-Aldrich Co. and Milli Q water) to form a slurry. The solution is chilled at 4°C overnight to allow for rehydration and swelling. The solution is then blended into a uniform, homogeneous viscous mixture and degassed in a bell jar to remove excess trapped air bubbles. Hydroxyapatite (Sigma-Aldrich, Cat.# 900203) is then added, and the mixture is blended. Acetic acid is added in 50µl increments until the mixture reaches a fluid consistency. Elastin (derived from Bovine Neck Ligament, Sigma-Aldrich, Cat. # E1625) is then added, the mixture is blended, and the mixture is degassed to further remove any air bubbles. 1.5 mL of the mixture is then dispensed with a syringe into 6-well plates and left to air-dry in a fume hood to form a thin film in each well. The plates containing the scaffolds are then packaged and X-ray-irradiated to ensure complete sterility.

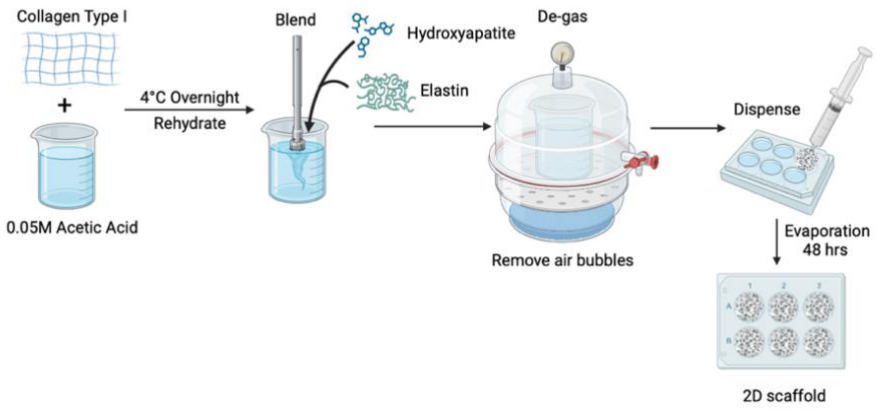

Figure 2. *Schematic of 2D scaffold fabrication process.* Collagen type I and 0.05M acetic acid are mixed and left to chill overnight. The solution is then blended, Hydroxyapatite and Elastin components are added, and the solution undergoes another series of blending and de-gassing until it is completely homogenized and free of air bubbles. The solution is uniformly dispensed into the bottom of 6-well plates and left to air-dry in a biosafety cabinet. Image created with BioRender.com

2.2 CFU Assay

To determine if the functional clonogenic capacity of cells is altered by CD36 inhibition and association with the ECM scaffold, CFU assays were performed. Cells cultured either on polystyrene or scaffolds with or without CD36 inhibition were recovered and used to produce CFUs by seeding either 500 cells (if AML OCI-2) or 50,000 cells (if primary AML cells) suspended in 50µl of media with 500µl of MethoCult (Cat.# 4434, Stem Cell Technologies) into each of the six inner-most wells of a 24-well plate. The peripheral wells were filled with PBS to maintain humidity during incubation. The cells were then incubated for 14 days and routinely monitored. On day 14, microscopic images and videos were taken to count the colonies in each well.

2.3 Flow Cytometry Panel Design

Flow cytometry panels were designed to evaluate cell viability, surface phenotype, and lipid uptake across different experimental conditions. Antibody panels were optimized based on fluorophore compatibility to minimize spectral overlap. Single-colour compensation controls were prepared using compensation beads. Viability was assessed using 7-AAD exclusion. Data acquisition and spectral unmixing were performed using the Agilent NovoCyte Opteon and NovoExpress software. The composition of the AML panel is shown in Table S1.

2.4 Preliminary testing with AML OCI2 cells

2.4.1 AML OCI-2 Cell Culture

Acute myeloid leukemia OCI-2 cell lines were obtained from Dr. Minden's lab (Princess Margaret Hospital). Cells were expanded and cultured in media with αMEM (Cat.# 12-169F, Lonza) with 10% Fetal Bovine Serum (FBS, Cat. #12483-020, Thermo-Fischer Scientific), 1% L-glutamine (Cat. #25030164, Thermo-Fischer Scientific), and 1% Penicillin-Streptomycin (Cat.# 19378-016, Thermo-Fischer Scientific).

2.4.2 Optimization of Cell Recovery from Scaffolds

Following expansion, AML OCI-2 cells were seeded at a density of 300,000 cells per well in 6-well plates either containing the fabricated scaffolds or on polystyrene (control). The cells were

incubated for 72 hours and collected from each well into a separate tube. Each well was then washed either once, twice, three, or four times with PBS to collect any remaining cells on the scaffold. Washes were conducted using two techniques: indirectly on the side of the well's wall to avoid disturbing the scaffold, and directly on the scaffold. The cells were spun down and resuspended in 1mL of media and counted using Trypan blue and a cell countess machine.

2.4.3 Characterizing Phenotype of AML OCI-2 Cells

To validate the antibodies in a controlled, reproducible system, OCI-AML2 cells were initially utilized for volumetric counting and phenotypic analysis with a series of fluorescent antibody panels with the Agilent Flow Cytometer (Novocyte Opeteon). Cells were cultured on either PS or the ECM scaffold for 72 hours, recovered and stained with CD33 (APC), CD34 (SB600), CD45 (PE), CD38 (SB702), CD36 (FITC), DRD2 (with Alexa647-conjugated secondary antibody), for 30 minutes on ice (protected from light), washed 3x with PEF, and stained with 7-AAD (1:25 dilution with PEF, Cat. #6996-50, Fisher), and Hoechst (1:10,000 dilution with PEF, Cat. # H3570, Invitrogen). Unstained and single-stained reference controls were also included to establish compensation controls for spectral unmixing. The scatter population was defined by excluding debris from the unstained population. 7-AAD displaying events that were negative relative to the positively stained population were selected to discriminate against live and dead cells and were further gated as Hoechst positive cells to be classified as live gated cells. Gating strategies were standardized across all samples to allow comparison of surface marker expression and viability between PS and scaffold culture conditions. Mean fluorescence intensities (MFIs) for each fluorophore were analyzed using cells cultured on PS as the reference control. MFIs from scaffold-cultured cells were normalized to the corresponding PS values to enable direct comparison of marker expression levels.

2.3.4 Titration of Blocking Antibody FA6-152 Concentrations

Since the manufacturer did not provide an optimal blocking concentration for the FA6-152 blocking antibody, a range of concentrations was tested to determine the effective dose for CD36 inhibition. Cells were incubated at 1 µg/mL, 2 µg/mL, 4 µg/mL, and 5µg/mL for 1 hour in a total volume of 200 µL. A portion of the cells was collected for flow cytometry analysis (resuspended in PEF, stained with 7-AAD and Hoechst), and the rest was seeded at a density of 50,000 cells per

well in 200µl, in either AML-OCI2 media or primary AML media. After 72 hours of incubation, cells were harvested and either seeded for CFU analysis or stained with 7-AAD and Hoechst for flow cytometric analysis (Agilent Opteon). Three independent experimental replicates were conducted.

2.3.5 CD36 Inhibition on Lipid Uptake Assay

To verify the functional blocking ability of FA6-152, a lipid uptake assay was optimized and performed using a BODIPY-fatty acid analog (BODIPY 500/510 C_{12}, Thermo Fisher, Cat#D3823) to assess lipid content uptake in AML OCI-2 cells. Cells were incubated ± FA6-152 (4µg/mL) for one hour on ice, then with BODIPY (1/10,000 in PEF) for 15 minutes at room temperature. They were then seeded at a density of 50,000 cells per well in either PS or scaffold 96-well plates, in either: Basal media (AlphaMEM, 5% FBS, Penstrep), or serum-starved media (IMDM, BSA, NEAA, NaPyr, 2-Mercaptoethanol, IL-3). An aliquot of 100,000 cells after inhibition and Bodipy staining was used for flow cytometric analysis. Cells were washed with PEF and stained with 7-AAD and Hoechst. Single-stained reference controls were included, and analysis was performed using NovoExpress software. The same steps were repeated after 72 hours of incubation and cell harvesting. Three independent experimental replicates were conducted.

2.4 Primary AML PBMNC Cell Culture

Cryopreserved primary PBMNCs obtained from AML patients were provided by Dr. Mark Minden (Princess Margaret). Research has been reviewed and approved by the York University Ethics Review Board, ensuring compliance with the standards set by the Canadian Tri-Council Policy Statement (TCPS2) on Ethical Conduct for Research Involving Humans. Vials were thawed, and the cell suspension was maintained in phenol-free IMDM, 2-Mercaptoethanol, NaPyr, NEAA, IL-3 and BSA. Immediately before thawing, the media was supplemented with 0.1% IL-3. Cells were maintained at 37°C at 5% CO2 saturation.

2.4.1 Assessment of CD36 Inhibition in Scaffold-based Cultures of Primary AML Cells

Primary AML cells were thawed, resuspended in pre-warmed media, and centrifuged at 300xg for 10 minutes. Cells were then counted using TB exclusion on the Countess to assess initial viability and total yield. The recovered cell suspension was aliquoted for multiple downstream applications to evaluate both baseline and treatment-induced responses (protocol depicted in Figure 3).

Cells were incubated with or without FA6-152 (4µg/mL) for 1 hour on ice, washed and resuspended with PBS, then with BODIPY-labelled fatty acid for 15 minutes at room temperature. Cells were then washed, resuspended in stem cell media, and used for 1) CFU seeding (50,000 cells, n=2 wells), 2) Flow cytometry analysis for baseline immunophenotype analysis (approximately 1,000,000 cells per condition, washed and resuspended in PEF), and 3) seeding on either PS or scaffold 6-well plates at a density of 1,000,000 cells/well. After 72 hours, cells were recovered by washing directly on wells 3 times with PBS, spun down, resuspended in PEF, and used for CFU seeding and flow cytometry staining. Experiments were conducted with three different biological replicates: ID:120713, ID:130213, ID:110289.

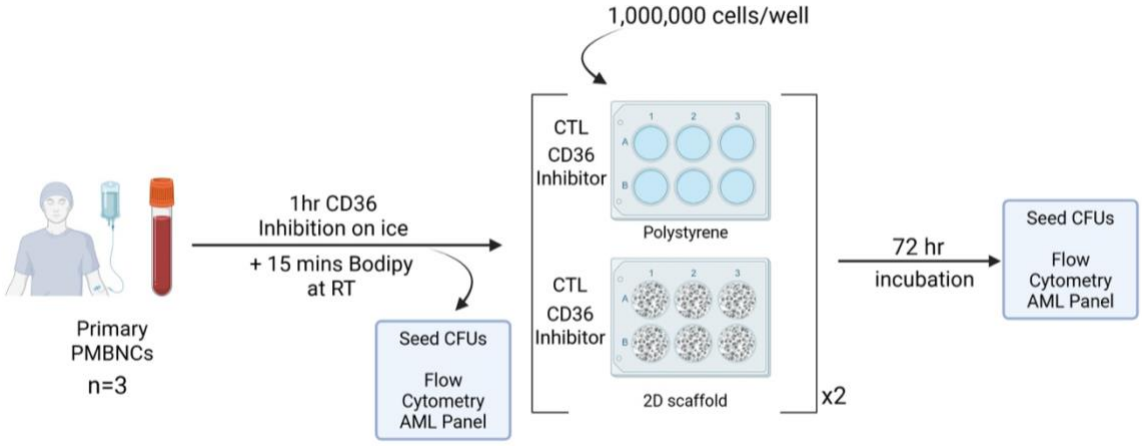

***Figure 3**. Experimental workflow to assess CD36 inhibition in scaffold-based cultures of Primary AML cells.* Thawed primary AML cells were processed and aliquoted for baseline (T=0) analyses, including RNA isolation, CFU assays, and flow cytometry. The remaining cells were treated ± FA6-152 (CD36 inhibitor) for one hour on ice, incubated with Bodipy-labelled fatty acid for 15 minutes at room temperature (RT), and seeded onto either polystyrene or ECM scaffolds. After 72 hours of incubation, cells were recovered for downstream CFU and flow cytometry analyses. Experiments were conducted using three biological replicates. Image created with BioRender.com

Chapter 3: Results

3.1 Optimizing Cell Recovery Assay

AML OCI-2 cells that were cultured and incubated in either polystyrene or scaffold 6-well plates for 72 hours were recovered (with 1-4 washes aimed directly or indirectly on the scaffold) and

counted using Trypan Blue dye and the automated Countess machine. Using a two-way ANOVA test, results showed that three direct washes yielded the most significant number of recovered cells from the scaffold compared to indirectly (Fig. 4B). The number of washes yielded the same number of cells when aimed directly for PS-cultured cells and was overall higher than indirectly (Fig. 4A). The number of cells recovered from directly washing 3 times on the scaffold were 2-fold lower than from PS (Fig. 4C). Overall, washing more than 3 times directly did not substantially increase the yield of live cells from the scaffold. There is still a substantial loss of cells with the best recovery technique from the scaffold when compared to PS.

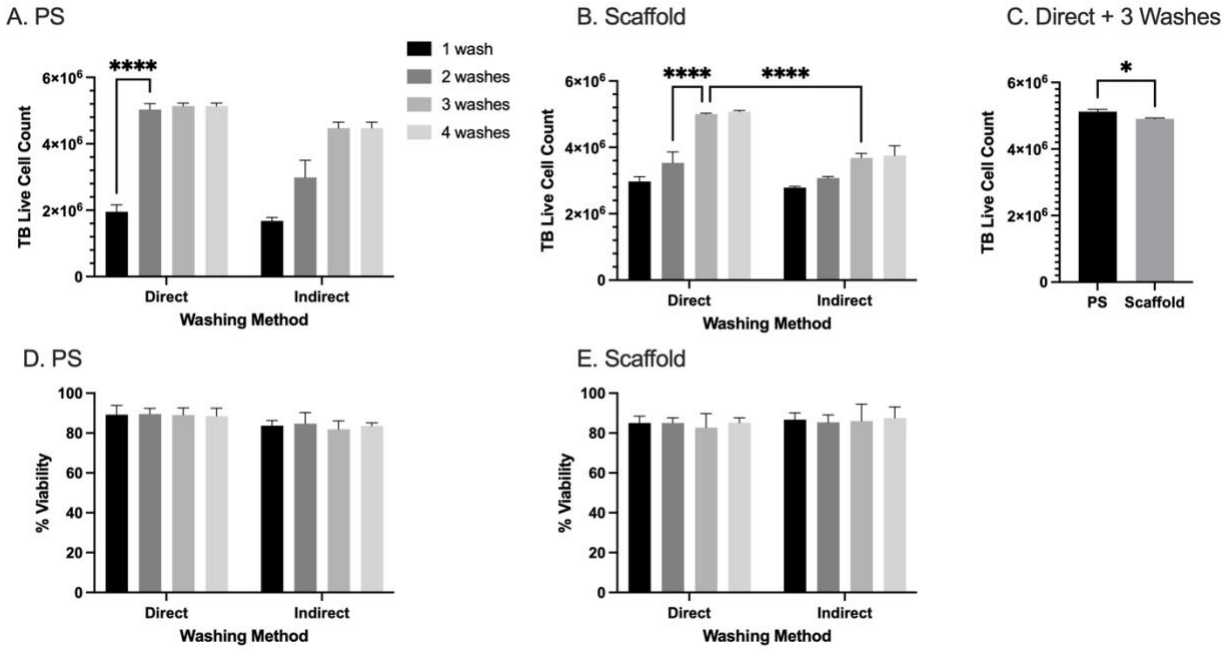

Figure 4. *Optimizing Recovery of OCI-AML2 cells on ECM Scaffold.* AML-OCI2 cells incubated on either **(A)** PS or **(B)** ECM scaffold, for 72 hours, were recovered by direct or indirect washing for 1-4 washes. **(C)** Live cell counts from PS and scaffold recovered by directly washing 3 times. Cellular viability was quantified using TB exclusion and a cell countess machine. Data reported as Mean ± SD, Two-way ANOVA test, (****) $p<0.0001$, unpaired t-test with Welch's correction (*) $p<0.05$, N=3.

3.2 Flow Cytometry-Based Characterization of Surface Markers and Viability Analysis in OCI-AML2 Cells

Flow cytometry was performed on AML OCI2 cells after 72 hours of incubation in either PS or scaffold to assess viability and surface marker expression between the two conditions. Initial gating for live and dead cell discrimination was accomplished by establishing a "scatter" gate of

cells based on forward scatter (indicates cell size, FSC-A) and side scatter (cell complexity, SSC-A) to exclude debris and identify cells of interest (Fig. 5A). Viable cells were subsequently identified as 7-AAD-negative and Hoechst-positive. The absolute number of live cells was determined using volumetric counting, which calculates the concentration of viable cells (Hoechst+/7-AAD-) per microliter of sample analyzed. This approach enables standardized quantification across conditions rather than raw live-cell counts, which can vary with the number of events collected and the acquisition time. Live cells were then gated based on CD33 and CD45 co-expression to identify and confirm that the cells are indeed of a myeloid lineage (Fig. 5B). The myeloid-gated population was further characterized as $CD36^{+}CD34^{-}CD38^{-}DRD^{-}$. Importantly, CD36 expression confirms the presence of the lipid uptake receptor, the intended target of inhibition in this study.

Overall, the absolute number of viable cells recovered from the scaffold was 0.87-fold lower than PS (*$p<0.05$, Fig. 5C), whereas viability between them was similar (Figure 5D). These results indicate that the ECM-based scaffold supports AML cell viability to a comparable extent as traditional PS culture.

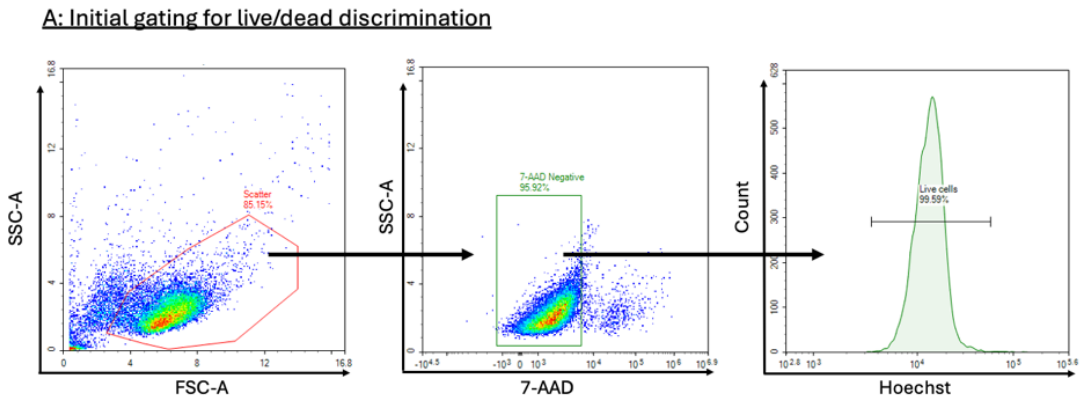

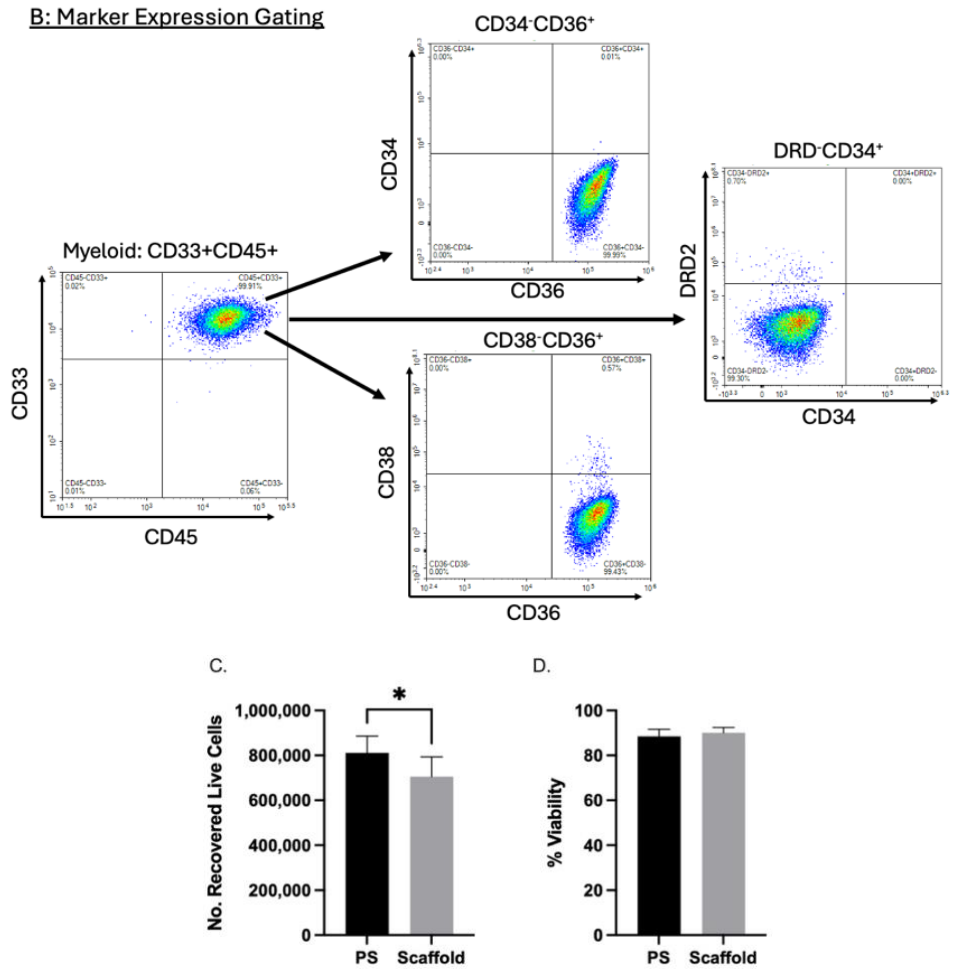

***Figure 5**. Representative flow cytometry of AML OCI-2 cell phenotype and survival.* Cells were seeded at a density of 300,000 cells per condition and incubated for 72 hours at 37 °C with 5% Co2. After incubation, cells were harvested and stained with 7-AAD, Hoechst, DRD2, CD36, CD33, and CD34 fluorophore-conjugated antibodies for flow cytometry analysis. **(A)** Scatter gating to exclude debris, further gated as 7-AAD negative and Hoechst positive to gate live cells. **(B)** Live cells gated on $CD33^{+}CD45^{+}$ to identify the myeloid population; further analyzed as $CD36^{+}CD34^{-}CD38^{-}DRD^{-}$. **(C)** The absolute number of recovered live cells determined by flow cytometric volumetric counting and viability staining for both conditions. **(D)** Percent Viability of cells for both conditions. Data reported as Mean ± SD, paired t-test, (*) $p<0.05$, N=3.

3.2.1 Scaffold-cultured cells Exhibit Elevated CD36 Expression

Although the immunophenotypic frequencies remained consistent between PS and ECM scaffold conditions, the MFI of each marker was analyzed to determine whether expression levels differed. The MFI of each marker in scaffold-cultured cells was normalized to the corresponding mean MFI in the control PS condition. The MFI for CD34, CD38, CD45, CD33, and DRD2 was comparable

between the two conditions, indicating no significant difference in expression levels. This suggests that the scaffold does not alter the phenotypic stability of OCI-2 cells over the culture period and supports cell maintenance without inducing detectable shifts in differentiation or lineage marker shifts. Interestingly, CD36 expression was higher in cells cultured on the scaffold, as indicated by a higher FITC MFI than cells cultured on polystyrene (* $p<0.05$, Fig. 6). This suggests that the ECM scaffold may enhance or sustain CD36 expression, supporting a more metabolically active leukemic phenotype.

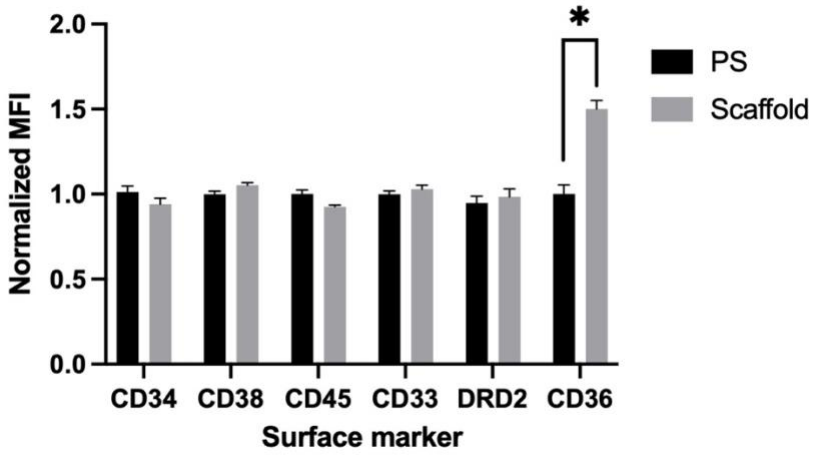

Figure 6. *Effect of Culture Condition on Surface Marker MFIs*. Normalized mean fluorescence intensities (MFIs) of surface markers on AML OCI-2 cells cultured on PS (polystyrene) or ECM-based scaffold for 72 hours. Flow cytometry was used to assess surface marker expression after culture under each condition. MFIs were normalized to PS controls and plotted to compare expression levels between PS and scaffold-cultured cells. Data reported as Mean ± SD, unpaired t-test, (*) $p<0.05$, N=9.

3.3 Titration of FA6-152 Blocking Antibody Concentrations

Since the manufacturer did not provide an optimal blocking concentration for the FA6-152 blocking antibody, a range of concentrations (1 µg, 2 µg, 4 µg, and 5µg) was tested to determine the effective dose for CD36 inhibition. After 72 hours of culture with inhibition in either basal or serum-starved media, recovered cells were analyzed by flow cytometry, and an aliquot was seeded for CFU analysis. Under basal media conditions, there was no effect on cellular viability,

proliferation, or CFUs at any concentration for both PS and scaffold-cultured cells (Fig. 7A-C). To better reflect the planned serum-free conditions for downstream primary AML experiments, the inhibitor was subsequently tested in standardized stem cell media lacking FBS. Under serum-starved conditions, scaffold-cultured cells exhibited reduced viability, absolute live cell counts, and fewer CFUs at concentrations of 4 and 5 µg/mL of the inhibitor. The concentration of 4µg/mL was selected for subsequent experiments.

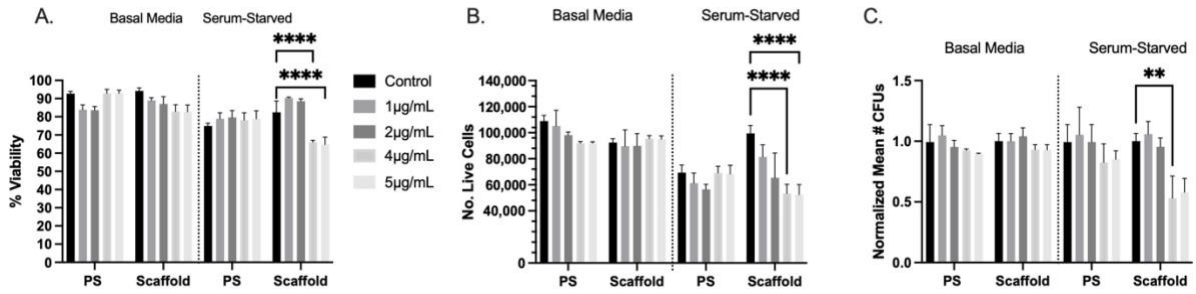

Figure 7. *Testing Different Concentrations of Blocking Antibody FA6-152 on AML OCI-2 Cells*. Cells were incubated with varying concentrations (1 µg, 2 µg, 4 µg, and 5µg) of FA6-152 in either basal media or serum-starved media on PS or scaffold 96-well plates. After 72 hours, harvested cells were either used for flow cytometry analysis or seeded for CFUs. **(A).** Percent viability determined with 7-AAD and Hoechst staining. **(B)** Absolute live cell counts determined with volumetric counting. **(C)** Mean number of CFUs normalized to PS control (respectively for basal media and serum starved conditions) recorded after 14 days of initial seeding. Data reported as Mean ± SD, Two-way ANOVA, (****) $p<0.0005$, N=9.

3.4 CD36 Inhibition Reduces Proliferation and Fatty Acid Uptake for Scaffold-Cultured AML OCI2 Cells

As a preliminary screen to evaluate the functional impact of CD36 inhibition, and if it differed between PS and ECM conditions prior to testing on primary AML patient samples, OCI-AML2 cells were treated with 4µg/mL of FA6-152 (CD36 inhibitor), stained with Bodipy and incubated on either PS or scaffold for 72 hours. Cells were recovered, analyzed by flow cytometry, and then seeded for CFUs.

Bodipy fluorescence intensity based on a threshold set where the cells in the upper quartile (top 50%) of fluorescence intensity relative to the control peak were classified as Bodipy^{hi} (Fig. 8A). In basal media, the amount of Bodipy^{hi} cells remained unchanged with inhibition for both conditions (Fig. 8B-iii). Viability, absolute live cell counts, bodipy MFI, and CFUs also remained

comparable between both PS and scaffold conditions with and without inhibition (Fig. 8B i-vi). Under serum-starved media, inhibition led to a decrease in viability (Fig. 8C-i) and absolute live cell counts (Fig. 8C-ii) in scaffold-cultured cells, while PS-cultured cells remained unaffected. The number of Bodipy^{hi} cells decreased upon inhibition in both conditions, with a more pronounced reduction in scaffold cultures. Similarly, Bodipy MFI declined under inhibition, and was abolished under scaffold inhibition. CFU assays performed 14 days after seeding showed reduced clonogenic potential in scaffold-inhibited cells (*$p<0.05$, Fig. 8C-vi). Overall, these findings suggest that, in serum-starved media, cells cultured on scaffolds are more susceptible to CD36 inhibition than those cultured on PS.

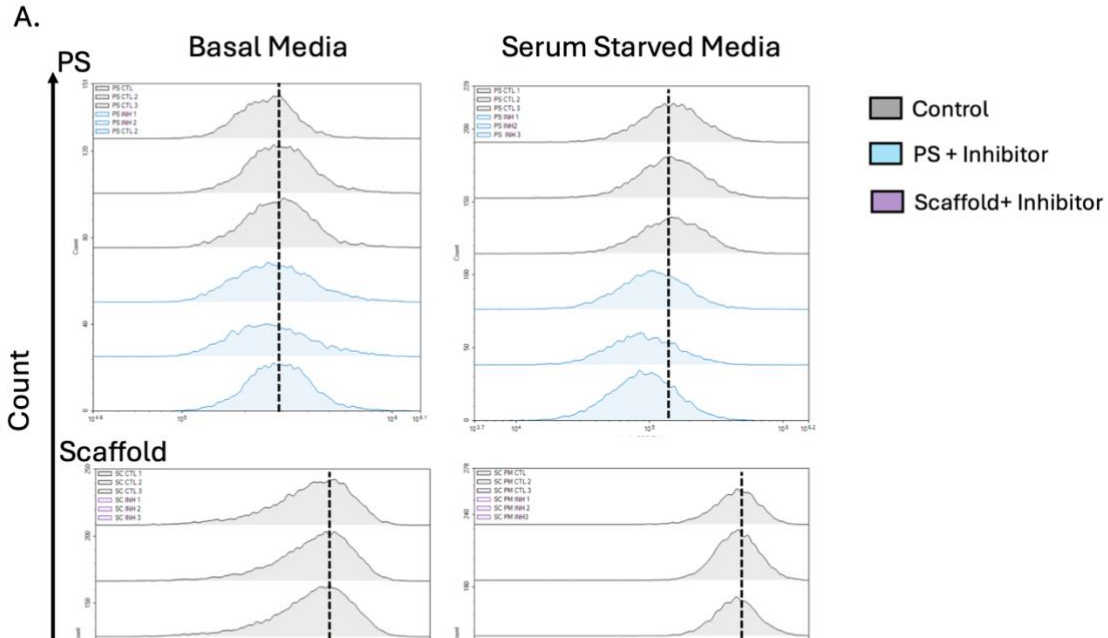

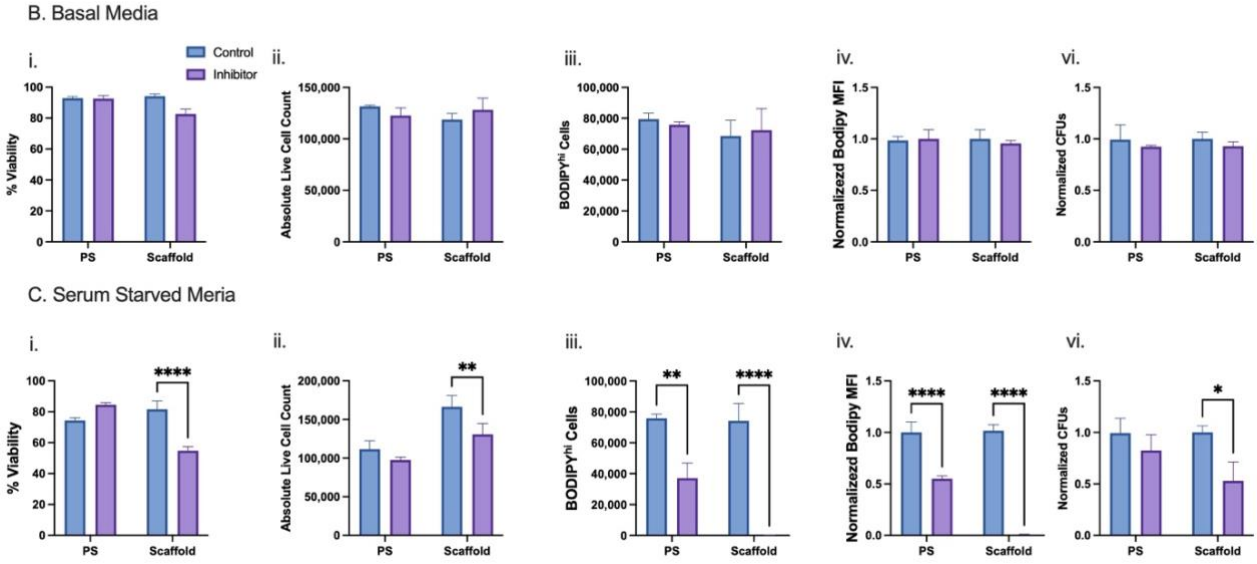

Figure 8. *Effect of CD36 inhibition on AML-OCI2 Cells.* **(A).** Histogram of Bodipy fluorescence following 72 hours of incubation without (grey area) and with (coloured) FA6-152 inhibitor on either PS or scaffold. Cells were either incubated in **(B)** Basal media and **(C)** Serum starved media for 72 hours and their viability (i), absolute cell counts determined with volumetric counting (ii), absolute counts of Bodipy^{hi} cells (iii), Normalized change in Bodipy MFI relative to the control (iv), and CFUs recorded and normalized to PS control 14 days after seeding from 72 hour incubation (vi). Data reported as Mean ± SD, Two-way ANOVA, Šídák's multiple comparisons test (**) $p<0.001$, (****) $p<0.0001$, N=9.

3.5 Baseline Characterization of Primary AML Samples

Primary AML cells were thawed and immediately incubated for one hour in the presence or absence of a CD36-blocking antibody (4µg/mL FA6-152). A portion of the cells from each condition was subsequently stained with Bodipy and then analyzed by flow cytometry to characterize their initial phenotype, assess viability, and evaluate baseline lipid uptake. The remaining cells were seeded at a density of 1,000,000 cells/well in either conventional PS 6-well plates or ECM-based scaffolds fabricated on 6-well plates for 72 hours.

3.5.1 AML Patient-Specific Variation in CD36 Expression and Fatty Acid Uptake

Given the central focus of this study on CD36 as a therapeutic target, CD36 expression was first examined across patients. It was observed that were was inter-patient variability in both frequency and absolute counts of CD36+ blast cells. Patient ID: 12713 displayed the lowest CD36+ frequency of 0.52%, ID: 130213 exhibited an intermediate frequency of 31.9%, and ID: 110289 had the highest CD36+ expression of 72.4% (Table 2, Fig. 9A).

With short-term CD36 inhibition, there was no significant change in CD36 cell frequencies. There was a significant reduction in the frequency of Bodipy+ cells for patient IDs 120713 and 110289 (*$p<0.05$, Fig. 9A). In contrast, ID 110289 also showed a reduction in fatty acid uptake, although this was not significant. Collectively, the frequency of Bodipy+ cells was reduced (**$p<0.005$, Fig. 9B). There was no change in MFI with inhibition. Collectively, these results indicate heterogeneity in CD36 expression and low initial Bodipy+ frequencies across all patient samples; however, overall fatty acid uptake was reduced with acute CD36 inhibition.

Table 2: Baseline CD36 and Bodipy expression frequencies across three primary AML patient samples. Flow cytometry was performed immediately following thawing and incubation for 1 hour, with and without CD36 inhibition, and with Bodipy staining to assess baseline CD36 expression and fatty acid uptake under acute inhibition. Reported values represent the average of three independent measurements for each patient (n=3).

	CD36+ Frequency		**Bodipy+ Frequency**	
Patient ID	Control	Inhibition	Control	Inhibition

120713	0.52%	0.6%	0.09%	0.02%
130213	31.86%	29.5%	1.45%	0.2%
110289	72.44%	70.66%	4.33%	2.92%

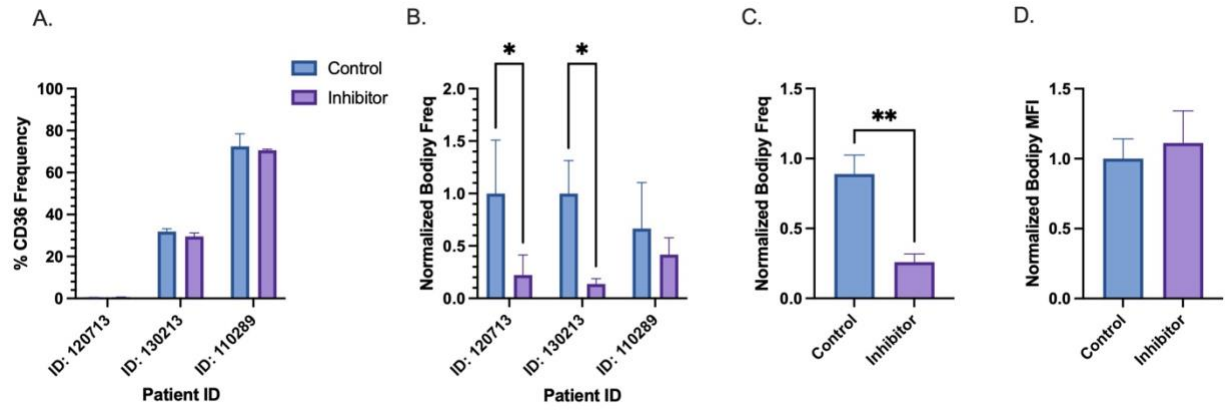

Figure 9. *Baseline CD36 frequency and Fatty Acid Uptake of Primary AML blasts with Acute CD36 inhibition.* Upon thawing, primary AML cells were incubated with 4µg/mL of FA6-152 inhibitor, stained with a panel of fluorescently conjugated antibodies, and analyzed with flow cytometry. **(A)** Percentage frequency for each patient expressing CD36+ cells**. (B)** Normalized Bodipy frequencies relative to untreated controls for each patient. **(C)** Compiled Bodipy frequencies from all three patient samples, normalized to each patient's control. **(D)** Compiled normalized Bodipy mean fluorescence intensity (MFI) across three patients. Data reported as Mean ± SD, Two-way ANOVA, Šídák's multiple comparisons test, (*) $p<0.05$, (**) $p<0.001$, N=3.

3.5.2 Baseline Phenotypic Profiles of Patient-Derived AML Samples

Flow cytometric analysis was performed using a sequential gating strategy where an initial scatter gate based on SSC-A and FSC-A was used to visualize the main cell populations, followed by exclusion of non-viable cells using 7-AAD staining. Live cells were defined as 7-AAD-negative events, with gating thresholds established from unstained controls. The live population was then plotted against CD33, and CD33+ cells were gated to capture the myeloid compartment of blasts. Within this blast gate, CD45 expression was evaluated to confirm low-to-intermediate levels, consistent with previously reported AML immunophenotypes. Subsequent analysis of blast populations included additional markers from the antibody panel, such as CD36. Positivity for

each marker was determined relative to unstained controls, and final frequencies were reported as the percentage of blast-gated cells expressing the indicated antigen (Fig. 10B).

3.5.2.1 Patient ID: 120713

The blast population displayed an immature AML immunophenotype characterized by a moderate CD34+ subset (≈ 14%) and low frequencies of myeloid lineage/maturation markers (<2%), alongside marked aberrant CD56 (≈ 91%) and CD10 (≈ 17%) within CD33+ blasts. Compared to other patients, this profile shows limited myeloid maturation features and minimal CD36 expression.

3.5.2.2 ID: 130213

Blast populations were characterized as mainly negative (≈ <1%) for CD34, CD123, DRD2, CD15, and HLA-DR. They were largely positive for CD117 and CD64 (≈ 90-98%), while moderate levels were detected for CD38, CD16, CD71, CD45 and CD36. The blasts also displayed aberrant co-expression of lymphoid markers CD10 (≈ 80%) and CD56 expression (≈ 35%). This profile suggests a more differentiated, monocytic-biased phenotype with reduced expression of primitive markers.

3.5.2.3 ID: 110289

The blast population exhibited moderate-low CD34 (≈ CD17%) and CD123 (≈ 7%) expression, with moderate positivity for CD38, CD16, and CD64, and moderate-high positivity for CD45 (≈ 76%) and CD36 (≈ 72%). The myeloid blasts also aberrantly co-expressed CD10 (≈ 72%), whereas they were negative for other lymphoid markers CD4, CD5, and CD56. This profile indicates an intermediate blast population with partial stem/progenitor features (CD34+), moderate myeloid differentiation (CD11b, CD45) and an aberrant lymphoid signature with CD10 expression.

Collectively, these baseline immunophenotypic profiles demonstrate a spectrum from primitive/immature (ID: 120713) to more differentiated/monocytic (ID: 130213) to intermediate with mixed features (ID: 110289), highlighting the patient heterogeneity in AML blasts at presentation.

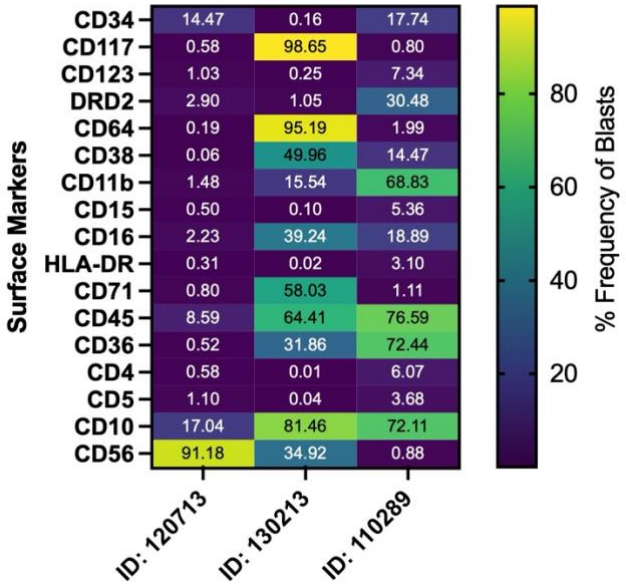

Figure 10. *Baseline Phenotype of AML Primary PBMNCs with Flow Cytometric Analysis.* Heat map depicting the percentage frequencies of blast-gated cells positive for each surface marker in the immunophenotyping panel for each patient.

3.5.3 Baseline Viability of AML Patient Samples

To ensure similar seeding of AML cells across experimental conditions, cell viability and cell counts were assessed after 1 hour of incubation in control or inhibitor media (Figure 11A, B). Viability was comparable between control and inhibited conditions for each patient, ensuring similar input across treatments. Patient ID: 120713 exhibited the lowest viability (40-50%), whereas Patients ID: 130213 and ID: 110289 had higher viabilities of 80-95%. Absolute live cell counts were normalized across conditions and comparable between control and inhibitor treatments for all three patients. This confirmed that brief equivalent numbers of viable cells were seeded in each culture condition.

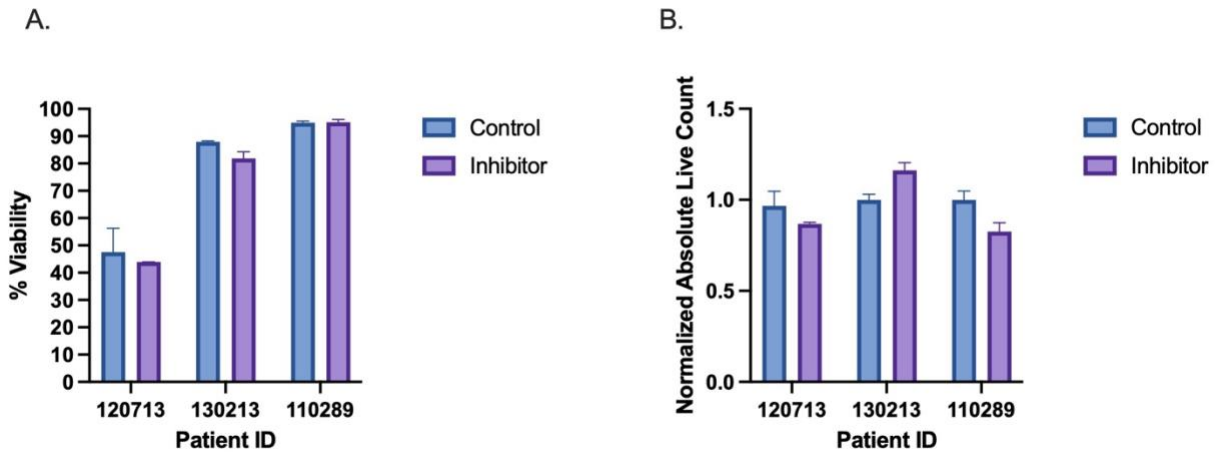

Figure 11. *Baseline Viability and Absolute Cell Count of Primary AML cells.* **(A)** Viability and **(B)** absolute live cell count of AML PBMNCs were determined by flow cytometric analysis using 7-AAD staining and volumetric counting upon one hour of CD36 inhibition after thawing cryopreserved samples. Absolute cell counts were normalized to each patient control (N=3, bars represent mean with SD). Data reported as Mean ± SD, N=3.

3.5.4 Baseline Frequencies of Stem Cell-Like Subpopulations

To determine the baseline composition of stem cell-like populations before culture, the frequencies of stem cell-like (CD34+CD38) populations in blasts were assessed. Figure 12A depicts flow cytometry plots of CD34+CD38- populations for each patient, with and without inhibition. Patient ID: 120713 had the highest frequency of CD34+CD38- cells (~7.32%; Fig. 12B). Patients ID: 130213 and ID: 110289 similarly exhibited low frequencies of CD34+CD38- cells (<1%). Notably, the frequency of CD34+CD38- cells decreased for ID: 120713 with acute inhibition (**$p<0.005$, Fig. 12B). The number of cell populations also declined, although not statistically significant (Fig. 12C). Other inhibited frequency cell subsets were similar to the control for each patient.

3.5.5 Baseline Colony-Forming Unit Potential

To assess the baseline clonogenic capacity of leukemic blasts, CFU assays were performed after one hour of incubation with or without inhibition. After 14 days of incubation, Patient ID: 120713 generated 12-13 colonies under control conditions, which were reduced to ~1 colony with acute

CD36 inhibition (Fig. 12F). In contrast, Patients ID:130213 and ID:110289 failed to produce any colonies under either control or inhibitor conditions, suggesting a lack of clonogenic potential in these samples.

3.6 Effect of CD36 Inhibition on AML Cell Viability and Proliferation

To determine whether CD36 inhibition affected the viability and proliferation of AML cells differently between PS and scaffold conditions, percent viability and absolute live cell counts were assessed by flow cytometry upon recovery after 72 hours of culture and normalized to the PS control. The viability remained relatively unchanged across conditions for each patient (Fig. 13A). However, the absolute number of blasts decreased in a patient-specific manner following CD36 inhibition, depending on the plate type. For patient ID: 120713, blast counts were significantly reduced under scaffold inhibition (*$p<0.05$, Fig. 13C). Patient ID: 130213 showed a significant reduction only under PS inhibition (****$p<0.0001$, Fig. 13Cii). For patient ID: 110289, PS inhibition led to a more pronounced reduction in blast numbers (***$p<0.001$), compared with scaffold inhibition (*$p<0.05$). When compiled and normalized to the respective plate type controls, PS inhibition had the most significant reduction in blast numbers (***$p<0.001$) than scaffold inhibition (**$p<0.01$, Fig. 13B).

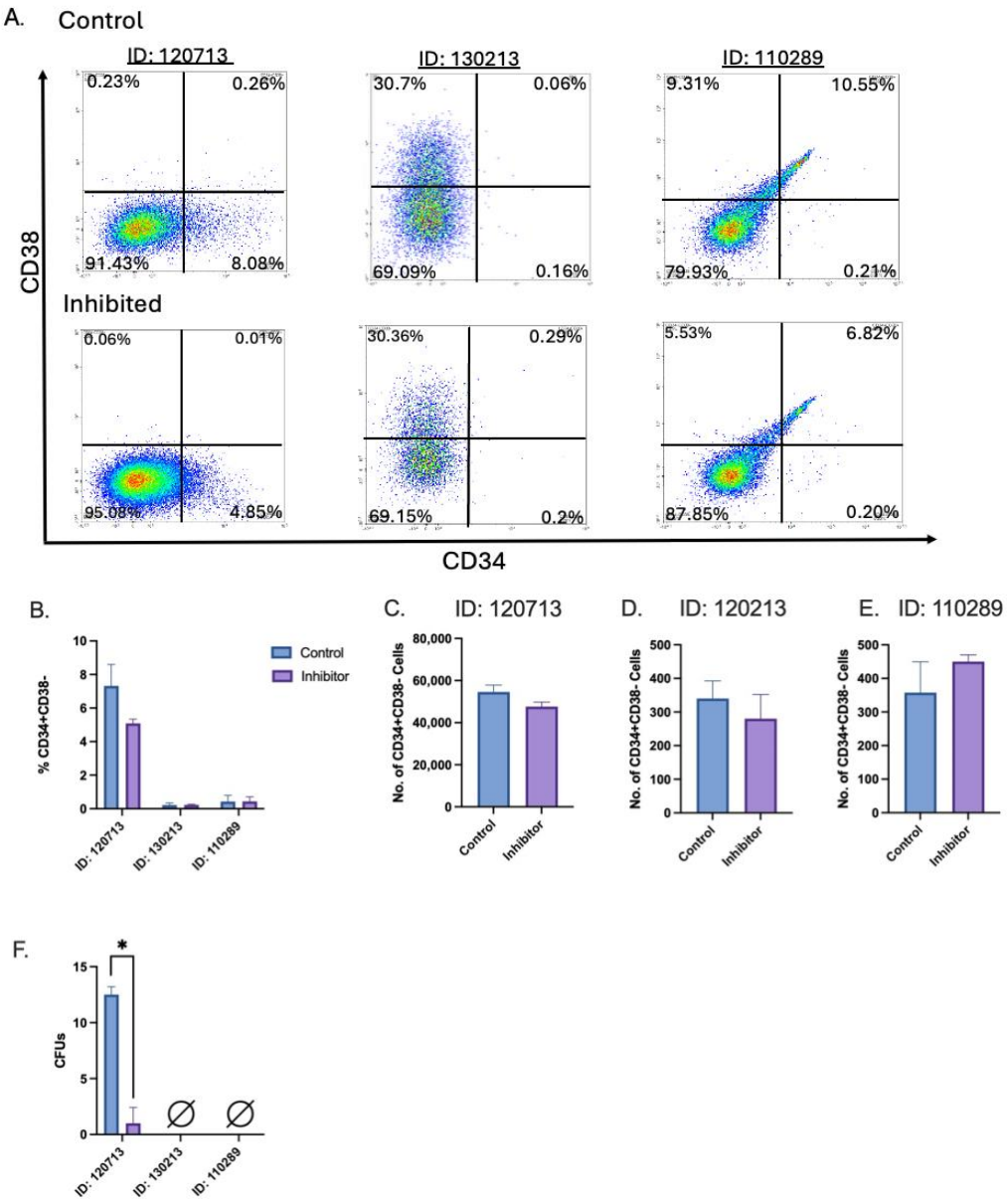

Figure 12. *Baseline Stem-like Populations and Clonogenic Capacity of Primary AML Patient Samples.* Upon thawing and incubation for one hour with 4 µg/mL of FA6-152 inhibitor, cells were stained with a panel of fluorescently conjugated antibodies and analyzed using flow cytometry. **(A)** Representative flow cytometry plots for each patient for both conditions, depicting CD34 versus CD38 marker expression (bottom left quadrant is CD34+CD38-) from live gated cells to identify primitive subsets. **(B)** Percent frequency of putative HSC-like cells (CD34+CD38-). **C-E)** Absolute cell counts of CD34+CD38- cells for each patient. **(F)** Colony-forming units (CFUs) were recorded 14 days after seeding from control or inhibited cells, following 1 hour incubation for each patient. Data reported as Mean ± SD, paired t-test two-tailed, (*)$p<0.05$, n=2.

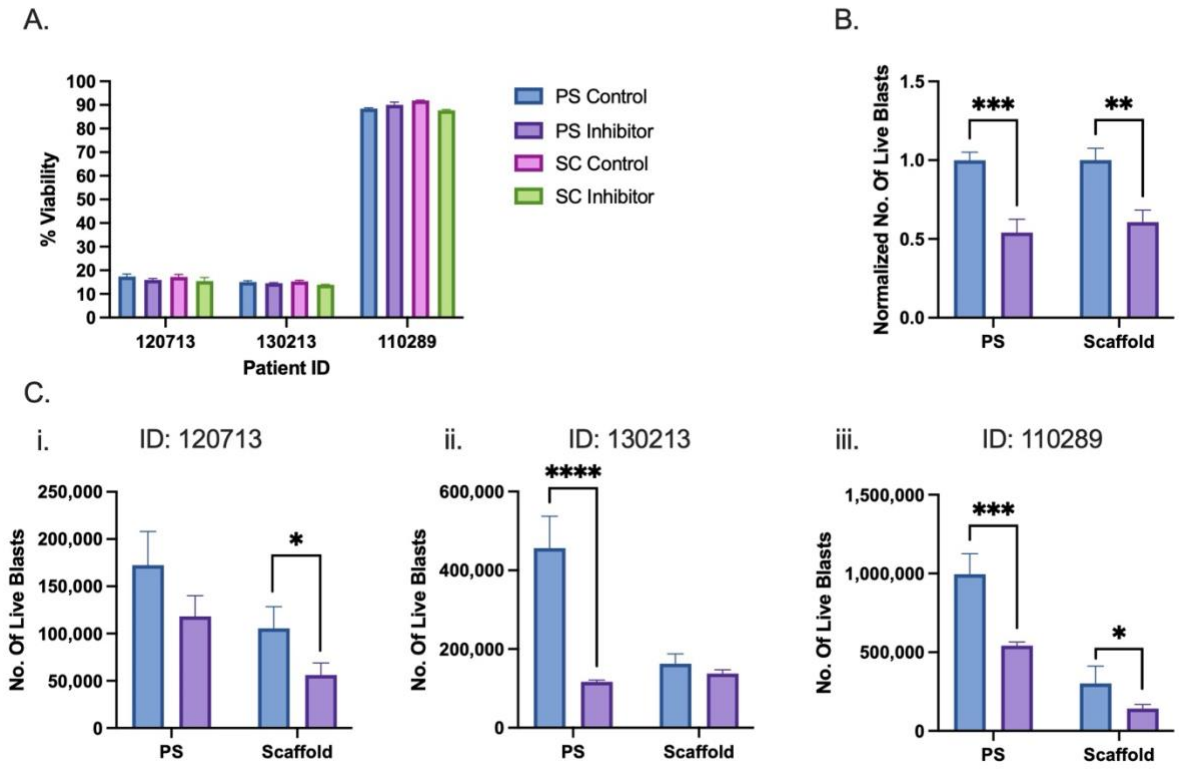

Figure 13. *Effect of CD36 Inhibition on Primary AML Cell Viability and Proliferation following 72-hour culture on PS or scaffold.* Flow cytometric analysis using 7-AAD staining was performed to assess blast cell viability and absolute live cell numbers from primary AML samples after 72 hours of culture on either PS or the ECM-based scaffold, with and without CD36 inhibition. **(A)**Percent blast viability for each patient across culture conditions. **(B)** Compiled absolute cell counts of live blasts normalized to their own respective controls. **(C)** Individual patient live cell counts were determined with volumetric counting. Data reported as Mean ± SD, N=3, Two-Way ANOVA with Šídák's multiple comparisons test, (*) $p<0.05$, (**) $p<0.01$, (***) $p<0.001$, (****) $p<0.0001$.

3.7 Effect of CD36 Inhibition on Fatty Acid Uptake

To assess the effect of CD36 inhibition on fatty acid uptake and whether it differentially affects uptake on PS or the scaffold, cells were initially stained with Bodipy upon inhibition, then cultured for 72 hours on either PS or the scaffold and subsequently recovered and analyzed by flow cytometry. Bodipy uptake was first assessed by comparing total Bodipy+ frequency, MFI, and absolute cell counts. Scaffold-cultured cells had less Bodipy frequencies and an absolute number

of Bodipy+ cells than PS-cultured cells (Fig 14A, B). With inhibition, scaffold-cultured cells exhibited a reduction in the frequency and absolute number of Bodipy+ cells when patient data were compiled (Fig. 14A, C). Patient ID: 130213 exhibited no effect with inhibition on fatty acid uptake for both PS and scaffold conditions (Fig. 14D, G). Patient ID: 120713 had a decreased reduction in the frequency of Bodipy+ cells under scaffold inhibition, and a reduction in the number of Bodipy+ cells under PS inhibition (****$p<0.0001$, Fig. 14GH) and scaffold inhibition (*$p<0.05$). Patient ID: 110289 only exhibited a reduction in the frequency of Bodipy+ cells under scaffold inhibition (***$p<0.001$, Fig. 14F). The MFI of Bodipy+ cells remained unchanged with inhibition for both PS and scaffold conditions. Collectively, these findings show that AML blasts cultured on the scaffold exhibit lower fatty acid uptake than those cultured on PS, and this reduction is further observed upon inhibition under scaffold incubation.

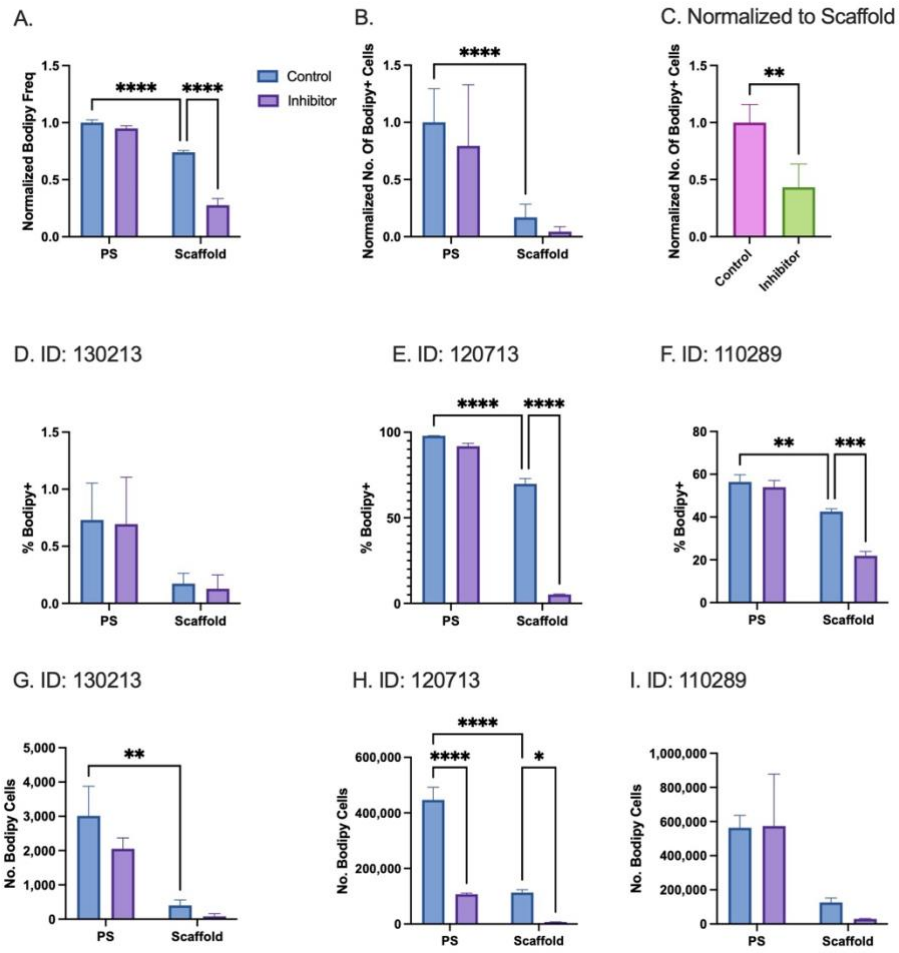

Figure 14. *Fatty Acid Uptake in Primary AML Patients with CD36 Inhibition.* Cells ± FA6-152 inhibitor were stained with Bodipy and incubated on either PS or scaffold conditions for 72 hours. Cells were then recovered for flow cytometry analysis. **(A)** Bodipy frequency normalized to each Patient's respective PS control. **(B)** Number of Bodipy+ cells normalized to each Patient's respective PS control. **(C)** Number of Bodipy+ cells normalized to each Patient's respective scaffold control. **(D-F)** Frequency of Bodipy under each condition for each patient. **(G-I)** Number of Bodipy+ cells under each condition for each patient. Data reported as Mean ± SD, N=3, Two-Way ANOVA with Šídák's multiple comparisons test, (*) $p<0.05$, (**) $p<0.01$, (***) $p<0.001$, (****) $p<0.0001$.

3.8 Effect of CD36 Inhibition on AML Phenotype

To assess whether CD36 inhibition differentially affects the phenotype of AML cells on either PS or scaffold, PBMNCs from three AML patient samples (each with technical triplicates) were cultured on either PS or scaffold conditions, with and without CD36 inhibition for 72 hours. Cells were then recovered, stained with a panel of fluorescently conjugated antibodies, and analyzed by

flow cytometry to capture live, total blast populations. For each condition, the frequency, MFI and absolute counts were normalized to the PS control (Fig. S2) and to the scaffold control (Fig. S3). Marker changes >1.5-fold were classified as significant increases, while those <0.5-fold were classified as decreases, and tallied according to whether they represented myeloid differentiation or immature phenotypes. Results were summarized for each patient individually and combined across all three patients (Tables S2-S3).

3.8.1 Variation in Phenotypic Responses Under Inhibition Across Primary AML Blasts

Each patient showed distinct trends in phenotypic frequency under inhibition, which varied depending on the plate type used for incubation. Relative to PS, Patient ID: 120713 exhibited increased frequencies of CD16 and HLA-DR under PS inhibition, suggesting myeloid activation (Fig. 16A). In contrast, scaffold control conditions showed increased CD123 and CD71, accompanied by a reduction in CD16. Scaffold inhibition relative to PS resulted in a broader reconfiguration of marker expression characterized by decreases in CD64, CD16, HLA-DR, and CD36, alongside increases in CD117 and CD123. For patient ID: 130213, CD36 inhibition and ECM culture produced broadly similar phenotypic trends across conditions. Relative to PS control, CD64 and CD16 were consistently decreased, whereas CD123, CD38, CD15, HLA-DR, CD71, and CD45 were increased under PS inhibition and both scaffold conditions. The only divergence from this pattern was a reduction in DRD2 expression observed under both scaffold conditions, with scaffold inhibition also showing reduced DRD2 cell numbers.

Patient ID: 110289 exhibited increases in CD38 and DRD2 under PS inhibition. In the scaffold control, CD15, CD123, and DRD2 were reduced, while CD38 and CD71 increased. Under scaffold inhibition, the frequencies of CD15, HLA-DR, and CD45 decreased, whereas those of CD11b, CD16, CD71, and CD11b increased.

Collectively, these data highlight the heterogeneity of phenotypic responses among patient samples and demonstrate that CD36 inhibition in the presence of an ECM scaffold elicits distinct and often more selective alterations compared to PS culture.

3.8.2 CD36 Inhibition Elicits Limited but Distinct Phenotypic Changes Within the ECM Scaffold

To determine if the phenotypic changes were significant within the scaffold system itself, data were normalized to each sample's scaffold control (Fig. 16B). Fewer phenotypic changes occurred under inhibition when the data were normalized to the scaffold than to PS. ID: 120713 only showed an increase in CD11b and CD123 frequency under inhibition. For ID: 130213, there was only an increase in CD11b across all metrics (frequency, MFI, absolute cell counts). For ID: 110289, there was an increase in CD117, CD11b, and CD16. HLA-DR was decreased in frequency, MFI and absolute counts. Overall, each patient displayed changes in unique surface markers under inhibition; however, CD11b was upregulated across all patients.

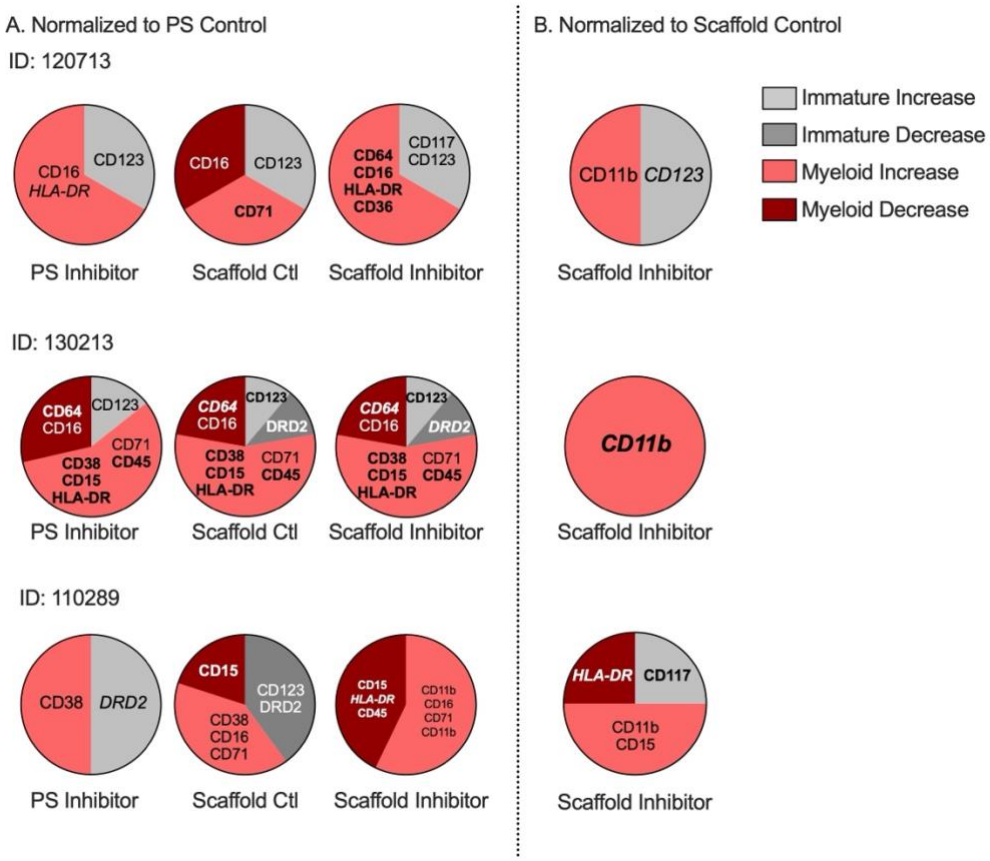

Figure 16. *Effect of CD36 Inhibition on AML Phenotype under different culture conditions.* After 72 hours of incubation ± FA6-152 inhibitor under either PS or scaffold conditions, cells were harvested and stained with a panel of markers for flow cytometric analysis. Significantly upregulated (>1.5) or downregulated (<0.5) surface marker frequencies, MFIs, and absolute counts for each patient are reported, normalized to **(A)** PS control and **(B)** scaffold control. Bolded and italicized markers indicate that the same trend was observed in MFI and absolute count parameters, respectively.

3.8.3 Upregulation of CD11b on Scaffold-Cultured Cells under Inhibition

The frequency and absolute cell count of CD11b+ blasts were analyzed due to converging trends of this surface marker being 1.5-fold higher in frequency for each patient under scaffold inhibition, relative to the scaffold control. When data were normalized to the respective plate-type controls, significant increases in CD11b frequency were observed for ID: 130213 and ID: 110289 under scaffold inhibition (Fig. 17B, C). Interestingly, the number of CD11b+ cells decreased under PS inhibition in patient ID: 110289 (Fig. 17F). Only ID: 130213 exhibited an increase in the number of CD11b+ cells under scaffold inhibition. Collectively, blasts under scaffold inhibition showed an increased frequency for CD11b (Fig. 17G); however, there was no significant difference in the number of CD11b+ cells, although an increase is apparent (Fig. 17H). There was no difference in CD11b MFI between conditions for all patients.

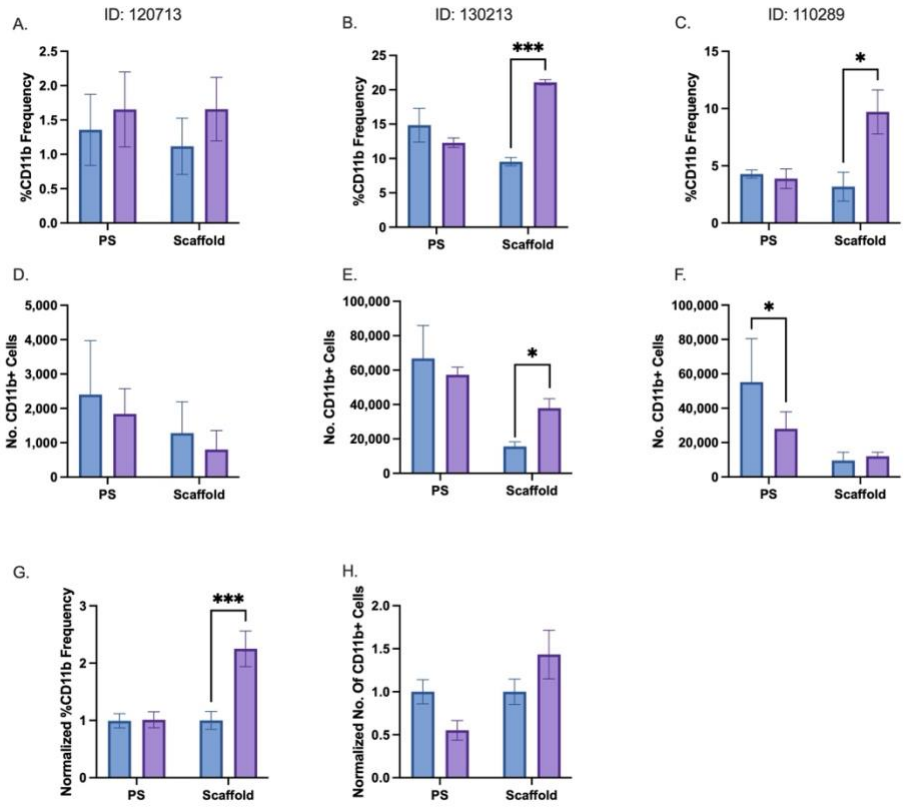

Figure 17. *Effect of CD36 Inhibition on Primary AML Myeloid Differentiation.* After 72 hours of culture on either PS or a scaffold ± CD36 inhibition, cells were recovered and stained with a panel of fluorescently conjugated antibodies for flow cytometric analysis. **(A-C)** Percent frequency of CD11b for each patient, **(D-F)** absolute number of CD11b+ cells for each patient. **(G)** Compiled frequencies and **(H)** number of CD11b+ cells of each patient normalized to the respective plate type control. Data reported as Mean ± SD, n=3, Two-Way ANOVA with Šídák's multiple comparisons test, (*) $p<0.05$, (***) $p<0.001$, (****) $p<0.0001$.

3.8.4 CD36 Inhibition Promotes Broad Myeloid Marker Increases Under PS, but Limited CD11b Upregulation within ECM Scaffold

Data were compiled for each patient to assess if CD36 inhibition had a significant effect on phenotype despite patient heterogeneity. Data were normalized according to each patient's respective conditional controls (Fig. 18A, B). Relative to each plate type control, PS inhibition exhibited a greater range of increased myeloid marker frequencies than scaffold inhibition (CD38, CD15, CD16, HLA-DR, CD71, and CD45 with PS inhibition) versus only CD11b under scaffold inhibition. In fact, scaffold data normalized to PS control also show similar increases in CD38, CD15, CD16, HLA-DR, and CD71. Relative to PS, only scaffold conditions revealed reductions of myeloid maturation markers CD64 and CD16. Overall, when data were normalized to the scaffold control, scaffold inhibition showed a more pronounced, uniform increase across the CD11b metrics.

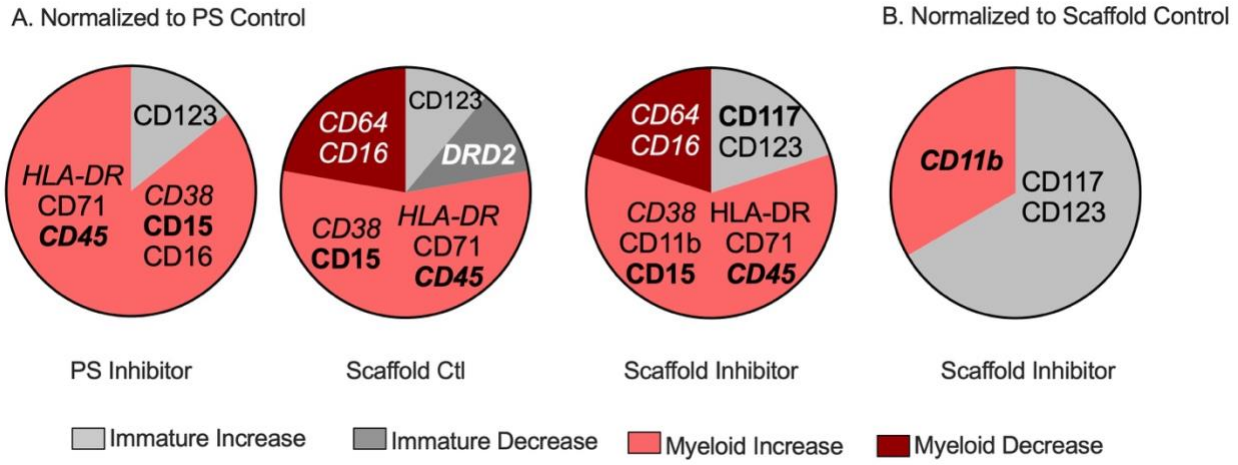

Figure 18. *Effect of CD36 Inhibition on Compiled AML Phenotype under Different Culture Conditions.* After 72 hours of incubation with a CD36 inhibitor under either PS or scaffold conditions, cells were harvested and stained with a panel of markers for flow cytometric analysis. Surface marker frequencies, MFIs, and absolute counts were compiled across 3 patients and normalized to **(A)** PS control and **(B)** scaffold control. Significantly upregulated and downregulated surface markers are annotated. Bolded and italicized markers indicate that the same trend was observed in MFI and absolute count parameters, respectively.

3.9 Effect of CD36 Inhibition on Clonogenic Potential

To evaluate whether CD36 inhibition influenced the functional clonogenic capacity of AML cells under different culture conditions, CFU assays were performed following 72 hours of incubation on either PS or scaffold with or without CD36 inhibition. After this incubation period, a portion of recovered cells from each condition was suspended in methylcellulose and colonies were recorded after 14 days of incubation.

Patient ID:120713 exhibited a marked reduction in colony formation with CD36 inhibition under both PS and scaffold conditions (Fig. 16A). In contrast, patient samples ID:130213 and ID:110289 failed to generate colonies under any condition, suggesting limited baseline clonogenic potential or loss of functional viability following *ex vivo* culture. Together, these results indicate that CD36 inhibition can suppress CFU formation in responsive samples, while the overall ability to form colonies remains patient dependent.

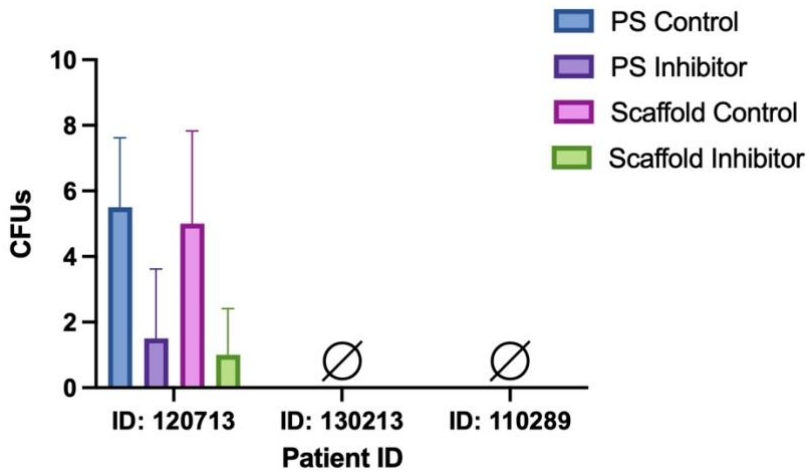

Figure 19. *Effect of CD36 Inhibition on Primary AML Clonogenic Potential.* Following 72-hours of incubation with or without CD36 inhibition, cultured on either PS or scaffold, cells were recovered and seeded for the Colony Forming Unit (CFU) assay. After 14 days of incubation, CFUs were counted and recorded.

Chapter 4: Discussion

4.1 Scaffold Efficacy

The ECM scaffold used in the study was based on a formulation previously developed and optimized by former lab members. They screened multiple combinations of collagen, elastin and hydroxyapatite to determine which composition best supported the survival and expansion of primary AML cells.

While this scaffold successfully integrates key bone marrow components and supports primary AML survival and expansion, its two-dimensional nature remains a limitation, as it cannot fully recapitulate the spatial complexity, diffusion gradients, or cell-cell interactions characteristic of a 3D marrow niche. In 2D cultures, cells experience uniform mechanical tension and unrestricted access to nutrients and oxygen, whereas 3D matrices impose physiologic gradients that more accurately mimic leukemic environments[170,171]. Moreover, this underestimates the influence of matrix porosity and stiffness on leukemic cell behaviour and drug response[172]. However, the 2D ECM system provides practical advantages such as easier imaging, washing, and cell recovery. Ongoing work in the lab is focused on optimizing cellular recovery from the 3D scaffold; however, the application has been limited by technical challenges associated with low cellular recovery, even for robust cell types such as AML OCI-2s. The denser matrix structure and reduced porosity of 3D constructs hinder the efficient retrieval of viable cells for downstream analyses, such as flow cytometry or CFU assays, thereby restricting their current experimental use. Thus, while ongoing work in the lab aims to optimize recovery from 3D scaffolds to achieve greater physiological relevance, the efficacy of the 2D ECM model was analyzed as an intermediate platform for systematic evaluation of ECM-dependent processes in AML.

Building on this foundation, the current work initially aimed to optimize the cellular recovery on ECM scaffold 6-well plates using AML OCI-2 cells, as previous experiments in the lab had only optimized recovery using a 96-well format. To standardize recovery for downstream applications which require millions of cells for analyses, the number of PBS washes (one to four) and the method of application (direct versus indirect) were systematically tested. This was to determine conditions that maximized cell yield while minimizing the risk of affecting viability and washing off scaffold debris that could interfere with analysis. Two-way ANOVA analysis demonstrated

that three washes yielded the highest recovery for both conditions, and direct washing on the well surface recovered significantly more cells than indirect side washing, particularly on the scaffold. However, PS recovery yielded nearly 2-fold more cells than from the scaffold, indicating a substantial number of cells are lost upon recovery. This warrants caution when comparing viable cell counts between the two. Although AML OCI-2 cells are classically known as a suspension line[173], these findings indicate that they exhibit measurable attachment to the ECM surface. The lower recovery from the scaffold vs PS suggests a partial adhesion of viable cells to the matrix, consistent with previous studies confirming that AML OCI-2 cells express integrin α2β1 and other β1-family heterodimers capable of binding to collagen and promoting niche-like interactions[174]. Such adhesion suggests that the ECM substrate engages authentic cell-matrix interactions rather than merely trapping cells within residual scaffold material. Together, this optimization established a robust and reproducible recovery protocol that highlights the inevitable loss of cells during recovery from the scaffold, while reinforcing the scaffold's physiological relevance for subsequent primary AML studies.

Subsequent analyses focused on determining whether scaffold culture altered immunophenotypic stability compared to PS in AML OCI-2 cells. Assessing this parameter was essential to ensure that the scaffold provided a biologically relevant yet non-perturbative environment before its application with primary patient samples. Expression of hematopoietic and myeloid surface markers (CD34, CD38, CD45, CD33, DRD2) was assessed by flow cytometry, and analysis confirmed that marker frequency and expression were similar across both conditions. This suggested that the ECM scaffold did not artificially induce differentiation, activation, or phenotypic drift independent of treatment.

CD36 frequency was also tested, and the cell line was confirmed to express high levels of CD36; however, there was a marked increase in CD36 MFI in scaffold-cultured cells. This elevation suggests that the ECM substrate influences the metabolic phenotype rather than altering their differentiation state. Given that CD36 functions as a fatty acid transporter and regulator of oxidative metabolism, its upregulation under scaffold conditions suggests that the scaffold has a capacity to elicit a more metabolically active phenotype reflective of *in vivo* behaviour. This observation provided a strong rationale for subsequent experiments testing whether CD36 inhibition elicits differential biological and therapeutic effects in primary AML cells cultured

under ECM versus PS. Collectively, the initial studies confirmed that the scaffold culture preserved phenotypic integrity over 72 hours and validated it as a suitable and supportive system for subsequent experiments testing CD36 inhibition in primary AML PBMNCs, where cell yield, survival, and phenotype are more variable and sensitive to culture conditions.

4.2.1 Scaffold Efficacy with Primary AML Cells

The genetic and clonal complexity of AML, along with the influence of the bone marrow niche, has been notorious for hindering the successful translation of preclinical findings into effective clinical strategies[175]. For instance, primary AML cells rapidly differentiate and undergo apoptosis in *ex vivo* culture without bone marrow support[176]. This presents a major experimental limitation, as the spontaneous loss of immature leukemic phenotypes *ex vivo* can mask key biological dependencies and therapeutic vulnerabilities. Therefore, whether the ECM scaffold used in these studies could effectively sustain primary AML phenotypic stability was also examined.

In primary AML cultures, scaffold conditions reduced the expression of terminal myeloid differentiation markers CD16 and CD64 relative to PS. This suggests that ECM engagement suppresses myeloid maturation. However, an inconsistency was observed, as scaffold conditions also showed an upregulation for the terminal differentiation marker CD15, indicating an increase in terminally activated monocytic lineages. This suggests that ECM-mediated effects on differentiation are not uniform and warrants caution in definitively concluding on the efficacy of this scaffold in eliciting global retention of myeloid differentiation. Regardless, for modelling AML biology, this is advantageous as it generally maintains blasts in a more primitive, stem-like state that better recapitulates *in vivo* conditions. From a therapeutic perspective, this same property underscores the ECM's role as a barrier to differentiation-based treatments. By sustaining blast-like features and suppressing most markers of terminal myeloid maturation, the ECM partially recreates this protective niche *in vitro*. It also highlights how the ECM may limit the efficacy of therapies designed to promote differentiation, as leukemic cells embedded within the matrix may remain refractory to cues that otherwise induce maturation in standard PS culture.

Furthermore, only one patient sample yielded colonies for CFU analysis, limiting the ability to draw definitive conclusions about whether the scaffold enhanced clonogenic capacity across

samples. For this patient, CFU numbers were comparable between PS and ECM conditions, suggesting that under the tested parameters, the scaffold did not markedly alter colony-forming potential. Assessing CFU potential in the additional patient samples with higher CD36 expression would have been extremely valuable for determining whether the scaffold provides a supportive environment for maintaining clonogenic capacity in different AML subsets.

Additionally, the number of primary AML cells recovered from the scaffold was substantially lower than from PS. This introduces uncertainty in evaluating scaffold-mediated proliferation, as it remains unclear whether reduced recovery reflects impaired expansion or incomplete retrieval. Given that cells may remain embedded within the ECM matrix despite multiple washing steps, the absolute proliferative capacity of scaffold-cultured cells cannot be fully resolved from these data. However, viabilities were largely equivalent between PS and scaffold conditions, indicating that the reduced yield reflects limitations in cell retrieval rather than increased cell death. Thus, the scaffold may still support survival to a similar extent as PS, but incomplete retention of cells within the matrix likely obscures an accurate assessment of proliferative output.

4.3 Patient Heterogeneity and CD36 Expression

The complex genetic nature and heterogeneity of AML have historically posed challenges for identifying suitable therapeutic targets[177]. Patient samples were selected for this study at random, with no prior information provided on AML subtype, treatment history, or patient age/gender. Although this lack of stratification limited the ability to associate responses with specific genetic or clinical backgrounds, it provided an unbiased and *ex vivo* representation of AML heterogeneity.

The baseline immunophenotypes were analyzed by flow cytometry in the absence of cytogenetic or molecular analyses. This limited the ability to definitively assign FAB or WHO classifications to each patient. Nonetheless, substantial inter-patient heterogeneity was evident across the three patient samples in both lineage-associated and aberrant marker expression.

Patient ID: 120713 displayed a predominantly immature profile, as the blasts lacked antigens associated with myeloid and monocytic maturation; however, they exhibited strongly aberrant CD56 positivity, even though they co-expressed the myeloid antigen CD33. Hence, this sample most closely resembles leukemic blasts with minimal differentiation (FAB-M0) or AML with no

maturation (FAB-M1)[85]. Patient ID: 130213 demonstrated a profile indicative of moderate monocytic differentiation characterized by CD117+, CD64+, CD38+, CD71+, CD16+ and intermediate CD11b expression. However, the blasts also aberrantly co-expressed CD10, rendering classification difficult. Although the overall marker profile closely resembles an M4 subtype[178], definitive diagnosis as mixed-phenotype acute leukemia (MPAL) would require confirmation of strong CD19 expression[179], which was not included in this panel. Patient ID: 110289 exhibited a more partial myeloid profile (largely positive for CD11b, CD45, intermediate CD64, CD16 and CD38 expression) with aberrant CD10 expression as well.

Notably, the frequency of CD36 expression varied markedly across patient samples, ranging from 0.52% in the most immature case (ID:120713) to 35% and 72% in the more differentiated samples. This trend reflects previously reported subtype-specific differences in CD36, where expression is lowest in immature subtypes (M0-M1), moderate in myelomonocytic cases (M4), and highest in monocytic and erythroid forms (M5-M6)[180,181]. It is reasoned that CD36 expression increases as progenitors commit to the monocytic lineage[181]. Additionally, CD36 upregulation accompanies monoblastic differentiation but not granulocytic maturation, reflecting its constitutive role in the monocyte lineage. In this study, the lowest CD36 expression was associated with the highest CD34+CD38- frequencies (most stem cell-like), whereas samples with higher CD36 frequency contained <1% of this fraction.

Only one other study has examined the impact of CD36 in primary AML blasts with low CD36 expression. Wegmann et al. (2024) reported that treatment with the CD36-blocking antibody FA6-152 had no measurable effect on viability or proliferation in the low-CD36 sample tested, while significant reductions were observed in the CD36-high cases[182]. However, that work was limited to examining viability after 24 hours and did not explore the functional or metabolic consequences. In contrast, the present study extends these findings by including patient ID 120713, thereby broadening the functional relevance across heterogeneous AML cases.

4.4 Effect of CD36 Inhibition on AML Clonogenic Capacity

While viability or metabolic assays can quantify surviving cells, they do not reveal whether leukemic progenitors retain the capacity for clonogenic self-renewal, which is a key attribute of

these disease-propagating cells. CFU assays, therefore, serve as critical assays that allow the quantification of progenitor self-renewal capacity and have been suggested to predict AML patient survival[184]. The ability of blasts to generate colonies reflects their clonogenic potential to propagate disease and contribute to relapse, rendering CFU assays a powerful tool for measuring functional stemness. Accordingly, the present study employed this assay to determine whether CD36 inhibition could attenuate clonogenic potential in AML, and to assess the influence of the ECM scaffold on this response.

After 72 hours of incubation, AML OCI-2 cells cultured on the scaffold exhibited a more pronounced reduction in CFUs than PS with inhibition. This trend suggests that the ECM amplifies CD36-dependent signalling pathways involved in fatty acid metabolism, rendering scaffold-cultured cells more susceptible to metabolic disruption upon inhibition, thereby affecting their clonogenic potential. In contrast, PS-cultured cells appeared less dependent on CD36 activity for clonogenic growth, highlighting the contextual importance of the ECM microenvironment.

Among the primary AML patient samples, only ID: 120713 produced CFUs at both baseline and post-72-hour treatment, whereas the others did not. CFU output from ID: 120713 decreased across both PS and scaffold conditions following inhibition, suggesting that functional leukemic progenitors within this sample rely at least in part on CD36-mediated metabolic processes to sustain colony formation.

The reduction of CFUs with CD36 inhibition aligns with prior studies implicating lipid-uptake pathways in regulating hematopoietic potential. Meng et al. (2023) demonstrated that HSPCs isolated from CD36-KO mice generated approximately 40% fewer colonies than WT controls, despite similar progenitor frequencies[185]. Similarly, a study conducted by Zhang et al. (2020) reported that knocking out apolipoprotein C2 (APOC2, a lipid handling protein that activates the CD36-ERK signalling axis) significantly reduced CFU formation in primary AML blasts[156]. However, they did not directly assess CFU output following CD36 inhibition itself, leaving the specific contribution of CD36 inhibition to leukemic clonogenic capacity unresolved. The present findings therefore fill an important gap, by directly linking pharmacologic inhibition of CD36 to diminished CFU output in both AML cell lines and primary blast cultures. This reinforces the

suggestive role of CD36 contributing to sustaining leukemic progenitor function, especially in the ECM context.

The lack of clonogenic output from the other two patient samples may indicate prior chemotherapy exposure and disease adaptation, as these samples had higher CD36 blast frequencies than ID: 120713. Elevated CD36 expression has repeatedly been associated with chemotherapy-resistant and quiescent leukemic populations that persist following treatment[186]. This interpretation is further supported by the findings of Farge et al. (2023), who have shown that post-chemotherapy residual AML blasts are enriched for CD36+ cells that maintain mitochondrial activity yet lack proliferative capacity[136]. Consistent with this, Canizo et al. (1996) demonstrated that AML patients who relapsed displayed diminished or dysregulated colony formation[187]. Hence in this context, the inability of CD36-high samples to form CFUs likely reflects a functionally exhausted or senescent progenitor pool, which is characteristic of post-treatment leukemic blasts. Another explanation could be that the samples contained extremely low frequencies of supposed immature progenitors or stem cell-like cells at baseline (<1% CD34+CD38-). In contrast, ID: 120713 had a higher proportion of this primitive population (7.32%). Given the rarity of such cells in the other samples, it is possible that the small subset of true leukemic progenitors was either below the detection threshold or lost during CFU seeding, leading to an apparent absence of colonies. This interpretation aligns with established findings that clonogenic capacity in AML predominantly resides within the CD34+CD38- compartment[188].

4.5 Effect of CD36 Inhibition and ECM Scaffold on Fatty Acid Uptake

AML cells exhibit remarkable metabolic plasticity, which enables them to survive under fluctuating nutrient and stress conditions in the bone marrow niche[188]. One of their main adaptations is switching from glycolysis to fatty acid oxidation and oxidative phosphorylation to meet their high metabolic demands[190]. AML blasts scavenge fatty acids released by bone marrow adipocytes and utilize them for fatty acid oxidation to fuel the TCA cycle and oxidative phosphorylation. While prior studies conducted by Farge et al. had concluded that inhibiting CD36 using the FA6-152 inhibitor does not impair fatty acid uptake in AML (suggesting that CD36 was dispensable for FA uptake), the study was conducted in normal media (not starved cells), which agrees well with our preliminary results showing that there is no difference in lipid uptake in basal

media. However, we also serum-starved the cells and demonstrated that the extracellular context modulates fatty acid uptake to a greater extent than PS. This was first evident with the initial testing of FA6-152 on the AML OCI-2 cell line. After 72 hours of incubation, cells cultured on the ECM scaffold with FA6-152 inhibition showed a greater reduction in fatty acid uptake than cells cultured on PS (as indicated by fewer Bodipy^{hi} cells).

Furthermore, scaffold-cultured cells exhibited reduced viability and proliferation, whereas PS-cultured cells remained unaffected under the same conditions. CFUs were reduced under inhibition for scaffold-cultured cells, although the difference was not statistically significant. These findings are comparable to those of Zhang et al., who treated THP-1 and MOLM-13 cells with FA6-152 and observed reductions in Bodipy staining and cell proliferation after 4 days of culture[156]. Therefore, these preliminary findings suggest that ECM-associated cues sensitize AML OCI2 cells to CD36 inhibition to a greater extent than PS. This provided a promising platform for evaluating the inhibitor with primary AML samples, considering the metabolic vulnerability of AML was further unmasked under physiologically constrained ECM conditions.

Across all three primary AML samples, fatty acid uptake was consistently lower for scaffold-cultured cells compared to PS-cultured cells. These findings suggest that the ECM plays a role in altering lipid metabolism in AML, which can be explained by several factors. For instance, this may be a consequence of altered mechanotransductive signalling in softer, matrix environments. Softer ECM conditions have been shown to reduce actomyosin contractility and cytoskeletal tension, which in turn modify Golgi mechanical stiffness that suppresses lipin-1 activity, ultimately reprogramming lipid metabolism towards lipid synthesis and storage rather than uptake[191]. Furthermore, a recent study showed that AML cells robustly uptake collagen, which supports their glycolytic metabolism and colony-forming capacity[191]. This indicates that ECM-derived substrates themselves can influence metabolic preference and aligns well with our findings that fatty acid uptake is lowered in the absence of ECM. While the interactions between BM niche adipocytes and fatty acid uptake in AML are well documented, no prior study has directly compared lipid uptake or FAO gene expression in AML blasts cultured on ECM scaffolds versus conventional PS culture. The present data, therefore, fill an important mechanistic gap by showing that ECM composition can directly influence lipid metabolism; however, transcriptomic profiling

and metabolic studies will be necessary to define the specific pathways underlying this ECM-mediated metabolic shift.

Notably, CD36 inhibition reduced fatty acid uptake mainly under scaffold conditions for AML OCI-2s, and for some primary patient samples. The patient-specific responses further highlight the metabolic diversity within AML. Patient ID: 130213 showed no measurable effect of CD36 inhibition, which can be attributed to the fact that this was the sample with the least amount of CD36 expression, and a very low frequency of cells taking up fatty acids, even under control conditions. In contrast, patient ID: 120713 displayed marked reductions in Bodipy+ cell numbers under both PS and scaffold inhibition, suggesting a stronger reliance on CD36-mediated fatty acid uptake. Patient ID: 110289 exhibited reductions under only scaffold conditions, implying that ECM interactions can unmask CD36 dependence not evident on PS. These divergent phenotypes reinforce the concept that different AML subtypes respond differentially to treatments, highlighting the need for personalized treatment in AML. The MFI of bodipy remained unchanged, suggesting that inhibition primarily decreased the fraction of cells capable of fatty acid uptake rather than uniformly lowering per-cell uptake levels. Unlike PS, ECM scaffolds introduce biologically relevant ligands that activate integrin and non-integrin-mediated signalling, each of which is known to promote lipid metabolism[193]. Although reduced fatty-acid uptake indicates a shift in metabolic state, the present data cannot determine which metabolic program AML blasts adopt, if any occur, when CD36-mediated lipid uptake is inhibited. Without direct metabolic measurements, it remains unclear whether cells compensate by altering mitochondrial activity, increasing glycolytic flux, or using alternative nutrient pathways. Comprehensive metabolic profiling would be necessary to definitively characterize whether and how CD36 inhibition reprograms metabolism within the scaffold microenvironment. Regardless, these findings indicate that even a 2D ECM microenvironment can restore essential biochemical cues, revealing CD36-dependent vulnerabilities that were otherwise masked in traditional PS culture.

4.6 Effect of CD36 Inhibition on Primary AML Proliferation and Viability

Assessment of CD36 inhibition across PS and scaffold conditions revealed substrate-dependent differences in cellular proliferation. While cell viability did not differ significantly across conditions, total live cell counts for ID:130213 and ID:110289 were reduced under PS inhibition,

and those for ID:120713 and ID:110289 were reduced under scaffold inhibition. Overall, cell proliferation was reduced more on PS than on the scaffold. This data indicates that the ECM scaffold plays a protective role for AML proliferation under suppressed lipid uptake (and potential metabolic stress) relative to PS.

4.7 Phenotype Analysis

Recent work has focused on targeting metabolic dependencies that AML cells exploit with the aim of inducing AML cell differentiation[194]. Classically, retinoic acid and arsenic trioxide have been therapeutically effective in treating acute promyelocytic leukemia (APL) by inducing terminal differentiation and apoptosis of leukemic promyelocytes without chemotherapy[195,196]. Unfortunately, this application has not been effectively translated into clinical benefit for other non-APL subtypes in AML[197]; however, research is still ongoing. To date, most evidence linking metabolic inhibition to AML differentiation has come from studies targeting OxPhos rather than fatty-acid uptake. For example, Shao et al. (2023) showed that inhibiting an OxPhos regulator facilitates the therapeutic differentiation of AML cells and eradicates AML blasts in relapsed/refractory leukemia[198]. They observed that transcription factors regulating terminal differentiation were specifically upregulated after inhibition, suggesting that the decline of OxPhos might be an important force driving terminal myeloid differentiation. The existing FAO-related literature in this context is limited. For example, inhibition of intracellular lipid-chaperoning pathways such as FAB4 has been shown to impair the proliferative rate of leukemia cells by inducing cell differentiation as seen by upregulated CD11b expression[199]. However, studies that specifically block fatty acid uptake have predominantly reported effects on viability, metabolic stress, or leukemic engraftment rather than clear differentiation phenotypes. As a result, whether restricting fatty-acid availability alone can induce myeloid maturation in AML remains largely unexplored. Extending this concept, the present study investigated whether targeting CD36-mediated lipid uptake, especially in an ECM environment, can similarly promote phenotypic maturation.

CD36 inhibition and ECM culture produced patient-specific phenotypic variations. Additionally, when comparing the effect of CD36 inhibition across substrates, a clear divergence emerged between PS and scaffold cultures. PS inhibition elicited a broad upregulation of myeloid

maturation markers (CD38, CD15, CD16, HLA-DR, CD71, and CD45) alongside CD123. In contrast, scaffold inhibition produced a far narrower response, limited to an increase in CD11b frequency, along with CD123 and CD117. This contrast suggests that the ECM microenvironment restricts the phenotypic plasticity of AML blasts while fatty acid uptake is reduced.

Furthermore, the finding of increased CD71 frequencies for patient samples (ID: 120713 and ID: 110289) exclusively in scaffold control conditions relative to PS aligns with the notion that CD71 is significantly increased in rapidly proliferating cells[200]. This provides further reinforcement that AML utilizes the ECM for survival and proliferation.

For patient ID: 130213, both scaffold control and inhibited conditions showed the same directional trends in myeloid marker expression as PS inhibition, when normalized to the PS control. This was characterized by decreased frequencies of CD64 and CD16, indicating suppressed myeloid maturation, and increased frequencies of CD38, CD15, CD71, and CD45, suggesting a more generalized activation or partial maturation profile. This consistency indicates that the phenotypic changes induced by CD36 inhibition of PS largely mirror those elicited by ECM engagement. However, when analyzed within the scaffold context, only CD11b was increased under inhibition. This suggests that while the ECM drives outcomes like those of CD36 inhibition (with PS), it also imposes a constrained phenotype, with only CD11b upregulated.

Additionally, the only divergence seen was that DRD2 frequencies were reduced under both scaffold conditions relative to PS, but the number of DRD2+ cells decreased with scaffold inhibition. Interestingly, this patient uniquely lacked the CD11b upregulation observed in the other under scaffold conditions when normalized to PS. This pattern suggests that decreased DRD2 may be associated with diminished matrix adhesion in this context. However, evidence connecting DRD2 to ECM-mediated adhesion is limited, having been demonstrated only in T cells through β1-integrin activation of fibronectin substrates (an ECM component not included in the present scaffold system)[201]. As such, a definitive mechanistic explanation for this trend remains unclear. Notably, when data were normalized to the scaffold control, DRD2+ frequencies remained unchanged under inhibition, indicating that the observed reduction relative to PS primarily reflects an ECM-associated effect rather than a direct consequence of CD36 inhibition.

To determine whether CD36 inhibition affects phenotype within the scaffold system itself, collective data normalized to the scaffold control showed increased CD11b frequency. CD11b characterizes both granulocytic and monocytic differentiation. It also pairs with CD18 to form the integrin Mac-1, which facilitates leukocyte attachment to the ECM[202]. Hence, the observed increase in CD11b frequency under scaffold-inhibition conditions suggests that CD36 inhibition promotes myeloid differentiation and stronger attachment to the ECM while fatty acid uptake is blocked. However, it would have been beneficial to confirm the true pairing between the two by including a fluorescently conjugated antibody specific for Mac-1 for phenotypic analysis. Regardless, the observed increase of CD11b expression aligns with multiple prior studies that have inhibited various aspects of metabolism connected to oxidative phosphorylation, leading to CD11b upregulation and decrease of stemness in AML[203,204]. Furthermore, this finding emerged particularly among patients with higher CD36 expression, suggesting that CD36 inhibition is more effective in AML subtypes with higher CD36 expression. Additionally, CD11b is required to sustain MAPK activation in AML[205].This suggests that ECM interactions may amplify CD11b-driven MAPK signalling as a compensatory survival mechanism when lipid uptake through CD36 is impaired. Furthermore, this phenotype represents a therapeutically exploitable vulnerability, whereby combining CD36 inhibition with agents disrupting CD11b signalling could enhance antileukemic efficacy.

Additionally, CD117 was also upregulated amongst the compiled patients exclusively under scaffold inhibition. CD117 is a well-established marker of immature myeloid progenitor cells and less differentiated blasts in AML[206]. However, it functionally serves as a receptor for SCF, activating PI3K/Akt, MAPK/ERK, and STAT signalling pathways, all of which contribute to enhanced cell survival, metabolic adaptation, and proliferative signalling[207]. Thus, the consistent upregulation of CD117 under scaffold inhibition may reflect a compensatory reliance on ECM-supported CD117 signalling. This interpretation aligns with the earlier observation that scaffold-cultured cells were less affected by a reduction in proliferation than the PS-inhibited counterparts. Hence, it is plausible that CD117 upregulation may represent a compensatory mechanism by which the ECM helps AML cells resist proliferative loss under CD36 inhibition, by shifting reliance from lipid-uptake pathways towards CD117-driven growth signals. While CD117 upregulation does not directly equate to increased proliferation, the data suggest that the ECM

context reinforces this signalling under inhibition, thereby modulating proliferative capacity and survival under metabolic stress. Further functional studies, such as co-inhibition of CD117 with CD36, are required to confirm this compensatory axis as a therapeutic vulnerability.

Furthermore, CD123 was consistently upregulated across all patient samples following inhibition in both PS and scaffold conditions. CD123 is the alpha chain of the IL-3 receptor, which is widely expressed on early AML progenitors and cytokine-responsive blast populations[208]. Unlike the scaffold-specific increase in CD117, the universal elevation of CD123 across both plate substrates reveals a core, microenvironment-independent adaptive response to metabolic stress induced by CD36 inhibition. The IL3-/CD123 axis activates the JAK2/STAT5[209], PI3K/Akt[210], and MAPK[211] pathways, which regulate key leukemic functions, including anti-apoptotic survival, cytokine-driven proliferation, cell cycle progression, metabolic support, and resistance to oxidative and nutrient stress[212]. These survival and growth pathways likely underlie a plausible mechanism by which AML cells adapt to CD36 inhibition to amplify compensatory survival signalling.

Chapter 5. Concluding Remarks

5.1 Conclusion

The bone marrow niche is a dynamic, tightly regulated microenvironment that maintains hematopoietic cells through coordinated cues that balance self-renewal, proliferation, and differentiation. AML disrupts this equilibrium by co-opting the cellular and extracellular components of the niche to promote leukemic survival at the expense of healthy hematopoiesis. Among these components, the ECM plays a critical role in shaping leukemic behaviour through its structural proteins and biochemical signals. Alterations in ECM composition and stiffness have been increasingly linked to therapy resistance, metabolic adaptation, and leukemic persistence, highlighting their emerging role as determinants of disease progression.

In recent years, CD36 has gained recognition as a metabolic vulnerability in AML due to its role in mediating fatty acid uptake, thereby contributing to metabolic adaptations that support survival and chemoresistance. However, despite evidence that CD36 inhibition can reduce leukemic engraftment and survival *in vivo*, the influence of the ECM on CD36-dependent metabolic processes has remained unexplored. The current study addressed this gap by investigating how ECM interactions modulate CD36-mediated lipid uptake and cellular responses in AML. By culturing both primary AML blasts and the AML OCI-2 cell line on an ECM-based scaffold and subjecting them to CD36 inhibition, this work represents the first attempt to examine the interplay between ECM engagement and lipid metabolic dependencies in AML.

Using a multi-model cellular analysis, this study provides the first evidence that ECM interactions significantly modulate CD36-mediated responses. Despite inter-patient heterogeneity, several phenotypic trends converged when compiled. Scaffold-cultured primary AML cells exhibited a greater reduction in fatty acid uptake yet a less pronounced decline in proliferation. This suggests that ECM interactions may buffer the metabolic stress induced by CD36 inhibition. Additionally, the exclusive upregulation of CD117 across primary samples under scaffold inhibition suggests a compensatory shift towards pro-survival/proliferative signalling in response to lipid restriction. In contrast, CD123 was globally upregulated in both PS and scaffold conditions under inhibition, likely reflecting enhanced cytokine responsiveness mediated through pro-survival pathways to

maintain survival under metabolic stress. Furthermore, the observed global increase in CD11b under scaffold inhibition across all three primary patient samples indicates an increased reliance on cell-matrix adhesion, which may provide compensatory survival and proliferative signalling. Thus, the ECM itself represents a co-targetable component which yields further investigation. Additionally, the upregulation of CD11b also suggests myeloid differentiation, a process leveraged in differentiation-based therapies.

Furthermore, the scaffold culture partially suppressed myeloid differentiation compared to PS, which is crucial for physiologically relevant models to maintain the primitive leukemic phenotype *ex vivo*. This offers greater biological insights into leukemic pathology and response to CD36 inhibition than traditional PS screening.

Together, these findings demonstrate that ECM interactions critically shape CD36-dependent metabolic and phenotypic responses in AML. It further reveals the implication of activated compensatory pathways to mitigate metabolic stress, which emphasizes the need for combinatorial strategies that disrupt both metabolic and environmental survival cues. While promising, the ECM model requires further refinement and mechanistic validation to strengthen its translational relevance.

5.2 Limitations and Future Directions

The experiments conducted serve merely as an initial step towards interrogating how the ECM modulates CD36-mediated lipid uptake in AML. A significant limitation of this study was the inability to conclusively confirm the detailed mechanistic changes in metabolism and functional myeloid maturation induced by CD36 inhibition. Moving forward, RNA sequencing analysis should be first performed for AML OCI-2 cells to validate and further characterize the metabolic and survival mechanisms underlying ECM-interactions with CD36. RNA sequencing was intended for primary AML samples; however, there was a lack of viable primary cells recovered after 72 hours of culture, even within the scaffold system. This limited the feasibility of other downstream analyses, such as RNA sequencing or metabolic flux profiling. Future work with primary samples should therefore either prioritize 1) optimizing the ECM scaffold to enhance

leukemic cell expansion and survival during extended culture periods for additional studies, or 2) focus on utilizing primary AML cell culture for extended metabolic studies and RNA sequencing analysis under CD36 inhibition. Additional niche components, such as hyaluronic acid, fibronectin, and laminin, should be incorporated to further recapitulate the native bone marrow niche. Also, co-culturing primary AML cells with adipocytes would better prevent spontaneous differentiation and further elucidate how niche-derived lipids and matrix interactions jointly regulate leukemic metabolism and survival under treatment pressure.

Furthermore, metabolic studies can provide insights into whether glycolysis or oxidative phosphorylation is differentially perturbed when cells are cultured on PS or the ECM scaffold under CD36 inhibition. Transcriptomic profiling would elucidate an ECM signature and molecular pathways downstream of CD36 that sustain FAO metabolism and survival in AML. It would also importantly confirm proper functional myeloid maturation under inhibition.

Additionally, future studies should investigate whether the ECM confers a protective advantage to AML cells under CD36 inhibition by fostering chemotherapy resistance. Specifically, assessing drug response profiles in scaffold-cultured versus PS-cultured AML cells following CD36 inhibition would help determine if ECM engagement mirrors the sensitizing effects conducted by others *in vivo*. Validating such results can promote standardization in using the ECM scaffold as an effective preclinical screening tool rather than PS.

References

1. Till JE, McCULLOCH EA. A direct measurement of the radiation sensitivity of normal mouse bone marrow cells. *Radiat Res*. 1961;14:213-222.

2. Seita J, Weissman IL. Hematopoietic stem cell: self-renewal versus differentiation. *WIREs Syst Biol Med*. 2010;2(6):640-653. doi:10.1002/wsbm.86

3. Bolkent S. Cellular and molecular mechanisms of asymmetric stem cell division in tissue homeostasis. *Genes Cells*. 2024;29(12):1099-1110. doi:10.1111/gtc.13172

4. Laurenti E, Göttgens B. From haematopoietic stem cells to complex differentiation landscapes. *Nature*. 2018;553(7689):418-426. doi:10.1038/nature25022

5. Akashi K, Traver D, Miyamoto T, Weissman IL. A clonogenic common myeloid progenitor that gives rise to all myeloid lineages. *Nature*. 2000;404(6774):193-197. doi:10.1038/35004599

6. Kondo M, Weissman IL, Akashi K. Identification of Clonogenic Common Lymphoid Progenitors in Mouse Bone Marrow. *Cell*. 1997;91(5):661-672. doi:10.1016/S0092-8674(00)80453-5

7. Spangrude GJ, Heimfeld S, Weissman IL. Purification and characterization of mouse hematopoietic stem cells. *Science*. 1988;241(4861):58-62. doi:10.1126/science.2898810

8. Vo LT, Daley GQ. De novo generation of HSCs from somatic and pluripotent stem cell sources. *Blood*. 2015;125(17):2641-2648. doi:10.1182/blood-2014-10-570234

9. Vo LT, Daley GQ. De novo generation of HSCs from somatic and pluripotent stem cell sources. *Blood*. 2015;125(17):2641-2648. doi:10.1182/blood-2014-10-570234

10. Lee-Thedieck C, Schertl P, Klein G. The extracellular matrix of hematopoietic stem cell niches. *Adv Drug Deliv Rev*. 2022;181:None. doi:10.1016/j.addr.2021.114069

11. Fröbel J, Landspersky T, Percin G, et al. The Hematopoietic Bone Marrow Niche Ecosystem. *Front Cell Dev Biol*. 2021;9:705410. doi:10.3389/fcell.2021.705410

12. Kfoury Y, Scadden DT. Mesenchymal cell contributions to the stem cell niche. *Cell Stem Cell*. 2015;16(3):239-253. doi:10.1016/j.stem.2015.02.019

13. Mehrasa R, Vaziri H, Oodi A, et al. Mesenchymal stem cells as a feeder layer can prevent apoptosis of expanded hematopoietic stem cells derived from cord blood. *Int J Mol Cell Med*. 2014;3(1):1-10.

14. Almalki SG, Agrawal DK. Key Transcription Factors in the Differentiation of Mesenchymal Stem Cells. *Differ Res Biol Divers*. 2016;92(1-2):41-51. doi:10.1016/j.diff.2016.02.005

15. Jones DL, Wagers AJ. No place like home: anatomy and function of the stem cell niche. *Nat Rev Mol Cell Biol*. 2008;9(1):11-21. doi:10.1038/nrm2319

16. Nakamura Y, Arai F, Iwasaki H, et al. Isolation and characterization of endosteal niche cell populations that regulate hematopoietic stem cells. *Blood*. 2010;116(9):1422-1432. doi:10.1182/blood-2009-08-239194

17. Perlin JR, Sporrij A, Zon LI. Blood on the tracks: hematopoietic stem cell-endothelial cell interactions in homing and engraftment. *J Mol Med Berl Ger*. 2017;95(8):809-819. doi:10.1007/s00109-017-1559-8

18. Gattazzo F, Urciuolo A, Bonaldo P. Extracellular matrix: A dynamic microenvironment for stem cell niche. *Biochim Biophys Acta*. 2014;1840(8):2506-2519. doi:10.1016/j.bbagen.2014.01.010

19. Krause DS, Scadden DT, Preffer FI. The hematopoietic stem cell niche—home for friend and foe? *Cytometry B Clin Cytom*. 2013;84B(1):7-20. doi:10.1002/cyto.b.21066

20. Lu P, Weaver VM, Werb Z. The extracellular matrix: A dynamic niche in cancer progression. *J Cell Biol*. 2012;196(4):395-406. doi:10.1083/jcb.201102147

21. Gross J, Lapiere CM. COLLAGENOLYTIC ACTIVITY IN AMPHIBIAN TISSUES: A TISSUE CULTURE ASSAY*. *Proc Natl Acad Sci U S A*. 1962;48(6):1014-1022.

22. Wells RG. The role of matrix stiffness in regulating cell behavior. *Hepatology*. 2008;47(4):1394-1400. doi:10.1002/hep.22193

23. Gattazzo F, Urciuolo A, Bonaldo P. Extracellular matrix: A dynamic microenvironment for stem cell niche. *Biochim Biophys Acta BBA - Gen Subj*. 2014;1840(8):2506-2519. doi:10.1016/j.bbagen.2014.01.010

24. Xiong J, Balcioglu HE, Danen EHJ. Integrin signaling in control of tumor growth and progression. *Int J Biochem Cell Biol*. 2013;45(5):1012-1015. doi:10.1016/j.biocel.2013.02.005

25. Tzaphlidou M. The role of collagen in bone structure: An image processing approach. *Micron*. 2005;36(7):593-601. doi:10.1016/j.micron.2005.05.009

26. Ricard-Blum S. The Collagen Family. *Cold Spring Harb Perspect Biol*. 2011;3(1):a004978. doi:10.1101/cshperspect.a004978

27. Revell CK, Jensen OE, Shearer T, Lu Y, Holmes DF, Kadler KE. Collagen fibril assembly: New approaches to unanswered questions. *Matrix Biol Plus*. 2021;12:100079. doi:10.1016/j.mbplus.2021.100079

28. Kalluri R. Basement membranes: structure, assembly and role in tumour angiogenesis. *Nat Rev Cancer*. 2003;3(6):422-433. doi:10.1038/nrc1094

29. Xiao Y, McGuinness ChanelleAS, Doherty-Boyd WS, Salmeron-Sanchez M, Donnelly H, Dalby MJ. Current insights into the bone marrow niche: From biology *in vivo* to bioengineering *ex vivo*. *Biomaterials*. 2022;286:121568. doi:10.1016/j.biomaterials.2022.121568

30. Wang K, Meng X, Guo Z. Elastin Structure, Synthesis, Regulatory Mechanism and Relationship With Cardiovascular Diseases. *Front Cell Dev Biol*. 2021;9:596702. doi:10.3389/fcell.2021.596702

31. Mithieux SM, Weiss AS. Elastin. In: *Advances in Protein Chemistry*. Vol 70. Fibrous Proteins: Coiled-Coils, Collagen and Elastomers. Academic Press; 2005:437-461. doi:10.1016/S0065-3233(05)70013-9

32. Moore J, Thibeault S. Insights Into the Role of Elastin in Vocal Fold Health and Disease. *J Voice*. 2012;26(3):269-275. doi:10.1016/j.jvoice.2011.05.003

33. Holst J, Watson S, Lord MS, et al. Substrate elasticity provides mechanical signals for the expansion of hemopoietic stem and progenitor cells. *Nat Biotechnol*. 2010;28(10):1123-1128. doi:10.1038/nbt.1687

34. Holst J, Watson S, Lord MS, et al. Substrate elasticity provides mechanical signals for the expansion of hemopoietic stem and progenitor cells. *Nat Biotechnol*. 2010;28(10):1123-1128. doi:10.1038/nbt.1687

35. Fujita A, Migita M, Ueda T, Ogawa R, Fukunaga Y, Shimada T. Hematopoiesis in regenerated bone marrow within hydroxyapatite scaffold. *Pediatr Res*. 2010;68(1):35-40. doi:10.1203/PDR.0b013e3181e1cfce

36. Lee-Thedieck C, Rauch N, Fiammengo R, Klein G, Spatz JP. Impact of substrate elasticity on human hematopoietic stem and progenitor cell adhesion and motility. *J Cell Sci*. 2012;125(16):3765-3775. doi:10.1242/jcs.095596

37. Reinisch A, Hernandez DC, Schallmoser K, Majeti R. Generation and use of a humanized bone-marrow-ossicle niche for hematopoietic xenotransplantation into mice. *Nat Protoc*. 2017;12(10):2169-2188. doi:10.1038/nprot.2017.088

38. Vakiti A, Reynolds SB, Mewawalla P. Acute Myeloid Leukemia. In: *StatPearls*. StatPearls Publishing; 2025. Accessed June 21, 2025. http://www.ncbi.nlm.nih.gov/books/NBK507875/

39. Arber DA, Orazi A, Hasserjian R, et al. The 2016 revision to the World Health Organization classification of myeloid neoplasms and acute leukemia. *Blood*. 2016;127(20):2391-2405. doi:10.1182/blood-2016-03-643544

40. Koschade SE, Stratmann JA, Finkelmeier F, et al. Relapse surveillance of acute myeloid leukemia patients in first remission after consolidation chemotherapy: diagnostic value of regular bone marrow aspirations. *Ann Hematol*. 2022;101(8):1703-1710. doi:10.1007/s00277-022-04862-3

41. Boddu P, Kantarjian HM, Garcia-Manero G, et al. Treated secondary acute myeloid leukemia: a distinct high-risk subset of AML with adverse prognosis. *Blood Adv*. 2017;1(17):1312-1323. doi:10.1182/bloodadvances.2017008227

42. Tests for Acute Myeloid Leukemia (AML). Accessed June 21, 2025. https://www.cancer.org/cancer/types/acute-myeloid-leukemia/detection-diagnosis-staging/how-diagnosed.html

43. Ishikawa Y. Recent progress in AML with recurrent genetic abnormalities. *Int J Hematol*. 2024;120(5):525-527. doi:10.1007/s12185-024-03848-3

44. Xiao W, Nardi V, Stein E, Hasserjian RP. A practical approach on the classifications of myeloid neoplasms and acute leukemia: WHO and ICC. *J Hematol OncolJ Hematol Oncol*. 2024;17:56. doi:10.1186/s13045-024-01571-4

45. Döhner H, Wei AH, Appelbaum FR, et al. Diagnosis and management of AML in adults: 2022 recommendations from an international expert panel on behalf of the ELN. *Blood*. 2022;140(12):1345-1377. doi:10.1182/blood.2022016867

46. Khoury JD, Solary E, Abla O, et al. The 5th edition of the World Health Organization Classification of Haematolymphoid Tumours: Myeloid and Histiocytic/Dendritic Neoplasms. *Leukemia*. 2022;36(7):1703-1719. doi:10.1038/s41375-022-01613-1

47. McKinnon KM. Flow Cytometry: An Overview. *Curr Protoc Immunol*. 2018;120:5.1.1-5.1.11. doi:10.1002/cpim.40

48. Döhner H, Wei AH, Appelbaum FR, et al. Diagnosis and management of AML in adults: 2022 recommendations from an international expert panel on behalf of the ELN. *Blood*. 2022;140(12):1345-1377. doi:10.1182/blood.2022016867

49. Zeijlemaker W, Kelder A, Wouters R, et al. Absence of leukaemic CD34+ cells in acute myeloid leukaemia is of high prognostic value: a longstanding controversy deciphered. *Br J Haematol*. 2015;171(2):227-238. doi:10.1111/bjh.13572

50. Holyoake TL, Alcorn MJ. CD34 + positive haemopoietic cells:Biology and clinical applications. *Blood Rev*. 1994;8(2):113-124. doi:10.1016/S0268-960X(05)80016-5

51. Zeijlemaker W, Grob T, Meijer R, et al. CD34+CD38- leukemic stem cell frequency to predict outcome in acute myeloid leukemia. *Leukemia*. 2019;33(5):1102-1112. doi:10.1038/s41375-018-0326-3

52. Wang X, Huang S, Chen JL. Understanding of leukemic stem cells and their clinical implications. *Mol Cancer*. 2017;16:2. doi:10.1186/s12943-016-0574-7

53. El-Meligui YM, Abd Elrhman HE, Salahuddin A, Hamouda MA, Kassem AB. Correlation Study on HLA-DR and CD117 (c-Kit) Expressions: Its Prognosis and Treatment Response in Acute Myeloid Leukemia Patients. *Pharmacogenomics Pers Med*. 2021;14:381-393. doi:10.2147/PGPM.S268986

54. Ikeda H, Kanakura Y, Tamaki T, et al. Expression and functional role of the proto-oncogene c-kit in acute myeloblastic leukemia cells. *Blood*. 1991;78(11):2962-2968. doi:10.1182/blood.V78.11.2962.2962

55. Williams MS, Basma NJ, Amaral FMR, Wiseman DH, Somervaille TCP. Blast cells surviving acute myeloid leukemia induction therapy are in cycle with a signature of FOXM1 activity. *BMC Cancer*. 2021;21:1153. doi:10.1186/s12885-021-08839-9

56. Rönnstrand L. Signal transduction via the stem cell factor receptor/c-Kit. *Cell Mol Life Sci CMLS*. 2004;61(19):2535-2548. doi:10.1007/s00018-004-4189-6

57. Munoz L, Nomdedeu JF, Lopez O, et al. Interleukin-3 receptor alpha chain (CD123) is widely expressed in hematologic malignancies. *Haematologica*. 2001;86(12):1261-1269. doi:10.3324/%25x

58. Guthridge MA, Stomski FC, Thomas D, et al. Mechanism of Activation of the GM-CSF, IL-3, and IL-5 Family of Receptors. *Stem Cells*. 1998;16(5):301-313. doi:10.1002/stem.160301

59. Blalock WL, Weinstein-Oppenheimer C, Chang F, et al. Signal transduction, cell cycle regulatory, and anti-apoptotic pathways regulated by IL-3 in hematopoietic cells: possible sites for intervention with anti-neoplastic drugs. *Leukemia*. 1999;13(8):1109-1166. doi:10.1038/sj.leu.2401493

60. Hercus TR, Dhagat U, Kan WLT, et al. Signalling by the βc family of cytokines. *Cytokine Growth Factor Rev*. 2013;24(3):189-201. doi:10.1016/j.cytogfr.2013.03.002

61. Testa U, Riccioni R, Militi S, et al. Elevated expression of IL-3Rα in acute myelogenous leukemia is associated with enhanced blast proliferation, increased cellularity, and poor prognosis. *Blood*. 2002;100(8):2980-2988. doi:10.1182/blood-2002-03-0852

62. Vergez F, Green AS, Tamburini J, et al. High levels of CD34+CD38low/-CD123+ blasts are predictive of an adverse outcome in acute myeloid leukemia: a Groupe Ouest-Est des Leucemies Aigues et Maladies du Sang (GOELAMS) study. *Haematologica*. 2011;96(12):1792-1798. doi:10.3324/haematol.2011.047894

63. Sawaguchi T, Goldman-Rakic PS. D1 Dopamine Receptors in Prefrontal Cortex: Involvement in Working Memory. *Science*. 1991;251(4996):947-950. doi:10.1126/science.1825731

64. Sachlos E, Risueño RM, Laronde S, et al. Identification of drugs including a dopamine receptor antagonist that selectively target cancer stem cells. *Cell*. 2012;149(6):1284-1297. doi:10.1016/j.cell.2012.03.049

65. Crocker PR, McMillan SJ, Richards HE. CD33-related siglecs as potential modulators of inflammatory responses. *Ann N Y Acad Sci*. 2012;12531(1):102-111. doi:10.1111/j.1749-6632.2011.06449.x

66. Haubner S, Perna F, Köhnke T, et al. Coexpression profile of leukemic stem cell markers for combinatorial targeted therapy in AML. *Leukemia*. 2019;33(1):64-74. doi:10.1038/s41375-018-0180-3

67. Liu J, Tong J, Yang H. Targeting CD33 for acute myeloid leukemia therapy. *BMC Cancer*. 2022;22(1):24. doi:10.1186/s12885-021-09116-5

68. The evolutionary ecology of the major histocompatibility complex | Heredity. Accessed August 18, 2025. https://www.nature.com/articles/6800724

69. Oelschlaegel U, Mohr B, Schaich M, et al. HLA-DRneg patients without acute promyelocytic leukemia show distinct immunophenotypic, genetic, molecular, and cytomorphologic characteristics compared to acute promyelocytic leukemia. *Cytometry B Clin Cytom*. 2009;76B(5):321-327. doi:10.1002/cyto.b.20475

70. Wetzler M, McElwain BK, Stewart CC, et al. HLA-DR antigen-negative acute myeloid leukemia. *Leukemia*. 2003;17(4):707-715. doi:10.1038/sj.leu.2402865

71. Toffalori C, Zito L, Gambacorta V, et al. Immune signature drives leukemia escape and relapse after hematopoietic cell transplantation. *Nat Med*. 2019;25(4):603-611. doi:10.1038/s41591-019-0400-z

72. Christopher MJ, Petti AA, Rettig MP, et al. Immune Escape of Relapsed AML Cells after Allogeneic Transplantation. *N Engl J Med*. 2018;379(24):2330-2341. doi:10.1056/NEJMoa1808777

73. van de Winkel JG, Anderson CL. Biology of human immunoglobulin G Fc receptors. *J Leukoc Biol*. 1991;49(5):511-524. doi:10.1002/jlb.49.5.511

74. Fcγ receptors as regulators of immune responses | Nature Reviews Immunology. Accessed August 18, 2025. https://www.nature.com/articles/nri2206

75. Dunphy CH, Tang W. The value of CD64 expression in distinguishing acute myeloid leukemia with monocytic differentiation from other subtypes of acute myeloid leukemia: a flow cytometric analysis of 64 cases. *Arch Pathol Lab Med*. 2007;131(5):748-754. doi:10.5858/2007-131-748-TVOCEI

76. Cell-intrinsic lysosomal lipolysis is essential for alternative activation of macrophages | Nature Immunology. Accessed August 18, 2025. https://www.nature.com/articles/ni.2956

77. Yakubenko VP, Lishko VK, Lam SCT, Ugarova TP. A Molecular Basis for Integrin αMβ2 Ligand Binding Promiscuity. *J Biol Chem*. 2002;277(50):48635-48642. doi:10.1074/jbc.M208877200

78. Davis GE. The Mac-1 and p150,95 beta 2 integrins bind denatured proteins to mediate leukocyte cell-substrate adhesion. *Exp Cell Res*. 1992;200(2):242-252. doi:10.1016/0014-4827(92)90170-d

79. Graf M, Reif S, Kröll T, Hecht K, Nuessler V, Schmetzer H. Expression of MAC-1 (CD11b) in acute myeloid leukemia (AML) is associated with an unfavorable prognosis. *Am J Hematol*. 2006;81(4):227-235. doi:10.1002/ajh.20526

80. Gadhoum SZ, Sackstein R. Lewis x/CD15 expression in human myeloid cell differentiation is regulated by sialidase activity. *Nat Chem Biol*. 2008;4(12):751-757. doi:10.1038/nchembio.116

81. Szlasa W, Wilk K, Knecht-Gurwin K, et al. Prognostic and Therapeutic Role of CD15 and CD15s in Cancer. *Cancers*. 2022;14(9):2203. doi:10.3390/cancers14092203

82. Simoes C, Gonzalez C, Vergez F, et al. Data-driven flow cytometry classification of blast differentiation in older patients with acute myeloid leukemia. *Blood Neoplasia*. 2024;1(3):100027. doi:10.1016/j.bneo.2024.100027

83. The Prognostic Implications of CD15 Antigen Expression in patients with acute myeloid leukemia. Sciety. January 31, 2025. Accessed August 19, 2025. https://sciety.org/articles/activity/10.21203/rs.3.rs-5905422/v1

84. Schwarzinger I, Valent P, Köller U, et al. Prognostic significance of surface marker expression on blasts of patients with de novo acute myeloblastic leukemia. *J Clin Oncol Off J Am Soc Clin Oncol*. 1990;8(3):423-430. doi:10.1200/JCO.1990.8.3.423

85. Li W. Flow Cytometry in the Diagnosis of Leukemias. In: Li W, ed. *Leukemia*. Exon Publications; 2022. Accessed August 19, 2025. http://www.ncbi.nlm.nih.gov/books/NBK586209/

86. Junge A, Bacher U, Mueller BU, Keller P, Solenthaler M, Pabst T. Adverse outcome of AML with aberrant CD16 and CD56 NK cell marker expression. *Hematol Oncol*. 2018;36(3):576-583. doi:10.1002/hon.2516

87. Jennifer B, Berg V, Modak M, et al. Transferrin receptor 1 is a cellular receptor for human heme-albumin. *Commun Biol*. 2020;3(1):621. doi:10.1038/s42003-020-01294-5

88. Liu Q, Wang M, Hu Y, et al. The Usefulness of CD71 Expression by Flow Cytometry in the Diagnosis of Acute Leukemia. *Blood*. 2012;120(21):2533. doi:10.1182/blood.V120.21.2533.2533

89. Wu B, Shi N, Sun L, Liu L. Clinical value of high expression level of CD71 in acute myeloid leukemia. *Neoplasma*. 2016;63(05):809-815. doi:10.4149/neo_2016_519

90. Rivera D, Alvarado Y, Garcia-Manero G, Borthakur G, Kantarjian H, Konoplev S. Clinical Characteristics and Outcomes of Patients Diagnosed with Acute Myeloid Leukemia with Expression of CD71. *Blood*. 2021;138:4449. doi:10.1182/blood-2021-151023

91. Deaglio S, Mehta K, Malavasi F. Human CD38: a (r)evolutionary story of enzymes and receptors. *Leuk Res*. 2001;25(1):1-12. doi:10.1016/s0145-2126(00)00093-x

92. Zhong X, Ma H. Targeting CD38 for acute leukemia. *Front Oncol*. 2022;12. doi:10.3389/fonc.2022.1007783

93. Aarhus R, Graeff RM, Dickey DM, Walseth TF, Lee HC. ADP-ribosyl cyclase and CD38 catalyze the synthesis of a calcium-mobilizing metabolite from NADP. *J Biol Chem*. 1995;270(51):30327-30333. doi:10.1074/jbc.270.51.30327

94. Zahran AM, Aly SS, Rayan A, et al. Survival outcomes of CD34+CD38−LSCs and their expression of CD123 in adult AML patients. *Oncotarget*. 2018;9(75):34056-34065. doi:10.18632/oncotarget.26118

95. Rheinländer A, Schraven B, Bommhardt U. CD45 in human physiology and clinical medicine. *Immunol Lett*. 2018;196:22-32. doi:10.1016/j.imlet.2018.01.009

96. Bhukaya L, Shukla J, Hershavardhini K, Abhilasha S. Aberrant antigen expression in children with acute lymphoblastic leukemia. *Pediatr Hematol Oncol J*. 2025;10(3):100485. doi:10.1016/j.phoj.2025.100485

97. Murphy T, Yee KWL. Cytarabine and daunorubicin for the treatment of acute myeloid leukemia. *Expert Opin Pharmacother*. 2017;18(16):1765-1780. doi:10.1080/14656566.2017.1391216

98. Mantzaris I. *Phase 1B Study of Venetoclax in Combination With Standard Intensive Chemotherapy With Daunorubicin Plus Cytarabine Followed by High-Dose Cytarabine in Adult Patients With Newly Diagnosed Acute Myeloid Leukemia and Advanced Myelodysplastic Syndrome*. clinicaltrials.gov; 2024. Accessed August 25, 2025. https://clinicaltrials.gov/study/NCT05342584

99. Vakiti A, Reynolds SB, Mewawalla P. Acute Myeloid Leukemia. In: *StatPearls*. StatPearls Publishing; 2025. Accessed November 20, 2025. http://www.ncbi.nlm.nih.gov/books/NBK507875/

100. Roboz GJ, Guzman M. Acute Myeloid Leukemia Stem Cells: Seek and Destroy. *Expert Rev Hematol*. 2009;2(6):663-672. doi:10.1586/ehm.09.53

101. Thol F, Ganser A. Treatment of Relapsed Acute Myeloid Leukemia. *Curr Treat Options Oncol*. 2020;21(8):66. doi:10.1007/s11864-020-00765-5

102. Short NJ, Rytting ME, Cortes JE. Acute myeloid leukaemia. *The Lancet*. 2018;392(10147):593-606. doi:10.1016/S0140-6736(18)31041-9

103. Joshi K, Zhang L, Breslin SJP, Zhang J. Leukemia stem cells in the pathogenesis, progression and treatment of acute myeloid leukemia. *Adv Exp Med Biol*. 2019;1143:95-128. doi:10.1007/978-981-13-7342-8_5

104. Cancer stem cell definitions and terminology: the devil is in the details | Nature Reviews Cancer. Accessed August 16, 2025. https://www.nature.com/articles/nrc3368

105. Lapidot T, Sirard C, Vormoor J, et al. A cell initiating human acute myeloid leukaemia after transplantation into SCID mice. *Nature*. 1994;367(6464):645-648. doi:10.1038/367645a0

106. Bonnet D, Dick JE. Human acute myeloid leukemia is organized as a hierarchy that originates from a primitive hematopoietic cell. *Nat Med*. 1997;3(7):730-737. doi:10.1038/nm0797-730

107. Dick JE. Stem cell concepts renew cancer research. *Blood*. 2008;112(13):4793-4807. doi:10.1182/blood-2008-08-077941

108. Taussig DC, Miraki-Moud F, Anjos-Afonso F, et al. Anti-CD38 antibody–mediated clearance of human repopulating cells masks the heterogeneity of leukemia-initiating cells. *Blood*. 2008;112(3):568-575. doi:10.1182/blood-2007-10-118331

109. Herrmann H, Sadovnik I, Eisenwort G, et al. Delineation of target expression profiles in CD34+/CD38− and CD34+/CD38+ stem and progenitor cells in AML and CML. *Blood Adv*. 2020;4(20):5118-5132. doi:10.1182/bloodadvances.2020001742

110. Hanekamp D, Cloos J, Schuurhuis GJ. Leukemic stem cells: identification and clinical application. *Int J Hematol*. 2017;105(5):549-557. doi:10.1007/s12185-017-2221-5

111. Galen P van, Hovestadt V, Ii MHW, et al. Single-Cell RNA-Seq Reveals AML Hierarchies Relevant to Disease Progression and Immunity. *Cell*. 2019;176(6):1265-1281.e24. doi:10.1016/j.cell.2019.01.031

112. Mesbahi Y, Trahair TN, Lock RB, Connerty P. Exploring the Metabolic Landscape of AML: From Haematopoietic Stem Cells to Myeloblasts and Leukaemic Stem Cells. *Front Oncol*. 2022;12. doi:10.3389/fonc.2022.807266

113. Vander Heiden MG, Cantley LC, Thompson CB. Understanding the Warburg Effect: The Metabolic Requirements of Cell Proliferation. *Science*. 2009;324(5930):1029-1033. doi:10.1126/science.1160809

114. Dembitz V, James SC, Gallipoli P. Targeting lipid metabolism in acute myeloid leukemia: biological insights and therapeutic opportunities. *Leukemia*. 2025;39(8):1814-1823. doi:10.1038/s41375-025-02645-z

115. Mishra SK, Millman SE, Zhang L. Metabolism in acute myeloid leukemia: mechanistic insights and therapeutic targets. *Blood*. 2023;141(10):1119-1135. doi:10.1182/blood.2022018092

116. Yang Y, Pu J, Yang Y. Glycolysis and chemoresistance in acute myeloid leukemia. *Heliyon*. 2024;10(15):e35721. doi:10.1016/j.heliyon.2024.e35721

117. Pavlova NN, Zhu J, Thompson CB. The hallmarks of cancer metabolism: Still emerging. *Cell Metab*. 2022;34(3):355-377. doi:10.1016/j.cmet.2022.01.007

118. Wang YH, Israelsen WJ, Lee D, et al. Cell-State-Specific Metabolic Dependency in Hematopoiesis and Leukemogenesis. *Cell*. 2014;158(6):1309-1323. doi:10.1016/j.cell.2014.07.048

119. Ema H, Suda T. Two anatomically distinct niches regulate stem cell activity. *Blood*. 2012;120(11):2174-2181. doi:10.1182/blood-2012-04-424507

120. Eliasson P, Jönsson JI. The hematopoietic stem cell niche: Low in oxygen but a nice place to be. *J Cell Physiol*. 2010;222(1):17-22. doi:10.1002/jcp.21908

121. Addanki S, Kim L, Stevens A. Understanding and Targeting Metabolic Vulnerabilities in Acute Myeloid Leukemia: An Updated Comprehensive Review. *Cancers*. 2025;17(8):1355. doi:10.3390/cancers17081355

122. Takubo K, Nagamatsu G, Kobayashi CI, et al. Regulation of Glycolysis by Pdk Functions as a Metabolic Checkpoint for Cell Cycle Quiescence in Hematopoietic Stem Cells. *Cell Stem Cell*. 2013;12(1):49-61. doi:10.1016/j.stem.2012.10.011

123. Simsek T, Kocabas F, Zheng J, et al. The Distinct Metabolic Profile of Hematopoietic Stem Cells Reflects Their Location in a Hypoxic Niche. *Cell Stem Cell*. 2010;7(3):380-390. doi:10.1016/j.stem.2010.07.011

124. Arranz L, Urbano-Ispizúa Á, Méndez-Ferrer S. Mitochondria underlie different metabolism of hematopoietic stem and progenitor cells. *Haematologica*. 2013;98(7):993-995. doi:10.3324/haematol.2013.084293

125. Norddahl GL, Pronk CJ, Wahlestedt M, et al. Accumulating Mitochondrial DNA Mutations Drive Premature Hematopoietic Aging Phenotypes Distinct from Physiological Stem Cell Aging. *Cell Stem Cell*. 2011;8(5):499-510. doi:10.1016/j.stem.2011.03.009

126. Ludin A, Gur-Cohen S, Golan K, et al. Reactive oxygen species regulate hematopoietic stem cell self-renewal, migration and development, as well as their bone marrow microenvironment. *Antioxid Redox Signal*. 2014;21(11):1605-1619. doi:10.1089/ars.2014.5941

127. Kim J whan, Tchernyshyov I, Semenza GL, Dang CV. HIF-1-mediated expression of pyruvate dehydrogenase kinase: A metabolic switch required for cellular adaptation to hypoxia. *Cell Metab*. 2006;3(3):177-185. doi:10.1016/j.cmet.2006.02.002

128. Jang YY, Sharkis SJ. A low level of reactive oxygen species selects for primitive hematopoietic stem cells that may reside in the low-oxygenic niche. *Blood*. 2007;110(8):3056-3063. doi:10.1182/blood-2007-05-087759

129. Filippi MD, Ghaffari S. Mitochondria in the maintenance of hematopoietic stem cells: new perspectives and opportunities. *Blood*. 2019;133(18):1943-1952. doi:10.1182/blood-2018-10-808873

130. Lagadinou ED, Sach A, Callahan K, et al. BCL-2 inhibition targets oxidative phosphorylation and selectively eradicates quiescent human leukemia stem cells. *Cell Stem Cell*. 2013;12(3):329-341. doi:10.1016/j.stem.2012.12.013

131. Åbacka H, Hansen JS, Huang P, et al. Targeting GLUT1 in acute myeloid leukemia to overcome cytarabine resistance. *Haematologica*. 2021;106(4):1163-1166. doi:10.3324/haematol.2020.246843

132. Tabe Y, Konopleva M. Resistance to energy metabolism - targeted therapy of AML cells residual in the bone marrow microenvironment. *Cancer Drug Resist*. 2023;6(1):138-150. doi:10.20517/cdr.2022.133

133. Jones CL, Stevens BM, D'Alessandro A, et al. Inhibition of Amino Acid Metabolism Selectively Targets Human Leukemia Stem Cells. *Cancer Cell*. 2018;34(5):724-740.e4. doi:10.1016/j.ccell.2018.10.005

134. Stevens BM, Jones CL, Pollyea DA, et al. Fatty acid metabolism underlies venetoclax resistance in acute myeloid leukemia stem cells. *Nat Cancer*. 2020;1(12):1176-1187. doi:10.1038/s43018-020-00126-z

135. Samudio I, Harmancey R, Fiegl M, et al. Pharmacologic inhibition of fatty acid oxidation sensitizes human leukemia cells to apoptosis induction. *J Clin Invest*. 2010;120(1):142-156. doi:10.1172/JCI38942

136. Farge T, Saland E, de Toni F, et al. Chemotherapy Resistant Human Acute Myeloid Leukemia Cells are Not Enriched for Leukemic Stem Cells but Require Oxidative Metabolism. *Cancer Discov*. 2017;7(7):716-735. doi:10.1158/2159-8290.CD-16-0441

137. Al-Khami AA, Zheng L, Del Valle L, et al. Exogenous lipid uptake induces metabolic and functional reprogramming of tumor-associated myeloid-derived suppressor cells. *Oncoimmunology*. 2017;6(10):e1344804. doi:10.1080/2162402X.2017.1344804

138. Samovski D, Jacome-Sosa M, Abumrad NA. Fatty Acid Transport and Signaling: Mechanisms and Physiological Implications. *Annu Rev Physiol*. 2023;85:317-337. doi:10.1146/annurev-physiol-032122-030352

139. Ye H, Adane B, Khan N, et al. Leukemic Stem Cells Evade Chemotherapy by Metabolic Adaptation to an Adipose Tissue Niche. *Cell Stem Cell*. 2016;19(1):23-37. doi:10.1016/j.stem.2016.06.001

140. Bolkun L, Pienkowski T, Sieminska J, et al. Metabolomic profile of acute myeloid leukaemia parallels of prognosis and response to therapy. *Sci Rep*. 2023;13(1):21809. doi:10.1038/s41598-023-48970-0

141. Stefanko A, Thiede C, Ehninger G, Simons K, Grzybek M. Lipidomic approach for stratification of acute myeloid leukemia patients. *PLOS ONE*. 2017;12(2):e0168781. doi:10.1371/journal.pone.0168781

142. Åbacka H, Masoni S, Poli G, et al. SMS121, a new inhibitor of CD36, impairs fatty acid uptake and viability of acute myeloid leukemia. *Sci Rep*. 2024;14(1):9104. doi:10.1038/s41598-024-58689-1

143. Tabe Y, Yamamoto S, Saitoh K, et al. Bone Marrow Adipocytes Facilitate Fatty Acid Oxidation Activating AMPK and a Transcriptional Network Supporting Survival of Acute Monocytic Leukemia Cells. *Cancer Res*. 2017;77(6):1453-1464. doi:10.1158/0008-5472.CAN-16-1645

144. Shafat MS, Oellerich T, Mohr S, et al. Leukemic blasts program bone marrow adipocytes to generate a protumoral microenvironment. *Blood*. 2017;129(10):1320-1332. doi:10.1182/blood-2016-08-734798

145. Guerrero-Rodríguez SL, Mata-Cruz C, Pérez-Tapia SM, Velasco-Velázquez MA. Role of CD36 in cancer progression, stemness, and targeting. *Front Cell Dev Biol*. 2022;10. doi:10.3389/fcell.2022.1079076

146. Jiang M, Karsenberg R, Bianchi F, van den Bogaart G. CD36 as a double-edged sword in cancer. *Immunol Lett*. 2024;265:7-15. doi:10.1016/j.imlet.2023.12.002

147. Chen Y, Zhang J, Cui W, Silverstein RL. CD36, a signaling receptor and fatty acid transporter that regulates immune cell metabolism and fate. *J Exp Med*. 2022;219(6):e20211314. doi:10.1084/jem.20211314

148. Guo HZ, Feng RX, Zhang YJ, et al. A CD36-dependent non-canonical lipid metabolism program promotes immune escape and resistance to hypomethylating agent therapy in AML. *Cell Rep Med*. 2024;5(6). doi:10.1016/j.xcrm.2024.101592

149. Chen L, Gao Z, Zhu J, Rodgers GP. Identification of CD13+CD36+ cells as a common progenitor for erythroid and myeloid lineages in human bone marrow. *Exp Hematol*. 2007;35(7):1047-1055. doi:10.1016/j.exphem.2007.04.003

150. Ladanyi A, Mukherjee A, Kenny HA, et al. Adipocyte-induced CD36 expression drives ovarian cancer progression and metastasis. *Oncogene*. 2018;37(17):2285-2301. doi:10.1038/s41388-017-0093-z

151. Feng WW, Wilkins O, Bang S, et al. CD36-Mediated Metabolic Rewiring of Breast Cancer Cells Promotes Resistance to HER2-Targeted Therapies. *Cell Rep*. 2019;29(11):3405-3420.e5. doi:10.1016/j.celrep.2019.11.008

152. Amantéa MC, da Silva RP, Soares LR, Pereira JL de M, de Souza APD. CD36 as a marker of acute myeloid leukemia prognosis: A systematic review. *Hematol Transfus Cell Ther*. 2025;47(3):103861. doi:10.1016/j.htct.2025.103861

153. Farge T, Nakhle J, Lagarde D, et al. CD36 Drives Metastasis and Relapse in Acute Myeloid Leukemia. *Cancer Res*. 2023;83(17):2824-2838. doi:10.1158/0008-5472.CAN-22-3682

154. Shafat MS, Oellerich T, Mohr S, et al. Leukemic blasts program bone marrow adipocytes to generate a protumoral microenvironment. *Blood*. 2017;129(10):1320-1332. doi:10.1182/blood-2016-08-734798

155. Mahalingam D, Harb W, Patnaik A, et al. First-in-human phase I dose escalation trial of the first-in-class tumor microenvironment modulator VT1021 in advanced solid tumors. *Commun Med*. 2024;4(1):10. doi:10.1038/s43856-024-00433-x

156. Zhang T, Yang J, Vaikari VP, et al. Apolipoprotein C2 - CD36 Promotes Leukemia Growth and Presents a Targetable Axis in Acute Myeloid Leukemia. *Blood Cancer Discov*. 2020;1(2):198-213. doi:10.1158/2643-3230.BCD-19-0077

157. Zheng TJ, Kohs TCL, Mueller PA, et al. Effect of antiplatelet agents and tyrosine kinase inhibitors on oxLDL-mediated procoagulant platelet activity. *Blood Adv*. 2022;7(8):1366-1378. doi:10.1182/bloodadvances.2022007169

158. Izzi V, Lakkala J, Devarajan R, et al. Expression of a specific extracellular matrix signature is a favorable prognostic factor in acute myeloid leukemia. *Leuk Res Rep*. 2018;9:9-13. doi:10.1016/j.lrr.2017.12.001

159. Bonardi F, Fusetti F, Deelen P, Gosliga D van, Vellenga E, Schuringa JJ. A Proteomics and Transcriptomics Approach to Identify Leukemic Stem Cell (LSC) Markers *. *Mol Cell Proteomics*. 2013;12(3):626-637. doi:10.1074/mcp.M112.021931

160. Alexander SPH, Kelly E, Mathie A, et al. THE CONCISE GUIDE TO PHARMACOLOGY 2019/20: Introduction and Other Protein Targets. *Br J Pharmacol*. 2019;176 Suppl 1(Suppl 1):S1-S20. doi:10.1111/bph.14747

161. Naci D, Berrazouane S, Barabé F, Aoudjit F. Cell adhesion to collagen promotes leukemia resistance to doxorubicin by reducing DNA damage through the inhibition of Rac1 activation. *Sci Rep*. 2019;9:19455. doi:10.1038/s41598-019-55934-w

162. Zöller M. CD44, Hyaluronan, the Hematopoietic Stem Cell, and Leukemia-Initiating Cells. *Front Immunol*. 2015;6:235. doi:10.3389/fimmu.2015.00235

163. Yu X, Munoz-Sagredo L, Streule K, et al. CD44 loss of function sensitizes AML cells to the BCL-2 inhibitor venetoclax by decreasing CXCL12-driven survival cues. *Blood*. 2021;138(12):1067-1080. doi:10.1182/blood.2020006343

164. Farge T, Saland E, de Toni F, et al. Chemotherapy Resistant Human Acute Myeloid Leukemia Cells are Not Enriched for Leukemic Stem Cells but Require Oxidative Metabolism. *Cancer Discov*. 2017;7(7):716-735. doi:10.1158/2159-8290.CD-16-0441

165. Hannigan G, Troussard AA, Dedhar S. Integrin-linked kinase: a cancer therapeutic target unique among its ILK. *Nat Rev Cancer*. 2005;5(1):51-63. doi:10.1038/nrc1524

166. Ruan Y, Kim HN, Ogana H, Kim YM. Wnt Signaling in Leukemia and Its Bone Marrow Microenvironment. *Int J Mol Sci*. 2020;21(17):6247. doi:10.3390/ijms21176247

167. Liu S, Calderwood DA, Ginsberg MH. Integrin cytoplasmic domain-binding proteins. *J Cell Sci*. 2000;113 (Pt 20):3563-3571. doi:10.1242/jcs.113.20.3563

168. Shishido S, Bönig H, Kim YM. Role of integrin alpha4 in drug resistance of leukemia. *Front Oncol*. 2014;4:99. doi:10.3389/fonc.2014.00099

169. Rothe K, Babaian A, Nakamichi N, et al. Integrin-Linked Kinase Mediates Therapeutic Resistance of Quiescent CML Stem Cells to Tyrosine Kinase Inhibitors. *Cell Stem Cell*. 2020;27(1):110-124.e9. doi:10.1016/j.stem.2020.04.005

170. Maltman DJ, Przyborski SA. Developments in three-dimensional cell culture technology aimed at improving the accuracy of in vitro analyses. *Biochem Soc Trans*. 2010;38(4):1072-1075. doi:10.1042/BST0381072

171. Baker BM, Chen CS. Deconstructing the third dimension – how 3D culture microenvironments alter cellular cues. *J Cell Sci*. 2012;125(13):3015-3024. doi:10.1242/jcs.079509

172. Sharipol A, Frisch BJ. Are we ready to integrate 3D culture systems in acute myeloid leukemia and bone marrow microenvironment research? *Front Hematol*. 2024;3. doi:10.3389/frhem.2024.1407698

173. Leibniz Institute DSMZ: Details. Accessed October 24, 2025. https://www.dsmz.de/collection/catalogue/details/culture/ACC-99

174. Naci D, Berrazouane S, Barabé F, Aoudjit F. Cell adhesion to collagen promotes leukemia resistance to doxorubicin by reducing DNA damage through the inhibition of Rac1 activation. *Sci Rep*. 2019;9(1):19455. doi:10.1038/s41598-019-55934-w

175. Cucchi DGJ, Groen RWJ, Janssen JJWM, Cloos J. *Ex vivo* cultures and drug testing of primary acute myeloid leukemia samples: Current techniques and implications for experimental design and outcome. *Drug Resist Updat*. 2020;53:100730. doi:10.1016/j.drup.2020.100730

176. Azadniv M, Myers JR, McMurray HR, et al. Bone marrow mesenchymal stromal cells from acute myelogenous leukemia patients demonstrate adipogenic differentiation propensity with implications for leukemia cell support. *Leukemia*. 2020;34(2):391-403. doi:10.1038/s41375-019-0568-8

177. Takahashi K, Tanaka T. Clonal evolution and hierarchy in myeloid malignancies. *Trends Cancer*. 2023;9(9):707-715. doi:10.1016/j.trecan.2023.05.004

178. Bruserud Ø, Selheim F, Hernandez-Valladares M, Reikvam H. Monocytic Differentiation in Acute Myeloid Leukemia Cells: Diagnostic Criteria, Biological Heterogeneity, Mitochondrial Metabolism, Resistance to and Induction by Targeted Therapies. *Int J Mol Sci*. 2024;25(12):6356. doi:10.3390/ijms25126356

179. Weinberg OK, Arber DA, Döhner H, et al. The International Consensus Classification of acute leukemias of ambiguous lineage. *Blood*. 2023;141(18):2275-2277. doi:10.1182/blood.2022019493

180. Khalidi HS, Medeiros LJ, Chang KL, Brynes RK, Slovak ML, Arber DA. The immunophenotype of adult acute myeloid leukemia: high frequency of lymphoid antigen expression and comparison of immunophenotype, French-American-British classification, and karyotypic abnormalities. *Am J Clin Pathol*. 1998;109(2):211-220. doi:10.1093/ajcp/109.2.211

181. Abd El-Aziz SM, Salem DA, Salah-Eldin MA. Clinical relevance of thrombospondin receptor (CD36) expression in Egyptian de novo adult acute myeloid leukemia. *Egypt J Haematol*. 2013;38(1):1. doi:10.7123/01.EJH.0000423008.85761.a3

182. Plesa A, Ciuperca G, Louvet V, et al. Diagnostics of the AML with immunophenotypical data. *Math Model Nat Phenom*. 2006;1(2):104-123. doi:10.1051/mmnp:2008006

183. Wegmann R, Bonilla X, Casanova R, et al. Single-cell landscape of innate and acquired drug resistance in acute myeloid leukemia. *Nat Commun*. 2024;15(1):9402. doi:10.1038/s41467-024-53535-4

184. Multivariate analysis of prognostic factors in acute myeloid leukemia: value of clonogenic leukemic cell properties. | Journal of Clinical Oncology. Accessed October 23, 2025. https://ascopubs.org/doi/abs/10.1200/JCO.1989.7.6.738

185. Meng Y, Pospiech M, Ali A, et al. Deletion of CD36 exhibits limited impact on normal hematopoiesis and the leukemia microenvironment. *Cell Mol Biol Lett*. 2023;28:45. doi:10.1186/s11658-023-00455-8

186. Zhang Y, Guo H, Zhang Z, Lu W, Zhu J, Shi J. IL-6 promotes chemoresistance via upregulating CD36 mediated fatty acids uptake in acute myeloid leukemia. *Exp Cell Res*. 2022;415(1):113112. doi:10.1016/j.yexcr.2022.113112

187. del Cañizo MC, Mota A, Orfao A, et al. Value of colony forming unit-granulocyte macrophage assay in predicting relapse in acute myeloid leukaemia. *J Clin Pathol*. 1996;49(6):450-452. doi:10.1136/jcp.49.6.450

188. Bonnet D, Dick JE. Human acute myeloid leukemia is organized as a hierarchy that originates from a primitive hematopoietic cell. *Nat Med*. 1997;3(7):730-737. doi:10.1038/nm0797-730

189. Jones RG, Thompson CB. Tumor suppressors and cell metabolism: a recipe for cancer growth. *Genes Dev*. 2009;23(5):537-548. doi:10.1101/gad.1756509

190. Tabe Y, Konopleva M, Andreeff M. Fatty Acid Metabolism, Bone Marrow Adipocytes, and AML. *Front Oncol*. 2020;10:155. doi:10.3389/fonc.2020.00155

191. Romani P, Brian I, Santinon G, et al. Extracellular matrix mechanical cues regulate lipid metabolism through Lipin-1 and SREBP. *Nat Cell Biol*. 2019;21(3):338-347. doi:10.1038/s41556-018-0270-5

192. Mills TS, Arnone M, Görsch E, et al. MRC2 expression modulates metabolism in acute myeloid leukemia stem cells. *Cancer Lett*. 2025;635:218068. doi:10.1016/j.canlet.2025.218068

193. Ata R, Antonescu CN. Integrins and Cell Metabolism: An Intimate Relationship Impacting Cancer. *Int J Mol Sci*. 2017;18(1):189. doi:10.3390/ijms18010189

194. Madan V, Koeffler HP. Differentiation therapy of myeloid leukemia: four decades of development. *Haematologica*. 2020;106(1):26-38. doi:10.3324/haematol.2020.262121

195. Breitman TR, Collins SJ, Keene BR. Terminal Differentiation of Human Promyelocytic Leukemic Cells in Primary Culture in Response to Retinoic Acid. *Blood*. 1981;57(6):1000-1004. doi:10.1182/blood.V57.6.1000.1000

196. Alimoghaddam K. A Review of Arsenic Trioxide and Acute Promyelocytic Leukemia. *Int J Hematol-Oncol Stem Cell Res*. 2014;8(3):44-54.

197. Testa U, Castelli G, Pelosi E. Recent Developments in Differentiation Therapy of Acute Myeloid Leukemia. *Cancers*. 2025;17(7):1141. doi:10.3390/cancers17071141

198. Shao X, Xu A, Du W, et al. The palmitoyltransferase ZDHHC21 regulates oxidative phosphorylation to induce differentiation block and stemness in AML. *Blood*. 2023;142(4):365-381. doi:10.1182/blood.2022019056

199. Yan F, Shen N, Pang J, et al. A vicious loop of fatty acid-binding protein 4 and DNA methyltransferase 1 promotes acute myeloid leukemia and acts as a therapeutic target. *Leukemia*. 2018;32(4):865-873. doi:10.1038/leu.2017.307

200. Acharya S, Kala PS. Role of CD71 in acute leukemia- An immunophenotypic marker for erythroid lineage or proliferation? *Indian J Pathol Microbiol*. 2019;62(3):418-422. doi:10.4103/IJPM.IJPM_604_18

201. Maguire JE, Danahey KM, Burkly LC, van Seventer GA. T cell receptor- and beta 1 integrin-mediated signals synergize to induce tyrosine phosphorylation of focal adhesion kinase (pp125FAK) in human T cells. *J Exp Med*. 1995;182(6):2079-2090. doi:10.1084/jem.182.6.2079

202. Maiguel D, Faridi MH, Wei C, et al. Small Molecule–Mediated Activation of the Integrin CD11b/CD18 Reduces Inflammatory Disease. *Sci Signal*. 2011;4(189):ra57. doi:10.1126/scisignal.2001811

203. Singh RP, Jeyaraju DV, Voisin V, et al. Disrupting Mitochondrial Copper Distribution Inhibits Leukemic Stem Cell Self-Renewal. *Cell Stem Cell*. 2020;26(6):926-937.e10. doi:10.1016/j.stem.2020.04.010

204. Sykes DB, Kfoury YS, Mercier FE, et al. Inhibition of Dihydroorotate Dehydrogenase Overcomes Differentiation Blockade in Acute Myeloid Leukemia. *Cell*. 2016;167(1):171-186.e15. doi:10.1016/j.cell.2016.08.057

205. Zhou C, Yang L, Zhao K, Jiang L. ITGAM sustains MAPK signaling and serves as an adverse prognostic factor and therapeutic target in acute myeloid leukemia. *Transl Cancer Res*. 2024;13(6). doi:10.21037/tcr-24-810

206. Cascavilla N, Musto P, D'Arena G, et al. CD117 (c-kit) is a restricted antigen of acute myeloid leukemia and characterizes early differentiative levels of M5 FAB subtype. *Haematologica*. 1998;83(5):392-397.

207. Foster BM, Zaidi D, Young TR, Mobley ME, Kerr BA. CD117/c-kit in Cancer Stem Cell-Mediated Progression and Therapeutic Resistance. *Biomedicines*. 2018;6(1):31. doi:10.3390/biomedicines6010031

208. Jordan CT, Upchurch D, Szilvassy SJ, et al. The interleukin-3 receptor alpha chain is a unique marker for human acute myelogenous leukemia stem cells. *Leukemia*. 2000;14(10):1777-1784. doi:10.1038/sj.leu.2401903

209. Testa U, Riccioni R, Militi S, et al. Elevated expression of IL-3Rα in acute myelogenous leukemia is associated with enhanced blast proliferation, increased cellularity, and poor prognosis. *Blood*. 2002;100(8):2980-2988. doi:10.1182/blood-2002-03-0852

210. Voytyuk O, Lennartsson J, Mogi A, et al. Src Family Kinases Are Involved in the Differential Signaling from Two Splice Forms of c-Kit*. *J Biol Chem*. 2003;278(11):9159-9166. doi:10.1074/jbc.M211726200

211. Wandzioch E, Edling CE, Palmer RH, Carlsson L, Hallberg B. Activation of the MAP kinase pathway by c-Kit is PI-3 kinase dependent in hematopoietic progenitor/stem cell lines. *Blood*. 2004;104(1):51-57. doi:10.1182/blood-2003-07-2554

212. Steelman LS, Franklin RA, Abrams SL, et al. Roles of the Ras/Raf/MEK/ERK pathway in leukemia therapy. *Leukemia*. 2011;25(7):1080-1094. doi:10.1038/leu.2011.66

Appendix

Table 1. List of fluorophores and corresponding antibody markers used in the primary AML immunophenotyping panel.

Fluorophore	Marker
cFluor V420	CD16
eFluor 450	CD45
cFluor V505	HLA-DR
cFluor V547	CD4
SB600	CD34
FITC	CD36
cFluor B548	CD15
B690	CD38
PE	Bodipy 500/510
cFluor V610	CD11b
BYG667	CD71
BYG710	CD117
BYG750	CD56
BYG781	CD10
APC	CD33
cFluor R685	CD5
cFluor R720	CD123
AF750	DRD2

Table 2: Effect of CD36 Inhibition on Primary AML Phenotype. Data were obtained using flow cytometry of blast-gated cells after 72 hours of incubation on either PS or scaffold, with or without CD36 inhibition. The table depicts metrics of surface marker frequency, MFI, and absolute counts that were significantly increased or decreased (greater than 1.5-fold or less than 0.5-fold) relative to each patient's respective PS control.

AML Blasts			PS Inhibitor			Scaffold Ctl			Scaffold Inhibitor		
			Freq	MFI	Abs Count	Freq	MFI	Abs Count	Freq	MFI	Abs Count
ID: 120713	Immature Markers	Increase	CD123	DRD2	0	CD123	0	0	CD117, CD123	0	0
		Decrease	0	CD123	0	0	CD123, DRD2	DRD2	0	CD34, CD117, CD123, DRD2	0
	Myeloid Markers	Increase	CD16, HLA-DR	CD38	CD15, HLA-DR	CD71	CD71	CD38	0	0	CD15, CD16, HLA-DR
		Decrease	0	0	0	CD16	CD64, CD15, CD45	0	CD64, CD16, HLA-DR, CD36	CD64, CD11b, CD15, CD16, HLA-DR, CD45, CD36	0
ID: 130213	Immature Markers	Increase	CD123	0	0	CD123	CD123	0	CD123	CD123	0
		Decrease	0	CD34, CD117, DRD2	DRD2	DRD2	CD117, DRD2	DRD2	DRD2	CD34, CD117, DRD2	DRD2
	Myeloid Markers	Increase	CD38, CD15, HLA-DR, CD71, CD45	CD38, CD15, HLA-DR, CD45	CD15, CD45	CD38, CD15, HLA-DR, CD71, CD45	CD38, CD15, HLA-DR, CD45	CD15, CD45	CD38, CD15, HLA-DR, CD71, CD45	CD38, CD15, HLA-DR, CD45	CD15, CD45
		Decrease	CD64, CD16	CD64, CD11b, CD71, CD36	0	CD64, CD16	CD64, CD11b, CD16, CD36	CD64	CD64, CD16	CD64, CD11b, CD71, CD36	CD64
ID: 110289	Immature Markers	Increase	DRD2	0	CD117 DRD2	0	0	CD117	0	0	CD117
		Decrease	0	0	0	CD123 DRD2	CD34, CD117, CD123, DRD2	0	0	CD34, CD123, DRD2	0
	Myeloid Markers	Increase	CD38	CD16, HLA-DR	CD15	CD38 CD16 CD71	0	HLA-DR, CD71	CD11b CD38 CD16 CD71	0	0
		Decrease	0	CD11b	0	CD15	CD64, CD38, CD11b, CD15, CD16, HLA-DR, CD71, CD45, CD36	CD16	CD15 HLA-DR CD45	CD64, CD38, CD11b, CD15, CD16, HLA-DR, CD71, CD45, CD36	CD16, HLA-DR

Table 3: Effect of CD36 Inhibition on AML Phenotype cultured on ECM scaffold. Data was obtained using flow cytometry of blast-gated cells after 72 hours of incubation on either PS or scaffold, with or without CD36 inhibition. The table depicts metrics of surface marker frequency, MFI, and absolute counts that were significantly increased or decreased (greater than 1.5-fold or less than 0.5-fold) under scaffold inhibition relative to each patient's respective scaffold control.

AML Blasts			Scaffold Inhibitor		
			Freq	MFI	Abs Count
ID: 120713	Immature Markers	Increase	1 CD123	0	0
		Decrease	0	0	0
	Myeloid Markers	Increase	CD11b	CD64, CD15, HLA-DR	0
		Decrease	0	CD38	0
ID: 130213	Immature Markers	Increase	0	0	0
		Decrease	0	0	CD34
	Myeloid Markers	Increase	CD11b	0	CD11b
		Decrease	0	CD64	CD64, CD38, CD15, HLA-DR, CD71, CD45, CD38
ID: 110289	Immature Markers	Increase	CD117	CD117	0
		Decrease	0	0	0
	Myeloid Markers	Increase	CD11b, CD16	0	0
		Decrease	HLA-DR	CD16, HLA-DR, CD71	0

Table 4: Effect of CD36 Inhibition on the Phenotype of Compiled Primary AML Samples

Compiled Blasts		PS Inhibitor			Scaffold Ctl (relative to PS ctl)			Scaffold Inh (relative to PS ctl)			Scaffold Inhibitor (relative to scaffold ctl)		
		Freq	MFI	Abs Count	Freq	MFI	Abs Count	Freq	MFI	Abs Count	Freq	MFI	Abs Count
Immature Markers	Increase	CD123	0	0	CD123	0	0	Cd117 Cd123	CD117	0	CD117 CD123	0	0
	Decrease	0	0	0	DRD2	DRD2	DRD2	0	0	CD34 CD117 DRD2	0	0	0
Myeloid Markers	Increase	CD38 CD15 CD16 HLA-DR CD71 CD45	CD15 CD45	CD38 HLA-DR CD45	CD38 CD15 HLA-DR CD71 CD45	CD15 CD45	CD38 CD45	CD38 CD11b CD15 HLA-DR CD71 CD45	CD15 CD45	CD38 CD45	CD11b	0	CD11b
	Decrease	0	0	0	CD64 CD16		CD64 CD11b CD16 CD36	CD64 CD16		CD64 CD11b CD16 CD71 CD36	0	0	0

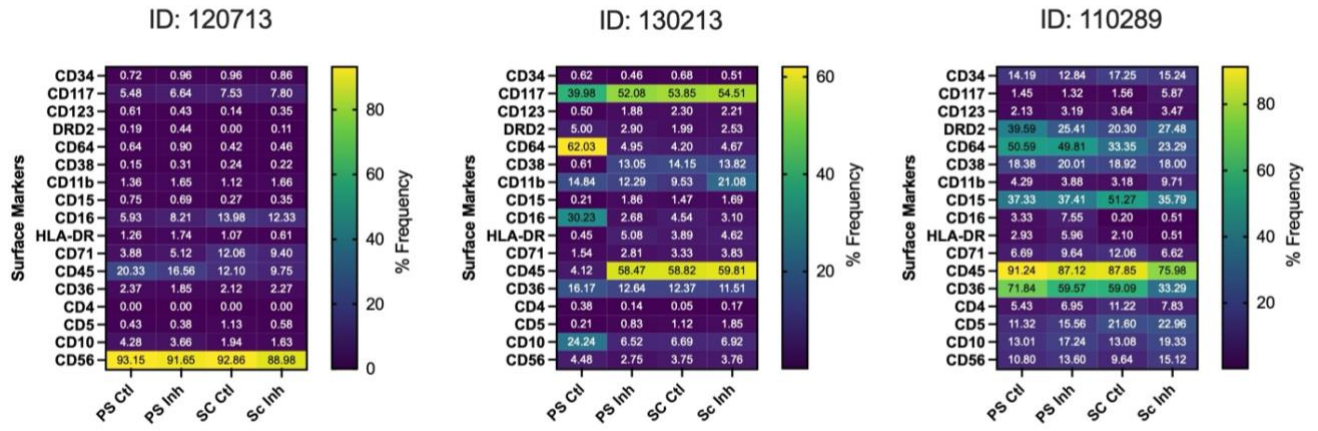

Supplemental Figure 1. *Primary AML surface marker Frequencies after 72 hours of culture.* Cells were incubated with or without CD36 inhibitor (Inh) and cultured on either PS (polystyrene) or ECM scaffold (SC). After 72 hours of incubation, cells were harvested and used for flow cytometry analysis. Heat maps depict surface marker frequencies for three patient samples (ID: 120713, ID: 130213, ID: 110289) for each condition.

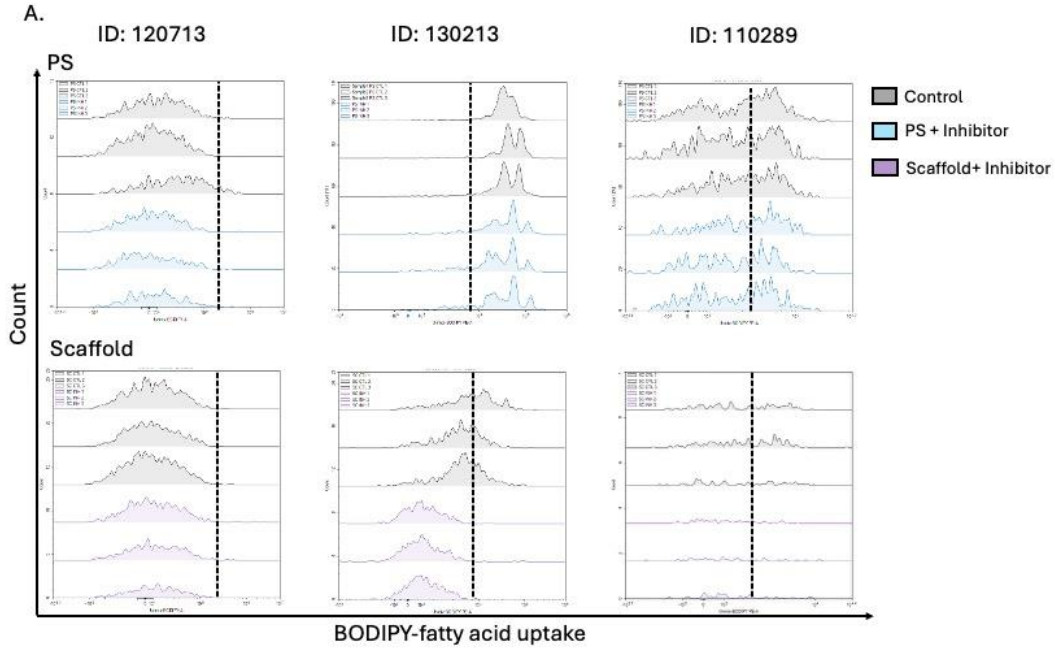

Supplemental Figure 2. *Representative Bodipy Fluorescence Histograms of Fatty Acid Uptake in Primary AML Patients with CD36 Inhibition.* **(A)** Histogram of Bodipy fluorescence following 72 hours of incubation without (grey area) and with (coloured) FA6-152 inhibitor on either PS or scaffold for each patient. Lines represent the gating threshold based on the unstained control.

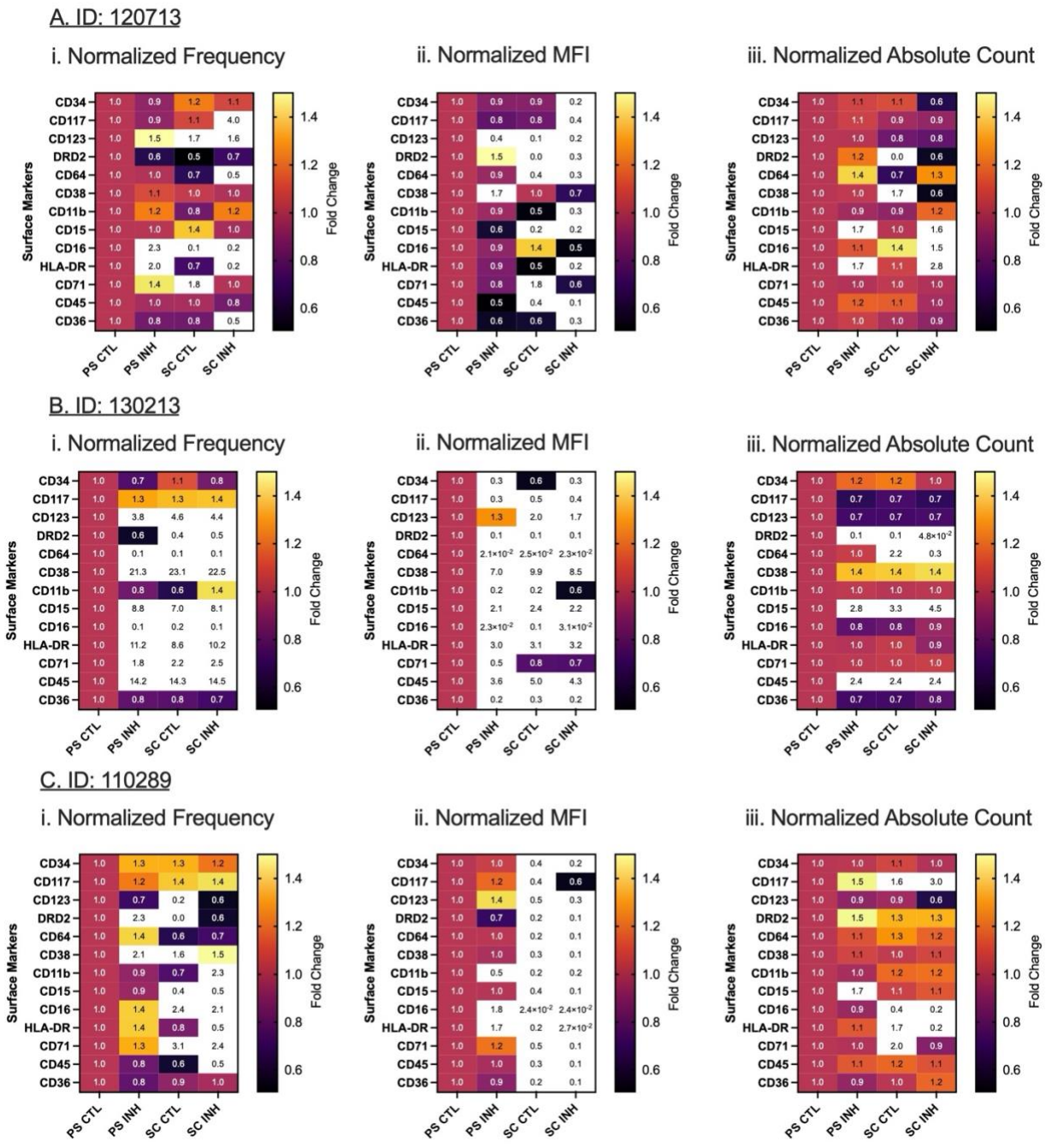

Supplemental Figure 2. *Phenotypic changes in AML blasts following 72-hour culture with CD36 inhibition normalized to the PS control.* **(A-C)** Heatmaps of three independent patient samples (ID: 120713, ID: 130213, ID:110289) depicting (i) surface marker frequencies, (ii) MFI, and (iii) absolute counts normalized data to PS control. Significant fold changes higher than 1.5-fold or lower than 0.5-fold are depicted in white.

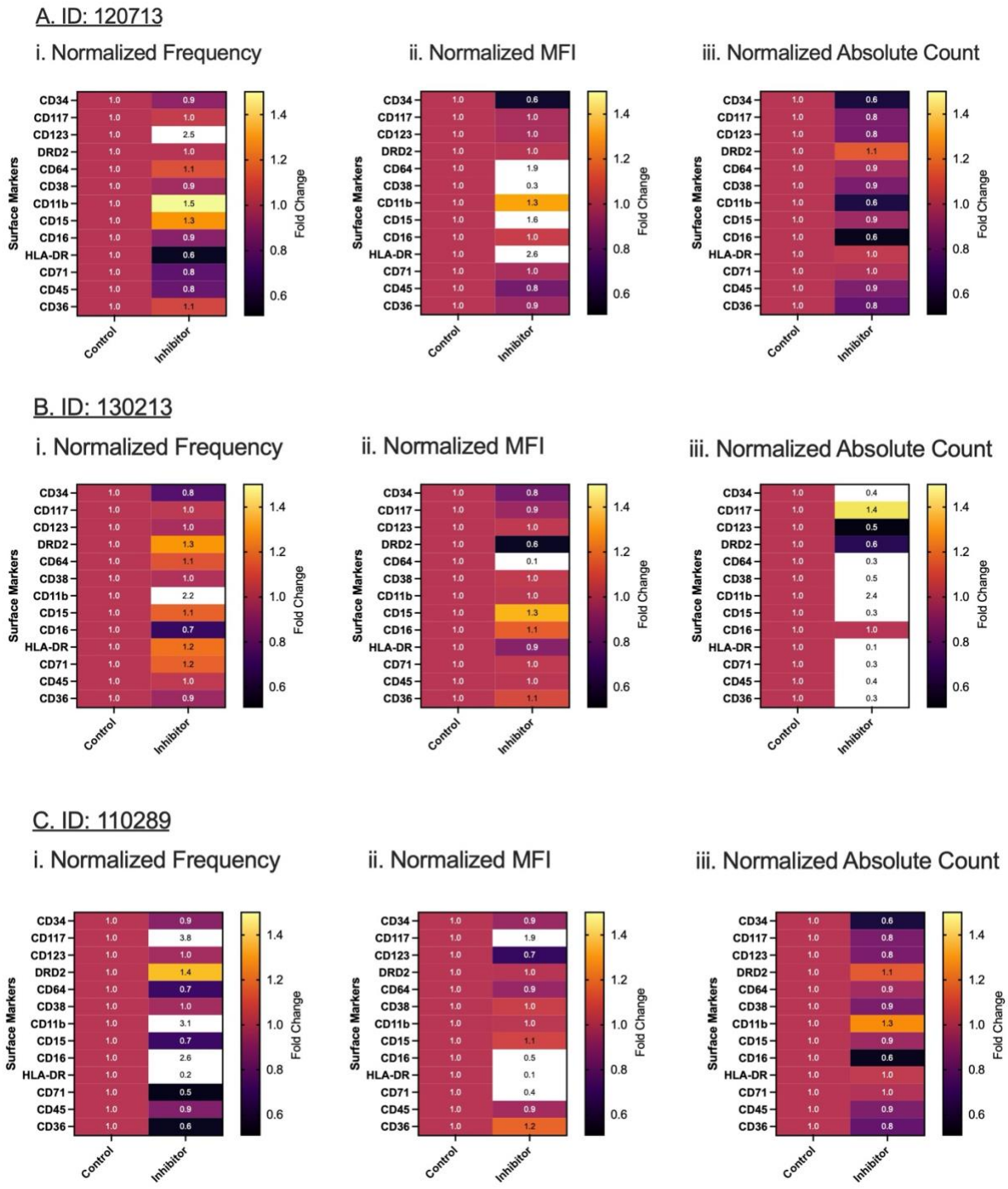

Supplemental Figure 3. *Phenotypic changes in AML blasts following 72-hour culture with CD36 inhibition normalized to the scaffold control.* **(A-C)** Heatmaps of three independent patient samples (ID: 120713, ID: 130213, ID:110289) depicting (i) surface marker frequencies, (ii) MFI, and (iii) absolute counts normalized data to their respective scaffold control. Significant fold changes higher than 1.5-fold or lower than 0.5-fold are depicted in white.